INTEGRATED DEGRADATION MODELS FOR POLYMER MATRIX COMPOSITES

by

Bethany J. Foch

B.S. Aeronautics and Astronautics Engineering
Massachusetts Institute of Technology, 1993

SUBMITTED TO THE DEPARTMENT OF AERONAUTICS AND ASTRONAUTICS
IN PARTIAL FULFILLMENT OF THE REQUIREMENTS FOR THE DEGREE OF

MASTER OF SCIENCE IN AERONAUTICS AND ASTRONAUTICS

AT THE

MASSACHUSETTS INSTITUTE OF TECHNOLOGY

JUNE 1997

Signature of Author:_

 ‿Department of Aeronautics and Astronautics Engineering
May 9, 1997

Certified by:_

Hugh L. McManus
Assistant Professor of Aeronautics and Astronautics
Thesis Supervisor

Accepted by:____

Professor Jaime Peraire
Chair, Graduate Office

INTEGRATED DEGRADATION MODELS FOR POLYMER MATRIX COMPOSITES

by
Bethany J. Foch

ABSTRACT

Aircraft systems such as the proposed High Speed Civil Transport (HSCT) experience severe cyclic environments during normal operations. Aircraft skins reach extreme temperatures due to high vehicle speeds; diffusion of moisture and oxygen into the material is accelerated by these temperatures; these in turn can cause property changes and/or permanent material degradation. Given that no predictive analytical model exists which captures the material response to this type of exposure, a set of models and computer codes was developed to aid in the calculation of the effects of severe, cyclic environments. A simplified solution, specifically designed for repeated cycles of varying moisture and temperature levels, results in a very efficient analytical tool. Using as inputs surface temperature, relative humidity (RH), oxidative environment, material properties and laminate geometry, these codes predict the material state, degraded properties, and resulting stress state as functions of position and time. Two independent computer programs fulfill this objective: the first is a new code to predict the diffusion of moisture and oxygen and the resulting chemical reactions; the second is an existing stress analysis tool. An infinite plate exposed to uniform environmental conditioning on its top and bottom surfaces is modeled. It is assumed that moisture and oxygen diffuse into the material following a one-dimensional Fickian law. Temperature is assumed constant through the thickness, and instantaneously equal to the time-varying ambient temperature. The onset of chemical reactions are activated by the presence of oxygen in the material and elevated temperatures. A recent study provides the basis for the reaction model used. The relevance of these models are supported with weight gain data from hygro–thermocycling and mass loss data from isothermal dry exposures. Cases relevant to the HSCT test program suggest two distinct results of cyclic moisture exposure. Near the laminate surface, rapid fluctuation of the moisture level occurs. In the interior of the laminate, the absorbed moisture level ignores the fluctuations and instead settles to an equilibrium value. Oxidative degradation due to this type of exposure are shown in preliminary calculations to be a concern only in the outer plies. A parametric study indicates that under severe cycling, non-trivial degradation occurs at the surface. Modified micromechanical and composite mechanics relations in the existing code allow the prediction of ply and laminate properties and stress states as a result of environmental exposure. In the cases studied, large thermal stresses predominated. Moisture cycling created cyclic stresses, with steep stress gradients. The computed stresses do not fully explain the increased cracking observed under exposure to moisture, suggesting that there are mechanisms for moisture-induced cracking beyond moisture-induced stresses. Degradation created severe stresses at the surface. This could explain the surface microcracking observed in numerous studies.

ACKNOWLEDGEMENTS

This thesis represents the culmination of several years of hard work and a few moments of clarity, neither of which were all mine. There are many people who have helped me through this process, aiding with both calculations and with mental stability. My advisor, Prof. Hugh McManus, is the one I must thank most for the first. There were many times that his intuition provided the answer, then I worked backwards from there to find out why.

My extended duration at MIT has put me in touch with many great teachers and researchers. Starting way back when with Unified, I have been grateful for the patience and availability of the professors in the Aero/Astro department. Throughout courses and presentations of research, Paul has encouraged a thorough understanding of the fundamentals through patient inquisitions. Mark sat patiently through all my questioning and always knew exactly how to phrase the answer so that the simplicity of the problem would work its way in. His questions about my research were not always met with the same speedy response, but his interest was always appreciated. It was always reward enough to give a talk just to hear Professor Dugundji say that he really enjoyed it.

Thanks a million to Deb, who has always taken care of everything with the utmost ability and efficiency. I have been so grateful for your company and for our chats during my visits to Hugh's outer office. I'm so glad you came back. Thanks also to Ping, who knows the inner workings of the funds upon which we all rely. You were a savior when I didn't know my account number from my ID number. And thanks to Al Supple, the true voice of experience.

FOREWORD

This work was conducted in the Technology Laboratory for Advanced Composites (TELAC) in the Department of Aeronautics and Astronautics at the Massachusetts Institute of Technology. This work was sponsored by the Boeing Commercial Airplane Group under contract numbers NAG3-1893 and TO-523781-07LLN.

TABLE OF CONTENTS

7

TABLE OF FIGURES

TABLE OF TABLES

NOMENCLATURE

A	multiplying factor for calculating material saturation level
A_{ni}	mode amplitude for solution of moisture diffusion
b	mass loss metric
b_{tot}	average mass loss across laminate thickness
B	exponential factor for calculating material saturation level
B_{ni}	mode amplitude for solution of oxygen diffusion
$\overline{C}(ply_n,t)$	average concentration in ply n at time t
C_{eq}	equilibrium moisture level
C_m	specific concentration of moisture
C_{mo}	initial specific moisture concentration
$CTEkl$	coefficient of thermal expansion
C_{ox}	normalized oxygen concentration
C_∞	relative humidity dependent moisture saturation level
d_{eq}	moisture fluctuation surface layer thickness
D_{ij}^m	anisotropic 3-d diffusivity of moisture
D_z^m	through-thickness diffusivity of moisture
D_z^{ox}	through-thickness diffusivity of oxygen
D_o^{ox}	diffusion constant for oxygen
D_o^m	diffusion constant for moisture
E_{Akl}	activation energy required for reaction k acting on component l
E_A^m	activation energy of moisture diffusion
E_A^{ox}	activation energy of oxygen diffusion
E_{ijkl}	anisotropic 3-D Young's modulus
h	laminate thickness
i	index for cycle specification

k index for reaction

k_{kl} reaction rate of reaction k acting on component l

l index for mass component

m_{kl} order of concentration dependency of reaction l acting on component k

m_k mass lost due to completion of reactions in component k

m_o initial mass of local material

n mode index for modal solution of diffusion

n_{kl} order of reaction kinetics of reaction l acting on component k

N_p number of plies in laminate

n_{P_b} exponential constant used in determining degraded material property

N_s number of points through thickness at which calculations performed

N_{sp} number of points per ply at which calculations performed

P degraded material property

P_o original material property

R real gas constant

R_{kl} non–dimensional material constant representing oxygen concentration required to complete reaction l in material component k

r_{ox} reaction consumption factor

r_{ox}^* reduction in oxygen concentration due to reaction

s index for locations through thickness at which calculations performed

T temperature

T_{GD} dry glass transition temperature

T_{GW} wet glass transition temperature

T_o stress free temperature

T_{RT} room temperature

t time

t_i time at point i in cycle specification

t_{ply}	ply thickness
y_k	mass fraction of component k
z_s	location of position s
α_{kl}	mass loss metric for reaction l acting on component k
β_{kl}	coefficient of moisture expansion
Δm_k	change in mass in component k
ΔP_b	empirical constant for determining degraded material property
ΔT	change in temperature from stress free temperature
Δt_i	time interval between t_{i-1} and t_i
$\overline{\Delta t}^*$	adjusted time step used in d_{eq} calculations
$\Delta t_{m(i)}^*$	adjusted time step associated with moisture diffusion at t_i
$\Delta t_{ox(i)}^*$	adjusted time step associated with oxygen diffusion at t_i
$\Delta t_{rxn(i)}^*$	adjusted time step associated with reaction at t_i
Δz	step size used in stepwise integration
ε_{kl}	mechanical strain
σ_{ij}	stress in laminate
Φ	relative humidity
χ_{kl}	coefficient of degradation-induced shrinkage or expansion

CHAPTER 1

INTRODUCTION

1.1 PROBLEM

Polymer matrix composites are well suited for advanced aeronautical applications due to their high strength–to–weight ratios as well as the potential they provide for tailoring fiber directions to meet structural requirements. New fiber and matrix materials are being developed that are capable of meeting ever more demanding design requirements. Recent work has included development of polymer matrices capable of withstanding high temperatures. These materials have proven advantageous for extreme environment applications such as the primary structure of the proposed High Speed Civil Transport (HSCT). However, the uncertainty remaining in composite materials' long term behavior under mechanical and environmental loads limits their use. A material's response to extreme and demanding environments is complex, consisting of many coupled phenomena. Extensive experimental testing can provide some insight into material behavior. However, such tests are expensive and time consuming. Models which capture the mechanisms driving the material response are needed. Such models could be used to expand understanding of the material behavior, design appropriate accelerated and scaled tests, and ultimately provide design tools.

Structures such as those found on the HSCT experience cyclic loads and environments during flight. Materials under consideration for this application must withstand environmental exposure during the vehicle's entire lifetime, reaching 60,000 operational hours, or approximately 20,000 flights. During each flight, elements of this structure experience temperatures as high as 350°F and as low as –65°F, as well as periods of

exposure to humid air. An accurate material model must be able to capture behavior over many of these complex flight cycles. This model must incorporate the inherent complexity and coupling of the relevant effects. The current work provides a method for predicting the changing state of a material exposed to such harsh environments.

1.2 APPROACH

The goal of this work is to provide a design tool that captures the mechanisms of each of several environmental effects and predicts the resulting changes in material state. The first step in predicting the material behavior is modeling the process of temperature, moisture, and oxygen diffusion. Temperature across a laminate reaches equilibrium much faster than moisture or oxygen. As a result, it can be assumed that temperatures throughout a thin laminate will reach ambient values instantaneously. Gradients result from the much slower diffusion of moisture and oxygen into the material. Diffusion into the laminate is accelerated at high temperatures. In this work, the diffusion of moisture and oxygen into a laminate under varying ambient conditions is modeled, based on Fick's Law. An efficient mathematical analysis allows for fast calculation of the changing moisture and oxygen concentration during many cycles.

Over long periods, temperature, oxygen, and possibly moisture all cause chemical changes in the matrix material. These chemical reactions cause changes in properties and mass loss. The progress of these reactions is calculated in the current model using a previously developed technique.

The mathematical expressions developed to describe diffusion of oxygen and moisture and the resulting chemical reactions are encoded in a computer program to facilitate repeated, rapid calculations. User input includes all relevant material properties, profile of the cycle

14

(including duration, humidity, and temperature of pre–exposure), and number of cycles. Relevant material constants are also required in the input. Model predictions of the total weight change due to moisture uptake and chemical reactions show a close correlation with data from specimens exposed to one thousand test cycles. Comparison of predicted material mass loss with previous dry isothermal experiments also show reasonable agreement.

Varying thermal conditions, absorbed moisture, altered material properties, and changes in the mass of the material all affect the stress state in the structure. A constitutive equation including these effects, in conjunction with composite laminated plate theory (CLPT) and an empirical model of the changes in properties at the micromechanical level, provide the tools necessary to compute the stress state in the laminate. An existing code is used to calculate the stress state and the altered ply and laminate properties. The stresses resulting from exposure to sample test cycles create a potential for damage. Additional work is necessary to predict the resulting damage in order to fully characterize the response of materials to long term cyclic environments.

1.3   TERMINOLOGY

The terminology used to describe the effects being studied here is not well standardized. The terms related to this study are therefore defined below. We will follow established terminology whenever possible. The current work is a study of *environmental effects*. This term is often used to describe the effects of temperature and diffusion of moisture; the definition is expanded here to also include diffusion of oxygen, chemical changes in the material, and the resulting changes in the material stress state.

A *concentration* describes the normalized quantity of moisture or oxygen at a particular location. *Saturation* represents the maximum concentration of a substance that can be absorbed by a material for a given external condition. In general, the surface of the material is assumed to be equilibrated with the ambient level. *Specific moisture concentra. .)n* is expressed in terms of the mass of moisture in an infinitesimal volume of material, normalized by the dry mass of material in the volume. *Oxygen concentration* is expressed in terms of the mass of oxygen in the local control volume, normalized by the mass of oxygen that would saturate the material. This relative concentration metric is used for convenience, as it is difficult to measure either the mass of oxygen absorbed, or the saturation level for oxygen. The local concentration must not be confused with the *weight gain* (used here only for moisture), which is the total mass of moisture in a macroscopic specimen divided by the total dry mass of the specimen. The total weight gain is numerically equal to the volume–average concentration.

Once the level of moisture, oxygen, and temperature in the laminate are predicted, their effects on the material must be modeled. Chemical reactions in the polymer matrix are activated by temperature and by the presence of oxygen. Those reactions driven solely by temperature will be referred to as *thermal reactions.* Those which require oxygen to be present will be referred to as *concentration dependent reactions* or *oxidative reactions.* A *completeness of reaction metric* is introduced to record the progression of chemical reactions. Each reaction is tracked by an independent completeness metric, which reaches a value of one when the reaction is complete. Reactions cause a specific change in the state of the material that will be referred to as *degradation. Chemical degradation* is simply degradation caused by chemical reactions. Degradation is measured in terms of changes in the material properties and mass loss. Local mass loss across the laminate thickness is directly proportional to the reaction completeness metric. A *mass loss metric* records the mass lost in an infinitesimal volume of material, normalized by the original mass of the

volume. The *total mass loss* across the laminate thickness is the volume–average of the mass loss metric, and is expressed as a percent change in the mass of a macroscopic specimen from the original mass.

Past work has included non-standardized uses of the term *aging* in references to the various phenomena resulting from environmental exposure. *Physical aging* refers to the reversible rearrangement of molecules in the matrix to a more stable state. *Chemical aging* is often used to describe additional cross-linking in the matrix during elevated temperature exposure periods. This is also referred to as *post-curing*. Such additional cross-linking in the polymer chains causes an increase in material stiffness and glass transition temperature. Post-curing is not addressed in this study, as it is assumed that material will generally be fully post–cured as part of the manufacturing process. Chemical aging has also been used to describe chemical degradation. In general references to environmental exposure, investigators have used the term aging interchangeably with exposure time. Consideration of physical aging will not be included in this investigation. We will consider chemical aging, but we will use the term degradation to describe this effect. Aging will not be used here to refer to exposure.

A decrease in mass or density can cause *shrinkage* of the material. This is also a local effect, measured in terms of the stress–free change in dimensions of an infinitesimal, unconstrained volume of material, normalized by the original dimension. A macroscopic specimen can also exhibit changes in dimensions. These are *not* merely an average of the local shrinkage. They must be determined from a structural analysis of the distributions of shrinkage and changed material properties throughout the specimen.

Local stresses (*microstresses*) arise between the fibers and matrix due to changes in temperature, degradation–induced shrinkage, moisture–induced swelling, and the stress

concentrations that occur locally around fibers when a far–field load is placed on the composite. *Ply stresses* (homogenized stresses across a single ply) also arise from constraints between different plies due to changes in temperature, degradation–induced shrinkage, and moisture–induced swelling, as well as from applied loads.

Stresses may cause *surface cracks, microcracks,* or *fiber-matrix debonds.* Fiber-matrix debonds are separations between individual fibers and the surrounding matrix. Microcracks are cracks in the matrix between and parallel to the fibers. They can exist in sizes from the fiber–matrix scale all the way up to the height of entire plies. The later definition is usually used; these are also referred to as *ply cracks.* Surface cracks are observed starting at the surface of the composite, and penetrating inward some small distance. These can occur on both surfaces parallel to the plane of the laminate (in which case the cracks are often seen as random cracking of a surface resin layer, also referred to as *crazing*) or at cut edges, in which case they look like microcracks of limited length.

If cracks occur, the material is considered *damaged.* Damage is an irreversible change which limits a material's effectiveness in structural applications. Mechanical testing after exposure and a return to room temperature dry conditions provides *residual* material properties, often but not always associated with damage. Note that thermal stresses, especially from the manufacturing process, are sometimes referred to as *residual stresses,* but we will not use the term in this sense here.

1.4 OUTLINE

Background for this investigation is given in Chapter 2, which describes previous studies relevant to the current work. Chapter 3 provides an outline of the current problem and the approach used for its solution. The mathematical development of the model is included in

Chapter 4, as well as techniques used to integrate additional models into a comprehensive predictive tool. Chapter 5 consists of results, parametric studies, and comparison of results to available experimental data. A summary of this work and identification of areas which need further investigation is included in Chapter 6.

CHAPTER 2

BACKGROUND

As the use of polymer matrix composites in aerospace structures increases, more attention is being given to their long term behavior. The infiltration of moisture and oxygen at high temperatures for extended time periods has been seen to have a deleterious effect on the material's structural integrity. The exact nature of this collective change is not yet well characterized. Many investigations have been performed exposing a composite laminate to the environment, and reporting values in terms of change in weight or observed damage. The exposure is often in the form of a controlled wet or dry, hot or cold environment. The resulting material state, however, is a combined effect of many competing and coupled effects during such exposure.

The subject of "environmental effects" on composites has received much attention in the literature. These effects can include temperature, moisture, and chemical degradation. The effects of temperature are the most well understood of the environmental factors [1,2]. If the diffusion rate of temperature is much higher than that of any other substances, calculations of temperature-dependent effects are greatly simplified. In most materials, heat diffuses into a material approximately one million times faster than moisture; therefore, it is often assumed that a laminate reaches ambient temperature instantaneously, and temperature is constant throughout the material. For materials whose rates of moisture diffusion are on the same order of magnitude as heat conductivity, theories have been developed to account for the coupled distributions of moisture and temperature [3].

2.1 MOISTURE DIFFUSION

The diffusion of moisture into composite materials is very well documented. Several exhaustive reviews of moisture diffusion behavior and its effect on a composite laminate have been published [4-7]. Moisture absorption and desorption is most commonly reported in terms of material weight change as a function of exposure time to wet environments. When a material is initially exposed to moisture, fluid is absorbed in a near linear relationship with time. As exposure time lengthens, weight gain seems to asymptote to a maximum value. This trend suggests that increases in moisture content are dependent on the moisture concentration already in the material. Fick captured this behavior in an equation describing diffusion of a material through a medium by expanding the mathematical development presented by Fourier to describe heat conduction.

Crank suggested several forms for solutions to Fick's differential equation in his study of the mathematics of diffusion [8]. The most widely used solutions involve summation of sinusoidal modes or utilization of the error function. Both simulate the gradual decay of the slope of the absorption curve as the moisture value nears saturation. A thorough review of the applicability of these equations to the diffusion of moisture into a composite material is given by Shirrell and Halpin [9]. The evidence for Fickian moisture diffusion has been so strong that Fick's Law is often the exclusive model cited in reference texts for composite materials [10-12].

Subsequent investigations measuring the absorption of various fluids into composite materials showed that within a certain range of conditions, the Fickian approximation is quite accurate. Loos and Springer exposed several different graphite epoxy laminates to various fluids in order to quantify their absorption behavior [13]. Unidirectional laminates were fabricated from pre-impregnated fiber/matrix plies, and neat resin was identically

cured for comparison. Exposure to various types of fuel, as well as distilled water and humid air at various temperatures (300 to 322 K) enabled Loos and Springer to document diffusion rate constants and maximum moisture concentration. For each of these fluids, data correlated well with the Fickian prediction. The saturation levels were dependent only on relative humidity (not temperature) and were identical in laminates and their respective neat resin specimens.

Shen and Springer also found moisture absorption in both unidirectional and cross-ply composite laminates to correlate with the Fickian prediction [14]. These investigators proposed a relationship between the matrix diffusivity, the fiber volume fraction, and the diffusivity of the composite. It was assumed that fibers did not absorb any moisture. Exposing these composite materials to humid air and water at various temperatures (in the range 300 to 425 K), the researchers found good agreement between the diffusivity reduced from experimental data and the calculated prediction. The moisture uptake over time recorded during these experiments also correlated well with a modal solution of Fick's Law. In addition, diffusivity showed no dependence on the changing level of moisture in the laminate.

In order to characterize the diffusion of moisture into advanced thermoplastic composites, Ming performed a study comparing the moisture uptake in both neat resin and composites with increasing fiber volumes submerged in water at various temperatures (28°C to 97°C) [15]. An empirical expression for the composite diffusivity as a function of matrix diffusivity and the square root of fiber volume fraction was developed. Results from all tests agreed with the prediction given by Fick's Law. This study also included an investigation of the effects of hygrothermal exposure on mechanical properties. The short-beam shear strengths and flexure strengths at exposure temperature fell off rapidly with initial moisture uptake at 97°C, but settled to limit values after about 100 hours.

2.1.1 Micromechanics of Diffusion

A number of researchers have developed models that predict a material's diffusivity given only its constituent fiber and matrix properties. Finite element methods (FEM) have been used to predict diffusion behavior on a micromechanical level. The geometry of the unit cells for the FEM models varies, but all assume that the fibers do not absorb any moisture. Composite diffusivity, in these models, depends only on the diffusivity of the matrix and the interference of the fiber.

Kondo and Taki developed an FEM model to perform a parametric study on the effects of fiber volume fraction and the packing arrangement of the fibers [16]. These researchers found that experimental data for transverse moisture diffusivity best agreed with predictions for a random array of fibers (rather than a periodic regular distribution of square fibers). It was deduced that the model assuming a random distribution of fibers coincided with the inherent randomness in an actual unidirectional composite.

Another finite element analysis, performed by Bond, *et al.*, studied the effect of fiber geometry in a unit cell on transverse composite diffusivity [17]. Experimental results were given in terms of a ratio of transverse diffusivity over matrix diffusivity versus fiber volume fraction. The goal was to determine the ideal unit cell to predict accurate composite diffusivity. Random, tetragonal, and hexagonal arrays were studied. It was determined that a randomly distributed fiber model predicts identical transverse diffusivities to a model with regular packed fibers of equivalent fiber volume fraction. Bond suggested that a regular packed unit cell may be used in FEM analyses, even if a random distribution of fibers exists in the real system. However, he notes that if a resin rich layer exists between plies, randomness cannot be assumed, and a reduction in through–thickness composite

diffusivity results. The studies done by Kondo and Taki and by Bond, *et al.* seem to come to contradictory conclusions about whether a regular unit cell can model a random fiber arrangement. This can be attributed to their choice of unit cell shape. Square unit cells do not accurately model randomly arranged fibers, while tetragonal or hexagonal unit cells can.

Aditya and Sinha investigated the effect of the fiber's shape on the transverse diffusivity. Diffusion paths in unit cells with fibers of identical cross sectional area but varying shape (circular and elliptical) were modeled. These investigators suggested that fibers with increasing eccentricity along the transverse direction allowed greater diffusivity through the material [18].

2.1.2 Absorption Models

Given the diffusivity of the composite, moisture absorption and desorption can be predicted using Fick's Law. Several mathematical formulations have been developed in order to simplify the process of predicting moisture sorption. A model developed by Springer, entitled "W8GAIN", predicted the distribution of moisture and temperature in a laminate exposed to constant ambient conditions [11]. In order to predict moisture distributions in laminates exposed to transient ambient conditions, Springer subsequently developed a cyclic exposure input to his code [20]. An analysis developed by Weitsman searched for the most efficient calculation for moisture sorption in a laminate over time-periods with fluctuating ambient conditions composing simple cycles [21].

A method developed by Miller predicts moisture concentration in a multi-material structure exposed to constant boundary conditions given only a hand calculator [22]. Miller's contribution is a method of converting a multi–layer system of different materials into a

single material for the purpose of analyzing the moisture through the entire material. The thickness of the second material was weighted by the diffusivity of the first. Calculations of the total change in weight can then be performed in one step. Each of these models is based on Fickian diffusion.

Aditya and Sinha proposed a method for determining a material's dependence on relative humidity that arose out of a limitation in the laboratory: the thermocycling oven could not be left on overnight [19]. These investigators proposed a two phase exposure cycle; the first phase consisted of a high temperature exposure to humid air, and the second a room temperature exposure (keeping relative humidity constant), representing the time that the oven would be turned off. The recorded weight gain during each constant temperature segment of this fluctuating environment followed Fickian behavior. Since maximum moisture concentration has been shown to be independent of temperature, periodic exposure could continue until additional moisture sorption (at either temperature) was negligible, and thus saturation was achieved.

2.1.3 Mechanical Effects of Moisture

Efforts have been made to correlate moisture sorption in composites with changes in material properties. Investigations on the effects of moisture in composite materials have reported altered material properties in wet specimens. Browning, *et al.* suggested two independent causes for these varied effects [24]. The first is a reversible chemical reaction activated by the presence of moisture and resulting in plasticization or softening of the polymer matrix. A second potential cause for changes in the material is swelling of the matrix combined with cracking at the fiber/matrix interface. These phenomenon may explain the reported decrease in various composite properties.

One of the most often reported material change during moisture absorption is a drop in the glass transition temperature [25,26]. Zhou and Lucas have reported that this change can be as large as a 10-20°C drop with every one percent weight gain due to moisture [26]. This has been attributed to a plasticization of the polymer structure due to the formation of weak Van der Waals bonds between the polymer and water molecules, leading to increased chain mobility and thus softening of the resin material. This theory supports the idea that water affects the material chemically as well as physically.

A decrease in mode two fracture toughness was noticed in wet materials in a study by Davies, *et al*. This effect was attributed to degradation in the interphase region between the fiber and matrix [27]. Lucas and Zhou also reported a significant degradation in this interfacial region due to moisture uptake, manifested as a reduction in the mode one delamination fracture toughness as measured in a notched short bar specimen [28]. A study by Upadhay and Prucz showed a drop-off in both transverse and shear strength in humid environments, while longitudinal strength changed little [29]. A parametric model was developed which related reduction in strength to moisture absorbed. The mode of failure (suggested by observed behavior and finite element analysis predictions) used in this model was debonding at the fiber/matrix interface.

Thermoplastics have proven attractive in applications in moist environments due to their low moisture uptake in comparison with thermosetting matrix materials. It has been reported that, at saturation levels, thermoplastic composites absorb one tenth of the moisture absorbed by thermoset systems [28]. A recent series of investigations on the effects of moisture on thermoplastic matrices showed a reversible drop in the glass transition temperature, with little change in other material properties [30]. A subsequent report suggested permanent mode one fracture toughness losses may result from soaking these specimens in water, but no change was seen in less humid environments [31].

26

2.1.4 Non-Fickian Behavior

A number of studies have reported non-Fickian moisture absorption in composite materials after extended periods of time. In a majority of these cases, divergence from Fickian behavior has coincided with the onset of degradation and cracking [26,30-32]. Water is absorbed mainly by the matrix; fibers are affected very little by moisture. The uptake of water in the matrix leads to swelling, causing a moisture induced strain due to mismatch in moisture expansion (similar to the effect of temperature on composite laminates). Studies have suggested that cracking results from this water-induced stress state, providing additional void locations for the uptake of water [28-31]. It has also been postulated that moisture gives mobility to end–groups of the polymer molecule, allowing additional cross–linking (or curing) to occur. The additional cross–linking at wet states may result in areas of high stress concentrations, on the scale of a fiber diameter, leading to microcracking [25].

These theories explain additional moisture uptake observed after saturation. At higher temperatures, however, a decrease in mass has been seen after saturation [26]. It has been suggested that chemical degradation at the material surface results in loss of resin, decreasing the overall mass. This concept will be discussed in more detail in the Chemical Effects section below.

A study by Cai and Weitsman presented an alternative to the Fickian diffusion model in order to account for this observed divergence [34]. These investigators noticed that many cases exist in which additional moisture is absorbed into a material after the initial leveling off under constant exposure to a humid environment. The goal of their study was to predict the time-dependent moisture concentration of materials exhibiting this behavior, as

well as provide a method of calculating diffusivities of "non-classical" materials. All previous models discussed in this section assumed an instantaneous equilibrium condition between the ambient moisture condition and the material surface. In Cai and Weitsman's model, a time dependent boundary condition was introduced to capture the observed non-Fickian behavior. In this model, a material was exposed to a constant relative humidity. The concentration at the surface of the material equilibrated with the RH level according to an exponential time decay. The moisture concentration through the thickness of the material were then calculated using a well known solution to Fick's Law.

2.2 CHEMICAL EFFECTS

Material changes during exposure to air have been widely noted in the literature. Several forms of changes in the material are reported in various studies: a discoloration and embrittlement at the surface of the material; mass loss; and cracking both at the embrittled surface and within plies. Degradation has complicated the study of other factors, such as moisture and viscoelasticity, which require specimens to be exposed to high temperatures for long times. Presented below is an overview of investigations of the observed effects of exposure to hot, oxidative environments, and attempts to characterize the mechanisms driving this degradation.

2.2.1 Material Behavior

An example of the potential severity of exposure to hot, oxidative environments for long times is depicted in a study by Chester and Baker [35]. In this study, laminates were subjected to tropical conditions. Significant weight loss was observed in unpainted composite specimens. Resin at the exposed surface degraded significantly. In some areas, resin at the surface was lost completely, with free fibers visible under close inspection.

In the search for resin systems that can withstand high temperature applications, new polymers have been developed that are more stable at high temperatures. However, extended exposure to oxygen at extreme temperatures causes degradation even in these advanced polymer systems. A class of polymers known as polyimides has received much attention in the literature due to their relative stability in harsh environments [37]. Investigations have attempted to quantify the nature of the prominent chemical reactions that occur in a polymer exposed to air [38,39]. Roberts and Vanucci performed chemical analyses on various types of polyimides in an effort to identify the changes that occur in these materials as they are subjected to high temperatures. Of the materials studied, the one that best retained its original properties was a polyimide referred to as PMR-15. Although other candidates for high temperature applications exist, PMR-15 has been the subject of many studies in the effort to characterize chemical degradation [38-42].

Mechanical tests in many studies report decreases in material strength after exposure to hot, oxidative environments. Glass transition temperature tends to increase as a result of exposure [43-46]. The increase in glass transition temperature is explained by chemical changes in the material [44,45,46]. This phenomenon is thought to be a result of additional curing occurring in the matrix at elevated temperatures. Cross–linking between polymer chains, initiated during the cure cycle, continues when activated by temperature. An increase in strength and stiffness during initial exposure (followed by a decrease as the material begins to degrade) correlates with this chemical change in the matrix [46].

The most frequently cited mechanical property affected by prolonged high temperature exposure in studies concerned with time dependent oxidative effects is shear strength. All investigations showed a decrease from original values after exposure. After subjecting laminates to as much as 16,000 hours in air at 288°C, Nelson reported an eighty percent

drop in short beam shear strength [43]. Bowles reported a thirty percent loss in this property after only 300 hours at 371°C, exposed in nitrogen [48]. A sharp drop in shear strength was noted by Beckwith and Wallace during exposure in air at 176°C after 4000 hours, while slightly lower temperature environments caused no change up to 12,000 hours [49].

Madhukar, et al. investigated the effect of carbon fibers' surface treatment on the shear strength of composite materials exposed to air [50]. Treated fibers were coated with a proprietary material prior to consolidation, in an effort to strengthen the interface with matrix material. It was postulated that a weak interface between untreated fibers and the polymer matrix encouraged cracking at this joint, providing a path for oxygen infiltration. No drop in room temperature shear strength was seen in materials fabricated with surface modified fibers, while a non-trivial drop (twelve percent over 1000 hours at 316°C) occurred in the untreated fiber specimens.

2.2.2 Coupled Oxygen Diffusion and Reaction Models

The chemical reactions that occur at elevated temperatures are complex and difficult to model [38,51]. Recently, researchers have been able to separate coupled oxygen and thermal dependent reactions by carefully designed experiments. In order to separate oxidative effects from the influence of temperature, resin samples and composite laminates in several studies were exposed to elevated temperatures in a nitrogen environment. This enabled characterization of purely thermal reactions. Identical temperature exposures in an oxidative environment resulted in greater mass loss than the tests in pure nitrogen, suggesting some reactions are activated by the presence of oxygen.

A study by Xiang and Jones identified a three stage kinetic degradation process in PMR-15 impregnated carbon fiber woven composites [40]. The first stage involves oxidation of the resin at the material surface and formation of microcracks there; the second stage represents a diffusion dominated chemical degradation of the matrix; the third and final stage is oxidation of the carbon fibers. This model is more empirical than mechanistic; it relies on the outcome, rather than the cause, to characterize behavior.

A recent model separates the diffusion of oxygen into the material from subsequent thermal and oxidative reactions, leading to a prediction of mass loss. Cunningham and McManus performed thermogravimetric analyses at different heating rates on powdered samples to find values of the reaction constants of several separable chemical reactions. In this investigation, it was assumed that oxygen diffused into the material according to Fick's Law. A mathematical model was developed to predict degradation metrics, such as mass loss and growth of a surface layer [41,42].

2.2.3 Altered Mechanical Properties

The reactions that occur in polymers at high temperatures have been explored in depth by polymer chemists [52]. Very little modeling has been done to predict the extent of degradation of material properties due to these reactions. Part of the difficulty has been the lack of agreement on a set of metrics which describe this degradation. A relation must then be determined to link degradation metrics to the degraded matrix properties. Micromechanical relations could then predict the changed composite properties due to degradation. Some work has been done defining degradation metrics and linking them to material properties [53,54], but a comprehensive model relating chemical reactions to altered laminate properties does not yet exist.

2.3 STRESS STATE AND DAMAGE

The effects described above may cause stresses due to thermal strains, swelling, shrinkage, or changes in material properties. The potential dangers of thermal stresses are well documented [1,53,57]. In some cases, cool down from cure temperature creates thermal stresses significant enough to cause microcracking. Stresses caused by the presence of moisture and chemical changes in the material add to the total stress state. Chemical degradation also leads to altered material properties, resulting in a greater potential for damage at a given mechanical load level. When environmental and mechanical loads are applied in a cyclic manner, damage to a composite is greater than under static loading conditions [32].

2.3.1 Moisture Induced Swelling

Moisture causes swelling in the matrix, leading to stresses in the laminate plies and at the micro-structural level between the swelled matrix and the fibers. Shirrell and Halpin outlined a potentially dangerous scenario during the moisture sorption process [9]. Due to the fast equilibration with ambient humidity levels at the surface and slow diffusion into the center of the laminate, stress gradients may occur across a specimen's thickness. Restrained swelling of the laminate due to moisture results in a compressive stress. Dry plies in the interior will be affected by the expansion of moist surface plies, causing tensile stresses. Conversely, dry-out from a saturated state can result in plies at the surface loaded in tension, potentially leading to microcracking.

32

2.3.2 Mass Loss and Shrinkage

Exposing composites to oxidative environments results in material shrinkage and mass loss. Shrinkage of the material causes stresses between matrix and fibers. At the ply level, mismatches in stiffness between plies result in stresses. Mass loss causes changes in the matrix properties. Degraded material properties affect a laminate's ability to carry mechanical loads. Attempts to quantify these effects have caused investigators to define a coefficient of degradation–induced–strain which is related to strain in a manner similar to moisture and thermal expansion coefficients [54].

2.3.3 Damage

The onset of cracking in laminated composite specimens under mechanical loading has been captured by various modeling approaches. Laws and Dvorak, for example, developed a model using a shear lag method to predict material stresses [58]. Both Laws and Dvorak and Wang and Crossman formulated a strain energy release rate requirement to predict cracking [59,60]. A more complete overview of various studies of cracking is included in reference [61]. Only recently have models been developed that predict cracking due to progressive thermal loading. One code that attempts this was developed by Park and McManus, and expanded by Maddocks and McManus [62,63]. It uses a shear lag stress solution in conjunction with an energy requirement to predict the initiation of cracking. This investigation reported good agreement with experimental analysis.

2.3.4 Viscoelastic Effects

An additional complexity is the potential for viscoelastic behavior, which has been observed in studies of the effects of moisture [64,65]. It has been suggested that the

increased plasticity in the matrix and hygrothermal stresses caused by the presence of moisture result in accelerated relaxation of the stresses in a composite material. Flaggs and Crossman exposed laminates to moist environments at elevated temperatures in order to measure this time dependent mechanical response. When a high moisture concentration was maintained, stresses resulting from mechanical loading and swelling due to moisture relaxed after extended exposure times [64].

An investigation into deviation from Fickian diffusion and elastic response was performed by Harper and Weitsman. A change in curvature of unsymmetric laminates exposed to wet environments was measured. In some cases data agreed more closely with viscoelastic predictions. With increasing moisture cycling, data diverged even from this viscoelastic model, suggesting the onset of cracking [65]. This study suggests that moisture, as well as sustained mechanical loading, may result in a complex material response and damage.

2.4 SUMMARY

When exposed to complex environments, composite laminates undergo various changes. A change in temperature from the stress free (cure) temperature results in varying stresses across the thickness of a general composite laminate. For the newer, high temperature polymers, cooling to room temperature alone provides a several hundred degree Fahrenheit drop from cure temperature, creating a potential for microcracking. Moisture diffusion into a composite results in weight gain, altered material properties, and swelling of the matrix to accommodate the moisture, leading to hygral stresses. When high levels of absorbed moisture have been maintained for long periods of time, cracking has been observed. Oxygen diffuses into a laminate in a manner similar to moisture, but reacts with the matrix as it enters the material. Some chemical reactions also occur in the polymer driven purely

by thermal conditions. The combination of these reactions degrades the polymer material, resulting in loss of material, altered material properties, and surface cracking.

Many investigators have reported changes in material state due to environmental exposure. The motivation behind these studies is generally a desire to characterize the effects of the environment. However, no model has yet been developed that incorporates all of the contributing factors to predict a "degraded material state" and the properties of the laminate in this state. As investigators attempt to interpret complex results of environmental testing, a mechanistic model will assist in the analysis by both separating the effects and predicting aggregate results.

CHAPTER 3

PROBLEM STATEMENT

The purpose of this investigation is to develop a method for predicting the response of a material exposed to extreme cyclic environments for a long time. Given information about ambient temperature, relative humidity, oxidative environment, material properties, and laminate geometry, an integrated model is developed to compute moisture and oxygen concentrations through the laminate thickness, resulting material degradation, the effect of this degradation on material, ply, and laminate properties, and the resulting stress state, all as functions of position and time.

A new method for efficient calculation of the diffusion of moisture and oxygen is presented in this study. A well-known modal solution for moisture diffusion is adjusted to enable prediction of moisture absorption in a laminate subjected to a complex cyclic environment. A simple and efficient method for calculating modal amplitudes is developed. The diffusion of oxygen into the material is modeled similarly to that of moisture, with some alterations required due to the additional complexity introduced by the concurrent chemical reactions [42]. Ramps in temperature are accommodated using an adjusted time step.

These mathematical methods are encoded in a FORTRAN computer program. Moisture concentration through the laminate thickness as well as the total weight change due to moisture over time are predicted. The material degradation is also predicted, in terms of both mass loss metric through the thickness, and total mass lost from the material over time. Degradation and moisture profiles through the thickness are then used to determine changed material, ply and laminate properties.

Predicted changes in weight due to the presence of moisture and the extent of degradation are compared with experimental data. The Boeing Company recently performed studies on the response of IM7/PETI-5 laminates to cyclic environments. Unidirectional, cross–ply, and quasi–isotropic laminate configurations were exposed to multiple test cycles. In addition, comparison with mass loss from isothermal tests performed on PMR-15 neat resin samples are compared with degradation predictions.

The stress state resulting from temperature, moisture, and degradation is determined by employing an existing analysis tool (ICAN) [54]. By restructuring the output of the moisture and degradative analyses into ply–by–ply values, a file is created in the format appropriate for stress calculations. Shrinkage and the change in matrix properties are calculated from the temperature, moisture, and degradation state using an empirical model in ICAN. Microstresses and degraded ply properties are calculated using micromechanics. Ply stresses and laminate properties are calculated using a modified composite laminate plate theory (CLPT).

CHAPTER 4

ANALYSIS

This section consists of detailed development of the models used to predict the effects of moisture, oxygen, and temperature on a composite laminate. A new method for efficiently calculating the ingress of moisture and oxygen into a laminate under complex cyclic conditions is presented. Models of the chemical reactions activated by the presence of oxygen and by elevated temperatures are incorporated into the present development. The altered material state caused by moisture and chemical reactions is predicted. The state is also expressed in a format compatible with an existing code capable of determining degraded material properties and the resulting stress states.

4.1   GEOMETRY AND ENVIRONMENT ASSUMPTIONS

The geometry assumed is a flat plate, subjected identically on its top and bottom surfaces to a spatially uniform environment. This plate has a finite (and constant) thickness, but is assumed to be infinite in width and length. All environmental effects on a plate with this geometry can be expressed as a function of one dimensional (through the laminate thickness). The external environment attacks the material uniformly at every point on both surfaces. Due to the relative speed with which a composite laminate reaches ambient temperatures, temperature through the plate is assumed to be instantaneously equal to the ambient value and constant throughout the material.

The coordinate system used to perform calculations in this investigation is depicted in Fig. 4.1. Calculations are performed at N_s number of distinct points through the laminate
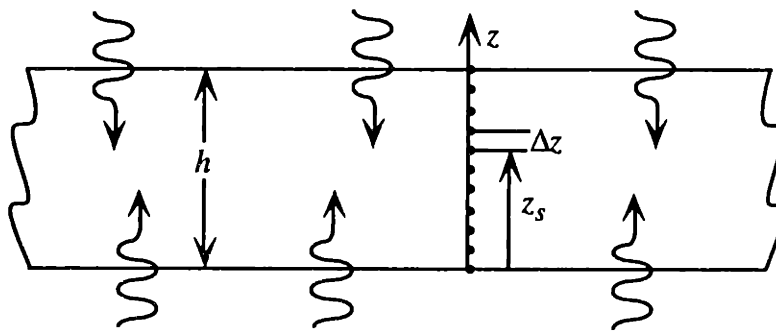
Figure 4.1: Coordinate system for one–dimensional diffusion and reaction model.

thickness. The position index is represented by s, and z_s designates a location in the laminate. The total thickness is divided into N_s-1 total segments, each of thickness Δz, where $\Delta z = z_s - z_{s-1}$. The laminate consists of N_p number of plies, divided into N_{sp} steps per ply, where $N_s - 1 = (N_{sp} - 1) * N_p$.

It has been shown that diffusion of moisture into a composite is dependent primarily on the matrix properties, while both the longitudinal and through–thickness diffusion of oxygen are enhanced by the presence of fibers. The bulk effect of these micromechanical interactions, however, can be captured by a homogenized, anisotropic value for the diffusivity of the composite. This provides the level of detail necessary to achieve an accurate model at the ply level, since fiber diameters are much smaller than a ply thickness.

Environmental exposure is modeled after typical temperatures seen at the surface of an HSCT vehicle in flight. Periods of high temperature (350°F) and low temperature (-65°F) and high and low humidity typical of real applications are included. Real structures are exposed to as many as 60,000 hours of flight time, translating to approximately 20,000 cycles. Shown in Fig. 4.2 is a test cycle with all of these conditions. This cycle is typical of the environment possible during flight, although not identical to a real flight.

An efficient analytical solution to the above problem is needed to compute moisture and oxygen concentration in laminates undergoing large numbers of complex thermal and environmental cycles. To this end, we will consider cycles including relative humidities that remain constant over specified lengths of time and temperatures that remain constant or change at a constant rate. Such cycles can be repeated an arbitrary number of times.

The cycles are designated by the system described below. Up to 100 specific times t_i in the cycle can be specified. At each time t_i, a temperature T_i is given (see Fig. 4.3). The period

40
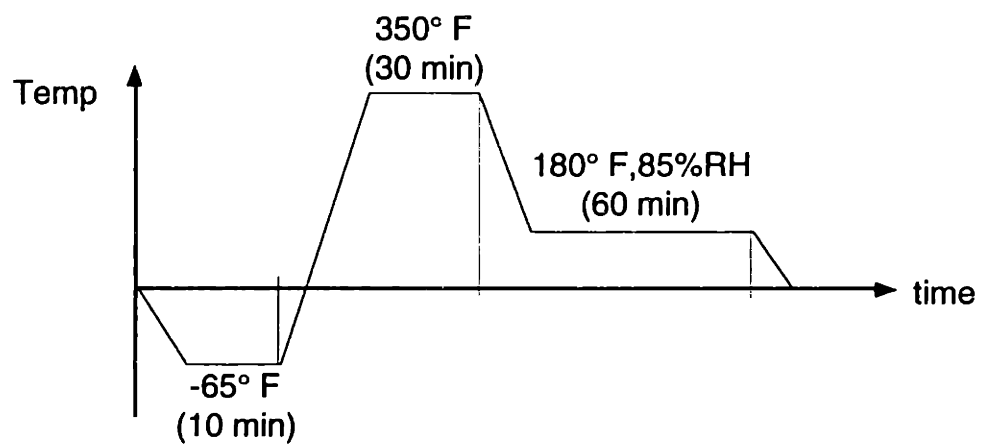
Figure 4.2: Sample environmental test cycle.

of time between t_{i-1} and t_i is referred to as interval i; a relative humidity Φ_i is specified for each interval (see Fig. 4.4). The concentration of moisture and oxygen is calculated at the end of each interval, so $C_m(z,t_i)$ is the moisture concentration at t_i. The saturation concentration value associated with the interval between t_{i-1} and t_i, when the relative humidity is Φ_i, is designated $C_{\infty i}$. Theoretical exposure to the designated cycle can be repeated an arbitrary number of times. Times during exposure are then specified by the cycle number and time in the cycle.

4.2 MOISTURE DIFFUSION

The current investigation adapts Fick's Law of diffusion to perform an analysis incorporating the effects of a cyclic environmental exposure on a material with a known initial state. Outlined below is the progression of this development for the diffusion of moisture. Given below is the tensor form of Fick's second law [8]:

$$\frac{\partial C_m}{\partial t} = \frac{\partial}{\partial x_i}\left(D_{ij}^m \frac{\partial C_m}{\partial x_j} \right)$$

(4.1)

where C_m is the concentration of moisture in the laminate, x_i and x_j denote material directions, and D_{ij}^m is the anisotropic diffusivity tensor for moisture. Due to the geometry used in this model, and the fact that exposure at the material surface is everywhere constant, we are only concerned with moisture gradients through the laminate thickness. The additional assumption that diffusivity is orthotropic eliminates the need for calculations of moisture transport along the length or width. Fick's law may therefore be simplified to its one–dimensional form:
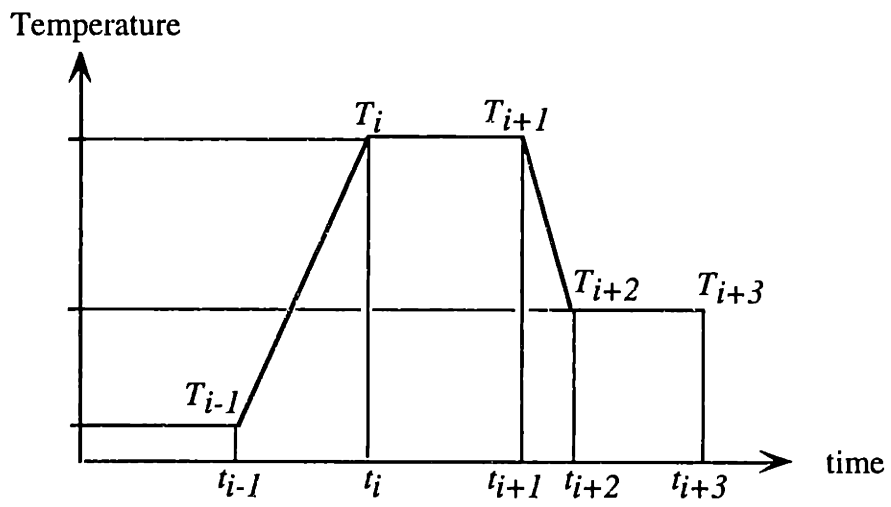
Figure 4.3: Temperature correspondence with indexed time segments.
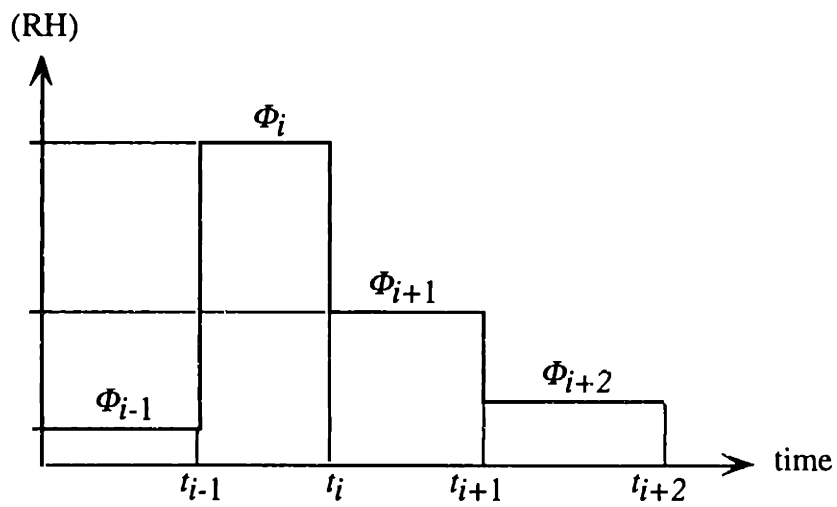
Figure 4.4: Humidity correspondence with indexed time segments.

$$\frac{\partial C_m}{\partial t} = \frac{\partial}{\partial z}\left(D_z^m \frac{\partial C_m}{\partial z} \right) \qquad (4.2)$$

where z represents through–thickness direction, and D_z^m is the corresponding component of diffusivity. It is assumed that this rate of diffusion increases exponentially with an increase in temperature [7,10,11]. This relationship can be described by an Arrhenius equation, with diffusivity reliant on the diffusion constant, D_o^m, activation energy, E_A^m, gas constant, R, and absolute temperature, T [8]:

$$D_z^m = D_o^m \exp\left[\frac{-E_A^m}{RT} \right] \qquad (4.3)$$

Temperature is always uniform through the thickness, (and E_A, D_o^m, and R are all constant in z), so Eq. 4.2 becomes

$$\frac{\partial C_m}{\partial t} = D_z^m \frac{\partial^2 C_m}{\partial z^2} \qquad (4.4)$$

In order to solve Eq. 4.4, we must first assume a solution form and define initial and boundary conditions. An acceptable solution is shown below:

$$C_m(z,t) = U + V\sin(uz)\exp(vt) \qquad (4.5)$$

where U, V, u, and v represent unknown constants to be determined via substitution into the governing differential equation and use of the initial and boundary conditions. The boundary conditions are:

$$\text{for all } t > 0,\ C_m(0,t) = C_\infty(t) \text{ and } C_m(h,t) = C_\infty(t) \qquad (4.6)$$

The quantity $C_\infty(t)$ represents the surface concentration at time t; and h represents the total thickness of the laminate. At every instant of exposure, the surface of the laminate is assumed to be saturated at the concentration corresponding to the current atmospheric relative humidity. Saturation concentration has been shown experimentally to be a function of relative humidity, Φ, and material constants A and B, which must be determined empirically [7].

$$C_\infty = A(\Phi)^B \tag{4.7}$$

4.2.1 New Method Development

In the time interval i (starting at t_{i-1}), substitution of Eq. 4.5 into 4.4 (with the boundary conditions given by Eq. 4.6) gives us a solution to the governing equation. The boundary conditions are given by the relative humidity, Φ_i, from which we can determine the saturation concentration, $C_{\infty i}$ (from Eq. 4.7). Substitution of Eq. 4.5 into Eq. 4.4 yields:

$$vV\sin(uz)\exp(vt) = -D_z^m u^2 V\sin(uz)\exp(vt)$$

$$\therefore v = -D_z^m u^2 \tag{4.8}$$

The boundary conditions (Eq. 4.6) give:

$$U = C_{\infty i}$$

and
$$U + V\sin(uh)\exp(vt) = C_{\infty i}$$

$$\therefore u = \frac{n\pi}{h}, \qquad n = 1,2,3,... \tag{4.9}$$

$$v = \frac{-n^2\pi^2 D_z^m}{h^2} \qquad\qquad n = 1,2,3,\dots \quad (4.10)$$

from the expression for v given in Eq. 4.8. In Eqs. 4.9 and 4.10, n represents the mode number. The solution is a sum of these modes. The variable V is arbitrary and its value is determined from the initial conditions. Let the term A_{ni} represent this variable for interval i and mode n, such that:

$$C_m(z,t_i) = C_{\infty i} - \sum_{n=0}^{\infty} A_{ni} \sin\left(\frac{n\pi z}{h}\right) \exp\left[\frac{-n^2\pi^2 D_z^m \Delta t_i}{h^2}\right] \qquad (4.11)$$

where Δt_i is the duration of interval i, $\Delta t_i = t_i - t_{i-1}$. The initial state of the material before the first interval we define as

$$C_m(z,0) = C_{mo}(z) \qquad\qquad (4.12)$$

By substituting Eq. 4.12 into 4.11 for $t = 0$ and exploiting the orthogonality of the sine function, we find [66]:

$$A_{n1} = \frac{2}{h}\int_0^h (C_{\infty 1} - C_{mo}(z))\sin\left(\frac{n\pi z}{h}\right) dz \qquad (4.13)$$

For interval i, we can use the solution at t_i as the initial condition. The general form for A_{ni} is then:

$$A_{ni} = \frac{2}{h}\int_0^h (C_{\infty i} - C_m(z,t_{i-1}))\sin\left(\frac{n\pi z}{h}\right) dz \qquad (4.14)$$

We can theoretically find A_{no} from Eq. 4.13, then use Eqs. 4.11 and 4.14 repeatedly to find the concentration at all times of interest. This method lacks efficiency. By substituting the expression given for $C_m(z,t_i)$ in Eq. 4.11 into Eq. 4.14, it is possible to bypass recalculation of the through–thickness concentration at each time step. Substitution (Eq. 4.11 into 4.14) and rearrangement gives us an intermediate solution, where m has been introduced to designate the mode number at t_{i+1} :

$$A_{m(i+1)} = \frac{2}{h} \left\{ \begin{array}{l} \int\limits_0^h \left(C_{\infty(i+1)} - C_{\infty i} \right) \sin\left(\frac{m\pi z}{h} \right) dz + \\[2mm] \int\limits_0^h \sum\limits_{n=0}^\infty A_{ni} \sin\left(\frac{n\pi z}{h} \right) \sin\left(\frac{m\pi z}{h} \right) \exp\left[\frac{-n^2\pi^2 D_z^m \Delta t_i}{h^2} \right] dz \end{array} \right\}$$

(4.15)

If we define W_n such that

$$W_n = A_{ni} \exp\left[\frac{-n^2\pi^2 D_z^m \Delta t_i}{h^2} \right]$$

(4.16)

The orthogonality of the sine function enables simplification of the second integral in Eq. 4.15:

$$\int\limits_0^h \sum\limits_{n=0}^\infty W_n \sin\left(\frac{m\pi z}{h} \right) \sin\left(\frac{n\pi z}{h} \right) dz = \left\{ \begin{array}{ll} 0 & \text{if } m \neq n \\[2mm] \dfrac{hW_n}{2} & \text{if } m = n \end{array} \right.$$

(4.17)

The first expression in equation 4.15 may be integrated explicitly, resulting in a simplified form for calculation of the new mode amplitudes:

$$A_{n(i+1)} = \frac{4}{n\pi}\left(C_{\infty(i+1)} - C_{\infty i}\right) + A_{ni}\exp\left(\frac{-n^2\pi^2 D_z^m \Delta t_i}{h^2}\right) \qquad (4.18)$$

where $\Delta t_i = t_i - t_{i-1}$, and n represents successive odd integer values. This form is useful in that it does not require the evaluation of integrals of the form of Eq. 4.14 except at the initial time step.

The previous development is appropriate for periods of constant temperature, as the moisture diffusivity, D_z^m, is constant, and can be calculated via Eq. 4.3. For the segments with changing temperatures, however, this calculation is complicated by the temperature dependence of D_z^m. The resulting variation in D_z^m invalidates the solutions above. This problem is solved by substituting Eq. 4.3 into Eq. 4.11 and defining a modified time step, $\Delta t_m{}^*$. This yields an equation for the calculation of the current moisture concentration during a temperature ramp:

$$C_m(z,t) = C_{\infty i} - \sum_{n=0}^{\infty} A_{ni}\sin\left(\frac{n\pi z}{h}\right)\exp\left[\frac{-n^2\pi^2 D_o^m \Delta t_m^*}{h^2}\right] \qquad (4.19)$$

where

$$\Delta t_m^* = \int_{t_{i-1}}^{t}\exp\left[\frac{-E_A^m}{RT(t)}\right]dt \qquad (4.20)$$

If the humidity and temperature exposure periods are repeated (cycled), we can calculate the values of $\Delta t_{m(i)}^*$ for each segment prior to doing the cyclical calculations

$$\Delta t_{m(i)}^* = \int_{t_{i-1}}^{t_i}\exp\left[\frac{-E_A^m}{RT(t)}\right]dt \qquad (4.21)$$

and Eq. 4.18 becomes

$$A_{n(i+1)} = \frac{4}{n\pi}\left(C_{\infty(i+1)} - C_{\infty i}\right) + A_{ni}\exp\left(\frac{-n^2\pi^2 D_o^m \Delta t_{m(i)}^*}{h^2}\right) \qquad (4.22)$$

This allows easy calculation of moisture concentrations for each segment. The coefficients A_{ni} are found by progressive application of Eq. 4.22, and then the concentration at any time can be found from Eq. 4.19. The calculations are repeated for as many cycles as needed.

The total moisture absorbed by the laminate, or weight gain, is calculated by averaging the specific moisture concentration across the laminate thickness. Integration of Eq. 4.19 in the interval $0<z<h$ and normalization by h gives an equation for the total moisture in the laminate in the time interval, Δt_i:

$$C_m(t) = C_{\infty i} - \sum_{n=0}^{\infty}\frac{2}{n\pi}A_{ni}\exp\left[\frac{-n^2\pi^2 D_o^m \Delta t_i}{h^2}\right] \qquad (4.23)$$

4.3 OXIDATIVE DIFFUSION AND REACTIONS

Here, a model based on previous work is used to calculate degradation of the matrix caused by high temperatures and the presence of oxygen. Oxygen diffusing into the material reacts with the matrix. Thermal reactions occur simultaneously. These reactions result in loss of mass from the matrix, and a degradation of material properties. A complete investigation into the various effects of these reactions is given in reference [42]. Given below is a mathematical development of the equations governing this behavior and the design of a computationally efficient model.

50

The development for the diffusion of oxygen is similar to that of moisture, with a few notable differences. An additional factor is necessary in the application of Fick's law to account for consumption of the diffusing oxygen by chemical reactions. This value, r_{ox}, is expressed in terms of an amount of the diffused substance consumed per unit time. The one–dimensional Fick's law describing this behavior is given by:

$$\frac{\partial C_{ox}}{\partial t} = \frac{\partial}{\partial z}\left(D_z^{ox}\frac{\partial C_{ox}}{dz}\right) - r_{ox} \tag{4.24}$$

where C_{ox} is the concentration of oxygen in the material. A dimensionless form for the concentration is used, rather than a change in mass due to the ingress of oxygen, which is difficult to measure. The material is saturated when $C_{ox}=1$. The boundary condition is assumed to be $C_{ox\infty}=1$ always. The through–thickness component of the diffusivity of oxygen, D_z^{ox}, is dependent on temperature and empirically determined constants, D_0^{ox} and E_A^{ox}.

$$D_z^{ox} = D_0^{ox}\exp\left(\frac{-E_A^{ox}}{RT}\right) \tag{4.25}$$

The additional factor necessary to account for the reacting substance makes solving Fick's law a more difficult problem. An approximate solution is used in this analysis, adjusting the development outlined for moisture to incorporate the consumption factor. If we assume that r_{ox} is relatively small in each interval, we can ignore the inhomogeneity in the governing differential equation, 4.24. We can then use the solution derived for moisture diffusion, subtracting a term representing the total concentration of oxygen consumed by reactions during the interval i, r_{ox}^*:

$$C_{ox}(z,t_i) = 1 - \sum_{n=0}^{\infty} B_{ni} \sin\left(\frac{n\pi z}{h}\right) \exp\left[\frac{-n^2\pi^2 D_z^{ox} \Delta t_i}{h^2}\right] - r_{ox}^*$$

(4.26)

where B_{ni} is the amplitude of each mode, n, calculated by the same method as shown above. The form of the Fourier transform used for calculation of each mode coefficient is given by:

$$B_{n(i+1)} = \frac{2}{h} \int_0^h \left(1 - C_{ox(i)}(z)\right) \sin\left(\frac{n\pi z}{h}\right) dz$$

(4.27)

where $C_{ox(i)}(z)$ represents the concentration of oxygen through the laminate thickness at t_i, and $B_{n(i+1)}$ is the amplitude used in calculating the concentration at t_{i+1}. Substitution similar to the previous method gives a somewhat simplified form for the modal amplitudes:

$$B_{n(i+1)} = B_{ni} \exp\left[\frac{-n^2\pi^2 D_z^{ox} \Delta t_i}{h^2}\right] + \frac{2}{h} \int_0^h r_{ox}^* \sin\left(\frac{n\pi z}{h}\right) dz$$

(4.28)

Eqs. 4.26 and 4.28 are applicable for periods of constant temperature exposure to oxidative environments. For segments with changing temperature, we can define a modified time step, $\Delta t_{ox(i)}^*$, which may be substituted for Δt_i in the same manner as outlined for moisture, giving:

$$C_{ox}(z,t_i) = 1 - \sum_{n=0}^{\infty} B_{ni} \sin\left(\frac{n\pi z}{h}\right) \exp\left[\frac{-n^2\pi^2 D_o^{ox} \Delta t_{ox(i)}^*}{h^2}\right] - r_{ox}^*$$

(4.29)

and

$$B_{n(i+1)} = B_{ni} \exp\left[\frac{-n^2\pi^2 D_o^{ox} \Delta t_{ox(i)}^*}{h^2}\right] + \frac{2}{h} \int_0^h r_{ox}^* \sin\left(\frac{n\pi z}{h}\right) dz$$

(4.30)

52

where

$$\Delta t^*_{ox(i)} = \int_{t_{i-1}}^{t_i} \exp\left[\frac{-E_A^{ox}}{RT(t)}\right] dt$$

(4.31)

This method of calculating oxygen concentration is developed in order to simplify and speed the computational process. However, the reactions occurring in the material are concentration dependent, necessitating calculation of oxygen concentration at each time step in order to predict the resulting reactions with the material. Oxygen diffusion is calculated using Eqs. 4.29 and 4.30 alternately. The integral in the expression for the mode amplitudes, $B_{n(i+1)}$, is evaluated explicitly by numerical integration at each interval.

4.3.1 Reaction Chemistry

Recent work by McManus and Chamis [54] identified two categories of material changes at elevated temperatures: additional cross–linking of polymer chains and degradation resulting in mass loss. Post–manufacturing cross–linking in the polymer chains is associated with an initial improvement in material properties. The current analysis has concentrated on degradative chemical effects, and will include only the reactions causing mass loss.

Reactions were modeled by Arrhenius–type equations, with each reaction defined by a unique reaction rate and activation energy [42]. For the purpose of this analysis, the matrix is assumed to be composed of several mass components. These components, y_k, are each a fraction of the total local mass, m_o such that

$$y_k = \frac{m_k}{m_o}$$

(4.32)

53

where m_k is the mass that would be lost upon completion of the set of reactions involving component k.

A reaction completeness metric, α, has been introduced to record the progress of the reactions. Each reaction is designated by subscripts k and l, such that α_{kl} represents the completeness of reaction l on component k.

If all reactions in a specific mass fraction, y_k, are summed, m_k would be zero when the aggregate reaction metric for that component, α_k, reaches a value of one. To find a form for this mass loss metric, we must first integrate the reaction rate (given in Eq. 4.36) over the time period of interest, giving a metric of the completeness of each reaction acting on each component of the material:

$$\alpha_{kl} = \int_0^t \frac{\partial \alpha_{kl}}{\partial t} dt \tag{4.33}$$

The reaction metric for all degradative reactions on each component of the material is found by summation over the reactions causing mass loss:

$$\alpha_k = \sum_{\text{all } l} \alpha_{kl} \tag{4.34}$$

It has proven useful in this analysis to express the material lost as a fraction of the original mass. In notation consistent with that used by McManus and Chamis, we define a metric, b, such that:

$$b = \sum_{\text{all } k} y_k \alpha_k \tag{4.35}$$

54

Formally, b is defined as the change in mass due to degradative reactions normalized by the total original mass of the material.

The progress of all potential reactions is modeled as:

$$\frac{\partial \alpha_{kl}}{\partial t} = C_{ox}^{m_{kl}} (1-\alpha_k)^{n_{kl}} k_{kl} \exp\left[\frac{-E_{Akl}}{RT}\right] \qquad (4.36)$$

where $\dfrac{\partial \alpha_{kl}}{\partial t}$ represents each reaction rate, T the absolute temperature, and exponents n_{kl} and m_{kl} the order of the reaction kinetics and the order of the concentration dependency, respectively. The concentration of oxygen is designated by C_{ox}, the reaction rate by k_{kl}, and the activation energy by E_{Akl}. In general, each reaction has a unique set of these constants.

The aforementioned oxygen consumption factor, r_{ox}^*, must be recalculated at each time interval, as it is a function of the reaction rate of all the oxygen dependent reactions acting on the material. In the notation introduced by Cunningham [42],

$$r_k = \sum_{\text{all } l} R_{kl} \frac{\partial \alpha_{kl}}{\partial t} \qquad r_{ox}^* = \sum_{\text{all } k} r_k \Delta t_i \qquad (4.37)$$

where R_{kl} are empirical constants, representing the amount of oxygen required to bring the reaction l to completeness in the given material component k, expressed as fractions of the saturation value.

In order to implement the method outlined above, let us assume the concentration of oxygen at time t_o, $C_{ox}(z,t_o)$, is zero everywhere. The completenesses of all reactions, α_{kl}, are also zero. We can calculate the concentration of oxygen in the first interval, Δt_1, using

Eq. 4.29, and the reaction rate using Eq. 4.36. The oxygen consumption factor depends only on the reaction rate of the oxygen dependent reactions; by multiplying this rate by the constant, R_{kl}, and summing over all material components available to the oxidative reactions, we find a value for the amount of oxygen used in chemical reactions during the first interval. This process is applicable for all intervals involving a constant temperature.

For intervals where the temperature is ramped, we must introduce a set of adjusted time steps, $\Delta t^{*}_{rxn(i)}$, for each reaction.

$$\Delta t^{*}_{rxn(i)} = \int_{t_{(i-1)}}^{t_{(i)}} \exp\left[\frac{-E_{Akl}}{RT(t)}\right] dt \qquad (4.38)$$

The oxygen concentration is calculated using Eq. 4.29. The reaction rates are found by discretizing Eq. 4.36 into a change in reaction metric over the time interval, to simplify analysis and facilitate calculations.

$$\Delta\alpha_{kl(i)} = C_{ox}^{m_{kl}} (1 - \alpha_k)^{n_{kl}} k_{kl} \Delta t^{*}_{rxn(i)} \qquad (4.39)$$

The completeness of each reaction at time t_i is then given by

$$\alpha_{kl(i)} = \alpha_{kl(i-1)} + \Delta\alpha_{kl(i)} \qquad (4.40)$$

Eqs. 4.34 and 4.35 can be used to derive the aggregate completeness metric, α_k, and the mass loss metric, b. The consumption of oxygen is found using a slightly modified form of Eqs. 4.37:

$$r_k = \sum_{\text{all } l} R_{kl} \frac{\Delta \alpha_k}{\Delta t_i} \qquad r_{ox}^* = \sum_{\text{all } k} r_k \Delta t_i \qquad (4.41)$$

The oxygen concentration calculated in Eq. 4.29 is spatially dependent, as is progress of the concentration dependent reactions (see Eq. 4.36). The reaction rate (Eq. 4.36), and therefore the completeness metric, α_{kl} (Eq. 4.34), are consequently also functions of z. (Additional temperature dependent reactions are bulk reactions, and therefore constant through the laminate thickness.) And since the mass loss metric, b, is calculated by summing the completeness metric for all reactions and all material components, it also varies through the thickness. This allows us to discretize the degradation through the laminate into a ply–by–ply analysis.

The total mass loss across the laminate thickness requires averaging the mass loss metric, b, over the interval $0 < z < h$. Due to the complexity of the necessary calculations, this integration is approximated using simplified numerical methods. The total mass loss is calculated using Eq. 4.42.

$$b_{tot} = \frac{1}{N_s} \sum_{n=1}^{N_s} b_n - \frac{b_1 + b_{N_s}}{2} \qquad (4.42)$$

4.4 STRESS STATE

An available code capable of handling all of the above effects, a modification of the Integrated Composites Analyzer (ICAN) [54], is used to do these calculations. In order to predict the stresses and strains that result from these environmental effects, output is formatted to act as an input deck for ICAN. The diffusion and reaction code requires a properly formatted ICAN input file as a starting point. Moisture concentration and

degradation values per ply at user specified times during exposure are inserted into the appropriate row and column by the diffusion and reaction code.

To input values into ICAN, we must translate the through–thickness specific moisture concentration C_m and mass loss metric b into a ply–by–ply form. Figure 4.5 shows the through–thickness cross section of a laminate made up of N_p plies each of thickness t_{ply}. The average moisture concentration in ply n at time t is:

$$\overline{C}(ply_n, t) = \frac{1}{t_{ply}} \int_{(n-1)*t_{ply}}^{n*t_{ply}} C_m(z,t)dz \tag{4.43}$$

The form used for calculating specific moisture concentration (4.29) is complicated, making calculation of a definite integral on this expression difficult. Instead, $C_m(z,t)$ is evaluated at discrete points z_s.

The expression $C_s(t)$ is used here to represent $C_m(z=z_s,t)$. Equation 4.43 becomes a numerical integral. For a laminate of N_p total plies divided into N_s-1 steps of equal size, Δz, with N_{sp} representing the number of steps per ply,

$$\overline{C}_m(ply_n, t) = \frac{1}{N_{sp} - 1} \sum_{s=N_{sp}(n-1)}^{N_{sp}(n)} C_s(t) - \frac{C_{N_{sp}(n)} - C_{N_{sp}(n-1)}}{2} \tag{4.44}$$

The computer code includes a user determined option to calculate the average at a specific point in the exposure (cycle number and interval index) or at the end of exposure.
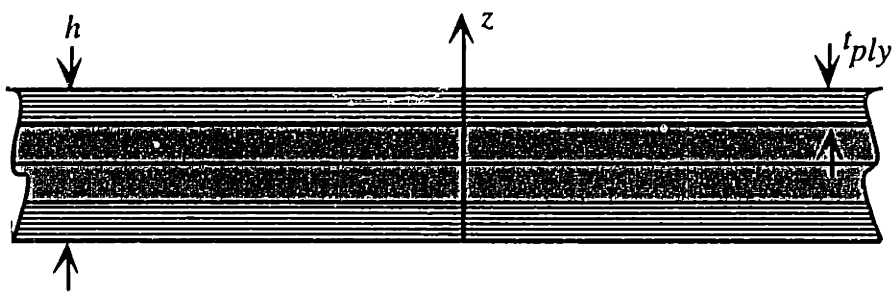
Figure 4.5: Cross section of laminate with four plies ($N_p = 4$).
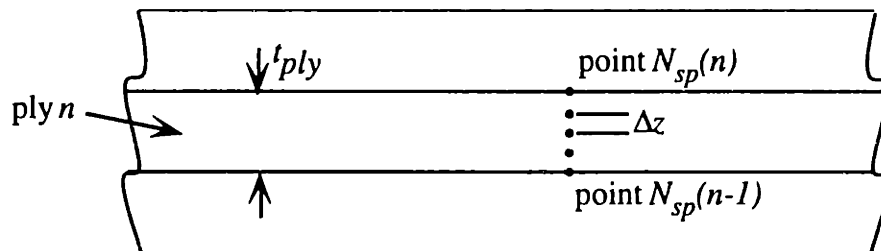
Figure 4.6: Coordinate system for ply–by–ply averaging calculations.

A similar method is employed for calculating the average degradation in each ply in terms of the mass loss metric, b.

$$b(ply_n, t) = \frac{1}{N_{sp} - 1} \sum_{s=N_{sp}(n-1)}^{N_{sp}(n)} b_s - \frac{b_{N_{sp}(n)} - b_{N_{sp}(n-1)}}{2} \tag{4.45}$$

Calculation of stresses requires two factors: changed material properties and swelling or shrinkage of the matrix. Material property changes to the matrix caused by degradation are approximated by ICAN using semi–empirical relations [53-56]. The change in glass transition temperature due to the presence of moisture is calculated using the following relation:

$$T_{GW} = \left(0.005 \cdot \overline{C}_m^2 - 0.10 \cdot \overline{C}_m + 1.0\right) \cdot T_{GD} \tag{4.46}$$

where T_{GW} is the glass transition temperature of a wet material, and T_{GD} is the dry value. The moisture concentration used is the average mosture concentration per ply calculated from Eq. 4.44.

Degraded mechanical and thermal properties due to mass loss and moisture–induced weight gain were calculated by the following relation:

$$P = P_o \cdot \left[1 - \Delta P_b(b)^{n_{P_b}}\right] \cdot \left(\frac{T_{GW} - T}{T_{GD} - T_{RT}}\right)^m \tag{4.47}$$

where P is the degraded property, P_o is the original property, T is the current temperature, and T_{RT} is room temperature. The exponent m has a value of 1/2 for mechanical properties (such as strength and stiffness) and $-1/2$ for thermal expansion coefficient. Values for ΔP_b and n_{P_b} are determined by fitting Eq. 4.47 to available data.

To calculate the stresses caused by shrinkage and swelling of the matrix, a comprehensive matrix constitutive relation is used. This relationship takes into account varying thermal conditions, absorbed moisture, and chemical degradation of the material:

$$\sigma_{ij} = E_{ijkl}(T, C_m, b)\left[\varepsilon_{kl} - CTE_{kl}\Delta T - \beta_{kl}C_m - \chi_{kl}b\right] \tag{4.48}$$

In Eq. 4.48, the anisotropic stiffness of the matrix, E_{ijkl}, is affected by the temperature during testing, T, the moisture concentration in the material, C_m, and the chemical state of the matrix, b. The coefficients of thermal and moisture expansion (CTE_{kl} and β_{kl} respectively) determine material expansion due to changes in temperature, ΔT, from the stress free temperature, T_o, and changes in moisture concentration from the dry condition. The degradative effects are accounted for in a coefficient of degradation induced expansion or shrinkage, χ_{kl}, a material property that predicts the stresses resulting in a chemically degraded material, given a change in mass, b.

Micromechanics are used to calculate ply properties from the degraded matrix properties and microstresses at the fiber diameter scale. Composite laminated plate theory (CLPT) is employed to find the laminate response, modified to include degradation [54]. A modified version of Eq. 4.48 substituting ply properties for matrix properties was used to find stresses at the ply level.

4.5 MODEL IMPLEMENTATION

A computer program was developed using the FORTRAN programmer's language that incorporates the above mathematical models. A user manual and the source code for this program is included in Appendix A. An algorithm outlining the computation process is

given in Fig. 4.7 Required input includes relevant material properties, ply thickness, and number of plies. This code was designed specifically for an environment with fluctuating humidity and temperature. A specification of this cycle is required, as is the number of cycles to be analyzed. It is also possible to expose the material to a humid environment for a user–defined period of time prior to cyclic exposure. Given this information, the code calculates the initial moisture and oxygen concentration in the laminate. Initial modal amplitudes for oxygen and moisture are computed from these initial values (using Eq. 4.13 and 4.27).

Computational efficiency is increased by calculating the adjusted time steps prior to repetition of the desired cycle. Each of the intervals in a specific cycle is associated with a set of values for the modified time steps, $\Delta t^*_{m(i)}$, $\Delta t^*_{ox(i)}$, and $\Delta t^*_{rxn(i)}$, necessary for concentration and reaction calculations. These values are stored in a matrix, and called upon during the cyclic analysis.

Moisture coefficients are calculated by successive application of Eq. 4.22. The specific moisture concentration is calculated by Eq. 4.19 only when requested by the user. Coefficients for oxygen concentration are calculated using Eq. 4.30, and oxygen concentration by 4.29. Finally, the progress of thermal and oxidative reactions are calculated using Eq. 4.36. Currently, three independent thermal reactions and one concentration dependent reaction are included in this model, consistent with the conclusions of Cunningham [42].

This process is repeated for each time segment in the cycle and for as many cycles as desired by the user. Results are given in several forms: through–thickness moisture and oxygen concentration and degradation at user–selected times, moisture concentration at
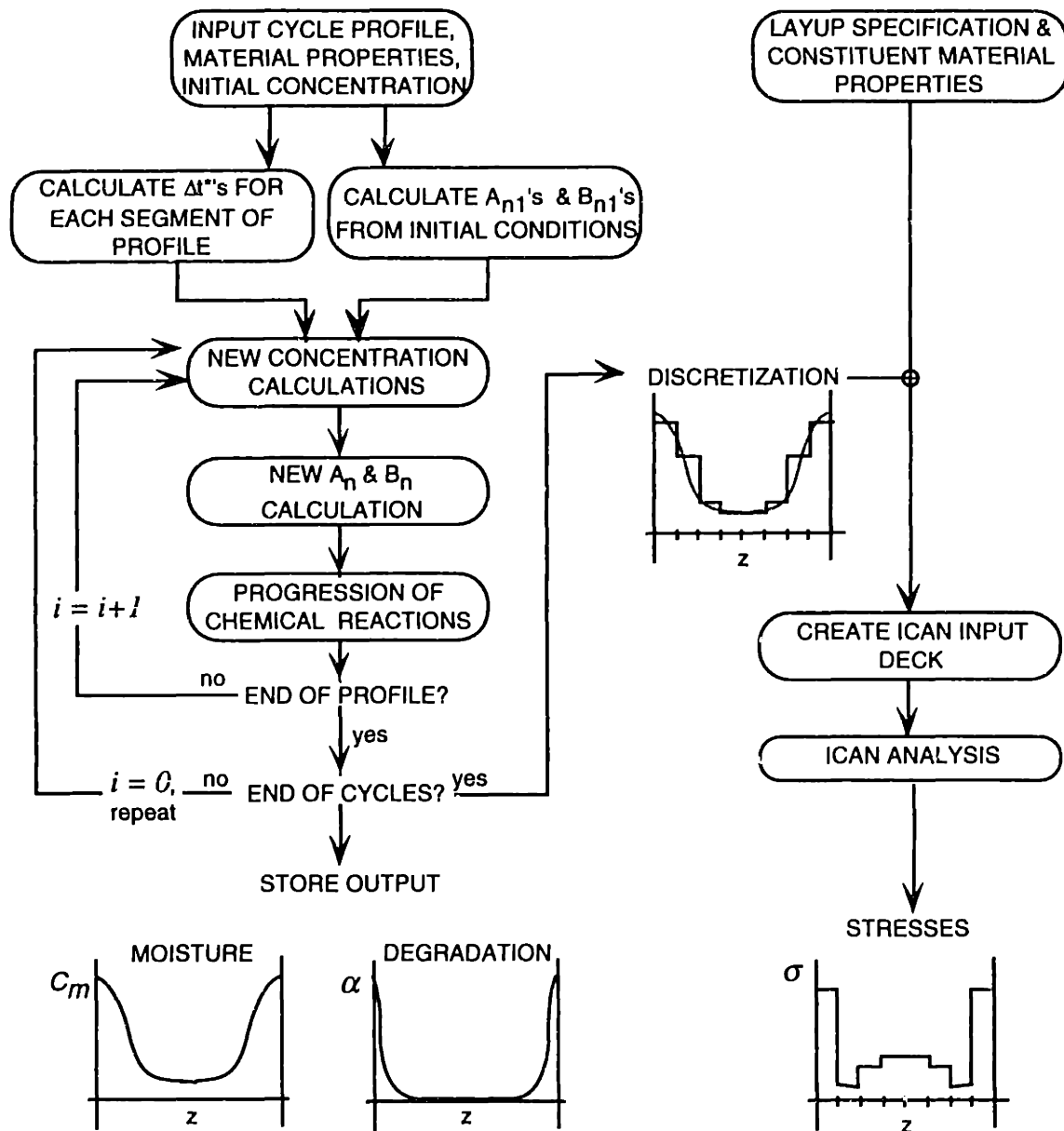
Figure 4.7: Algorithm used for calculations.

several points in the laminate, and time histories of the total weight gain due to moisture and mass loss due to degradation.

A simple technique was developed to link the program described above with an existing code in order to predict stresses and strains in the laminate resulting from degradation and the presence of moisture. The continuously varying through–thickness concentrations due to these effects are translated into ply–by–ply values and reformatted in order to take advantage of an existing analysis tool developed by McManus and Chamis [54]. This process consists of segmenting the continuous through–thickness output into averaged levels per ply. (A sample input file is given in Appendix B.) Averaged values can be at the end of exposure, or at a user–selected time during a specified cycle. Output from ICAN is in the form of degraded material, ply, and laminate properties and ply stresses and microstresses. From these predictions of stress fields in the laminate, the user may be able to determine the potential for the onset of damage.

CHAPTER 5

RESULTS AND DISCUSSION

Results predicted by the analytical model are reviewed in this section. Model predictions are compared with relevant experimental data. Trends in the results are analyzed. Parametric studies are included to investigate the changes in output resulting from varying material constants and cycles. Material degradation profiles are given for multi–cycle runs using the original and an accelerated test cycle. Stresses caused by moisture and degradation are calculated. Possible failure modes are discussed.

5.1 MATERIAL PROPERTIES

Relevant material properties for IM7/PETI-5 were supplied by The Boeing Company and McDonnell Douglas Aircraft [67]. Results from mechanical testing are reported in Table 5.1, along with temperature, moisture, and conductive properties of the material. Due to the scarceness of data, properties relating to oxygen diffusivity and reaction rates were taken from tests done on similar materials (primarily C6000/PMR-15) [42].

Figure 5.1 depicts the moisture diffusivity of IM7/PETI-5 material, measured at several temperatures. This data was provided by Northrup Grumman [67]. The temperature dependence was assumed to be of the form represented by Eq. 4.3. An exponential best fit to the data (using a tool available in the graphing program Kalaidagraph^{TM}) was used to derive the desired material properties: diffusion constant, D_o, and activation energy, E_A.

Table 5.1: IM7/PETI-5 Material Properties

E_{11}, GPa (Ksi)	Longitudinal Elasticity	A*	157.3 (22.8)
E_{22}, GPa (Ksi)	Transverse Elasticity	A	9.7 (1.4)
G_{12}, GPa (Ksi)	Shear modulus	A	4.20 (0.6)
ν_{12}	Poisson's ratio	A	0.33
G_{IC}, J/m² (Btu/in²)	Mode I critical fracture toughness (DCB)	D	1000 (6×10^{-4})
ρ, kg/m³ (lb/in³)	Density	A	1600 (0.06)
X_t, MPa (Ksi)	Tensile longitudinal strength	A	2160 (310)
X_c, MPa (Ksi)	Compressive longitudinal strength	A	1560 (230)
Y_t, MPa (Ksi)	Tensile transverse strength	A	70 (10)
Y_c, MPa (Ksi)	Compressive transverse strength	A	150 (22)
S, MPa (Ksi)	Shear strength	D	80 (12)
α_{11} $\mu\varepsilon/K$	Longitudinal coefficient of thermal expansion	A	−0.7
α_{22} $\mu\varepsilon/K$	Transverse coefficient of thermal expansion	A	36.9
k_1 W/m²K	Longitudinal thermal conductivity	A	8.65
k_2 W/m²K	Transverse thermal conductivity	D	0.35
$D_o{}^m$ mm²/s	Moisture diffusion constant	C	0.11
E_A kJ/mol	Moisture activation energy	C	35
A	Moisture saturation coefficient	B	0.013
B	Moisture saturation exponent	B	1
T_o (°F)	Cure temperature	B	600

* CODE:
A: McDonnell Douglas (IM7/PETI-5)
B: The Boeing Company (IM7/PETI-5)
C: Northrup Grumman (IM7/PETI-5)
D: estimated from similar materials
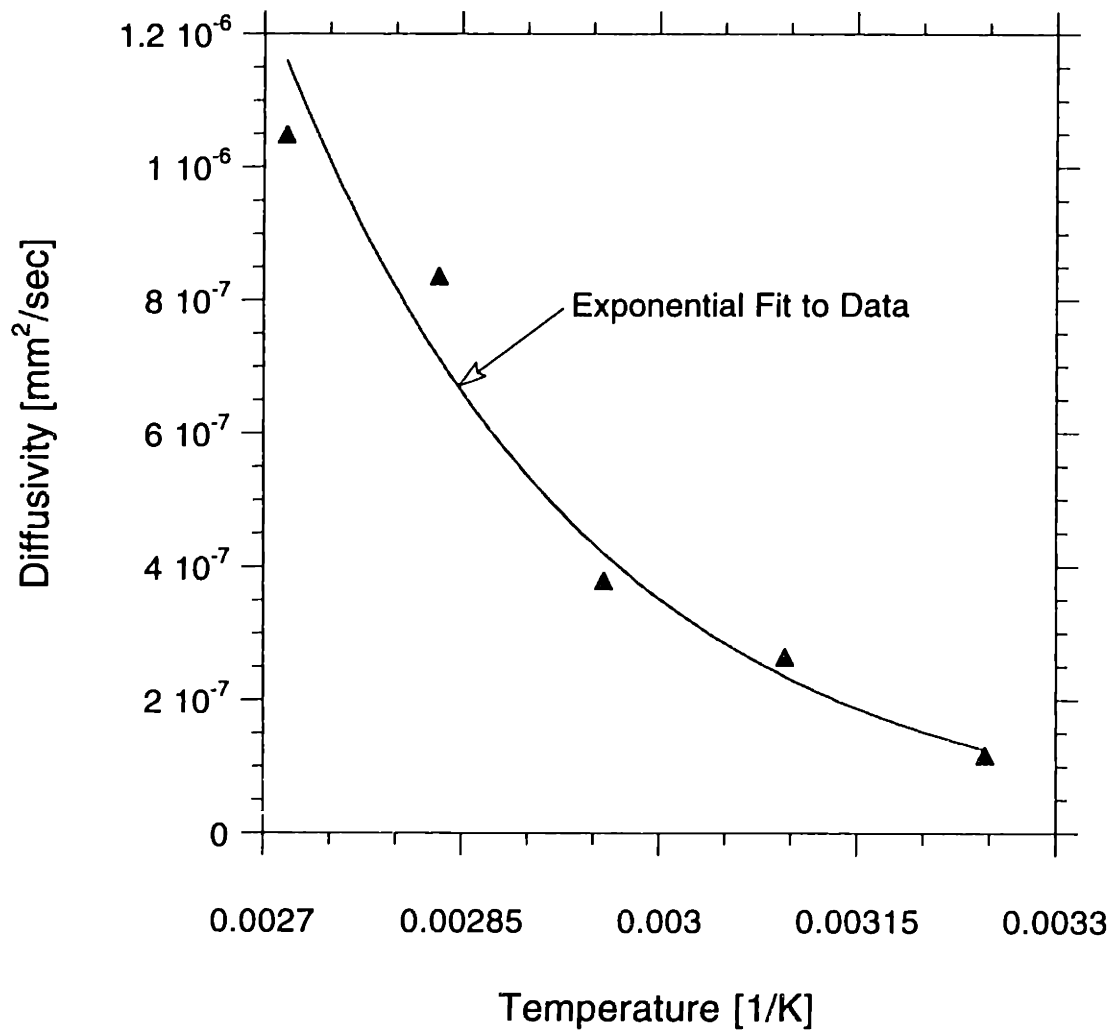
Figure 5.1: Exponential fit to diffusivity data to derive diffusion constants.

Test specimens referred to throughout this section include laminates sixteen plies thick, of unidirectional ($[0]_{16}$) or quasi-isotropic ($[0/\pm45/90]_{2s}$) lay-ups, and neat resin specimens. All results will be given assuming laminates of these geometries. Various exposure times, ranging from one to 5000 cycles, highlight different material behavior. The baseline exposure cycle used is the one given in Fig. 5.2, and will be referred to in this section as the "test cycle". Variations of this cycle are used in the parametric studies.

A normalized form of (specific) moisture concentration is presented in through-thickness plots in terms of the mass of the absorbed moisture as a fraction of the mass of the dry material. The total specific weight gain due to moisture absorption (the mass gained normalized by the dry mass) is equivalent to the average specific moisture concentration across the laminate. Degradation is reported in terms of the mass loss metric through the laminate thickness and total mass loss as a percentage of original mass. For situations involving a period of pre-exposure prior to cycling, the initial moisture condition and degradation state is calculated given the temperature, duration, and humidity of the pre-conditioning.

5.2 MOISTURE DIFFUSION

Presented below are typical model predictions of moisture concentrations given the type of cycle described earlier. Results are presented in terms of time histories of concentration at specific locations, weight change over time, or moisture concentration profiles at specific times. Times are specified by cycles elapsed, and select times within a cycle are noted by the designations t_A, t_B, and t_C on the test cycle, shown in Fig. 5.2.
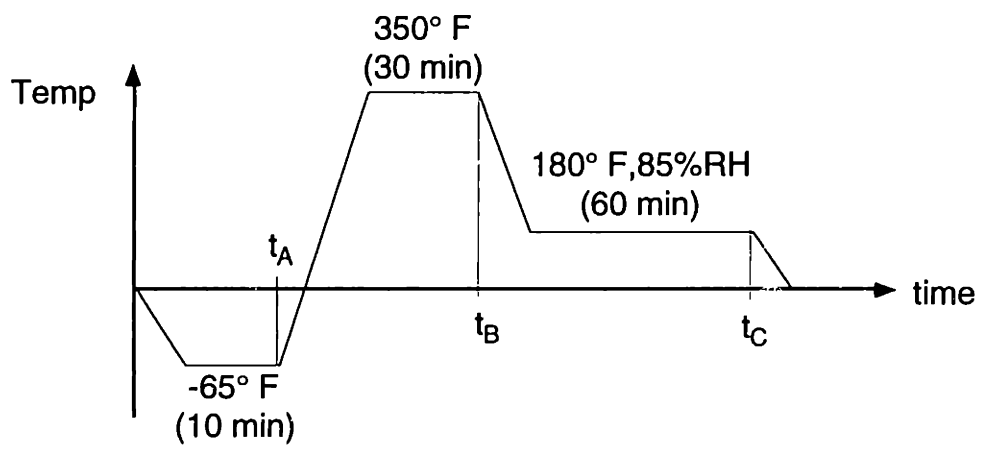
Figure 5.2: Test cycle with select times designated.

5.2.1 Trends in Moisture Sorption

Cyclic moisture exposure causes two types of response under the conditions studied. The first is fluctuation of the specific moisture concentration near the surface (shown in both Figures 5.3 and 5.4). The first time, t_A, designates the time just after cold, dry exposure. Due to the dry atmosphere, the very edge of the laminate dries out. However, little moisture diffuses out at this low temperature in the given amount of time. The hot, dry exposure just before t_B allows moisture near the surface to dry almost completely. The t_C marker designates the period just after the warm, wet exposure, when the surface is saturated. Comparison of Figures 5.3 and 5.4 shows that moisture level fluctuation near the surface continues relatively unchanged with each cycle. The second type of response is the slow soak of moisture in towards the center of the laminate. This internal behavior does not respond to the cycling; instead, we can observe a gradual change from cycle 2 (Fig. 5.3) to cycle 100 (Fig. 5.4).

Figure 5.5 shows a different perspective on these effects. Predictions of full time histories at different points in the material are shown. At the edge of the laminate, fluctuation of the moisture concentration is evident. The sharp rises and falls in moisture concentration at the edges are a result of the boundary condition defined earlier: the surface is always saturated at the current ambient humidity. At one ply thickness into the laminate, there are significant fluctuations in moisture concentration throughout each cycle. These changes are less pronounced than at the edge, and are more influenced by the temperature during the exposure period. At the center of the laminate, the slow change of moisture concentration can be seen, almost unaffected by the extreme behavior at the edges.

Both Figs. 5.6 and 5.7 show predictions of through–thickness moisture concentrations over many cycles at the point in the test cycle designated by t_B, where the surface is dry.
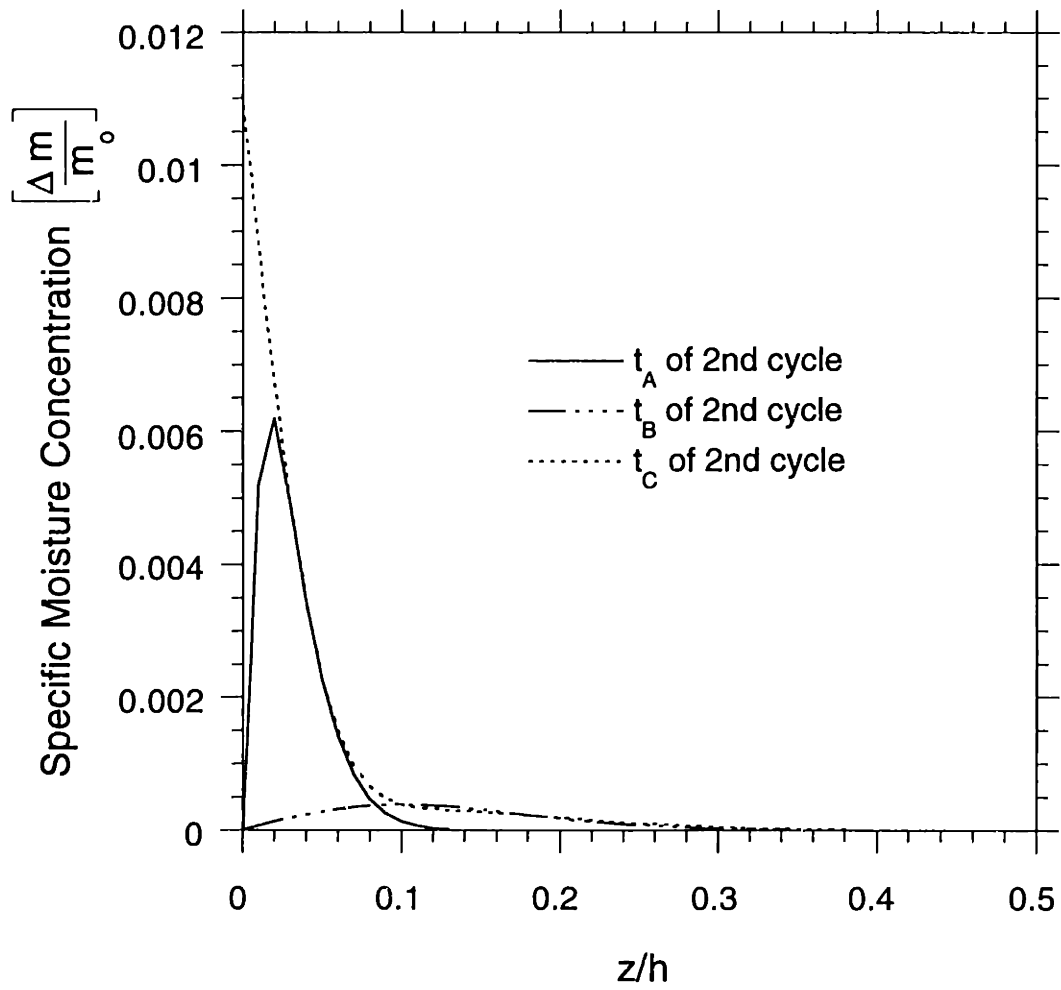
Figure 5.3: Snapshot of moisture levels at points in cycle 2.
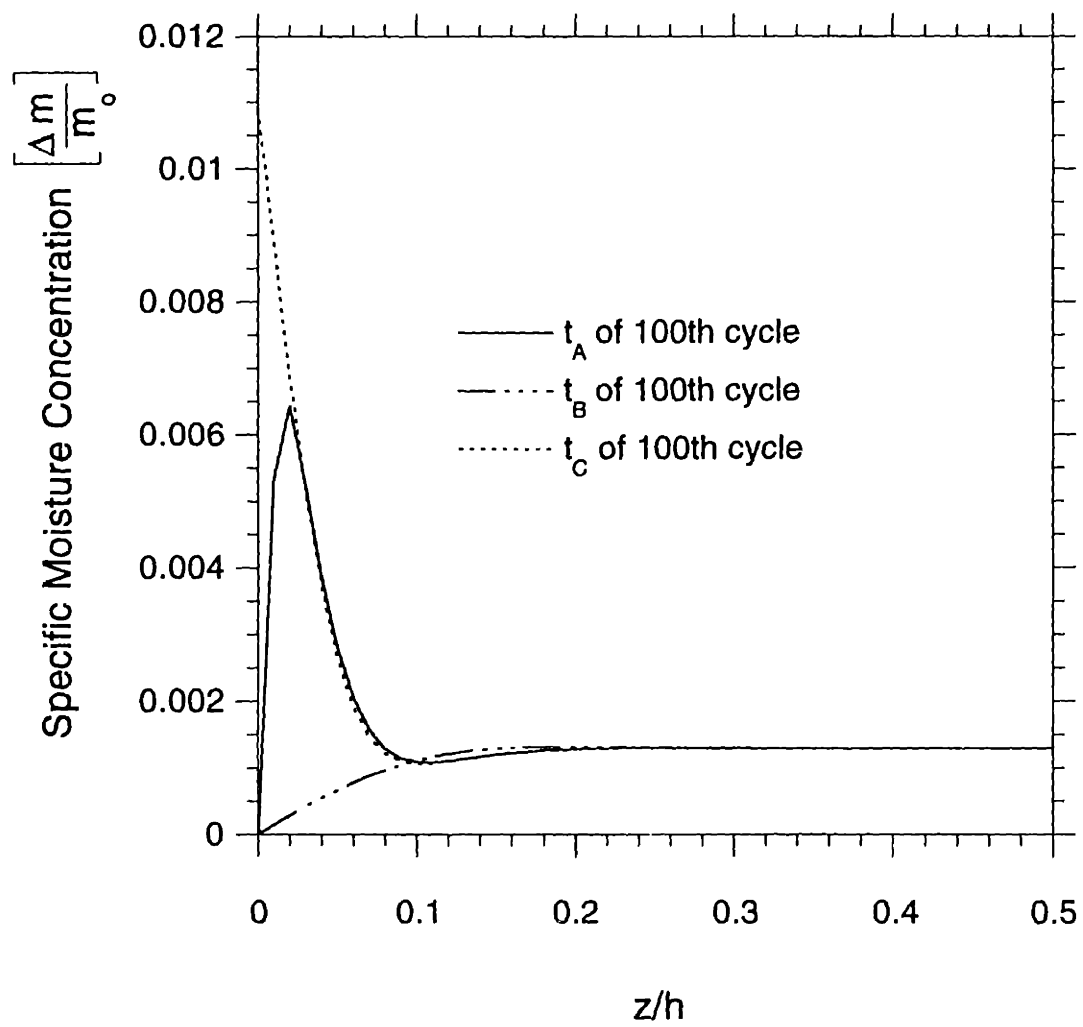
Figure 5.4: Snapshot of moisture levels at points in cycle 100.

These graphs show a pronounced gradient in the moisture concentration through the laminate thickness. The shape of this distribution changes as the moisture concentration approaches a "pseudo–equilibrium" condition. This state is characterized by an unchanging internal moisture concentration. Once this state has been reached, only the edges of the laminate experience changes in moisture concentration. The first plot, Fig. 5.6, shows an initially dry laminate exposed to the test cycle, while Fig. 5.7 shows the moisture concentrations resulting from a laminate exposed to 85%RH for 2 weeks at 160°F, then cycled. The final moisture concentrations after one hundred cycles are identical in these two plots, even though the initial conditions are different.

Output from runs with different initial conditions show similar equilibrium values in the center of the laminate. This value may be calculated using Eq. 5.1. It is simply a diffusion–rate–weighted average of the environmental conditions, and agrees with both values predicted by the full analyses and experimental data. The value predicted for the cycle shown in Fig. 5.2 and the material described in Table 1 is 0.13%.

$$
C_{eq} = \frac{\displaystyle\int_{cycle} C_{\infty} \exp\left[\frac{-E_A}{RT}\right] dt}{\displaystyle\int_{cycle} \exp\left[\frac{-E_A}{RT}\right] dt}
$$

(5.1)

The two distinct effects of moisture in the laminate under this type of cyclic exposure may be differentiated by a surface layer thickness, d_{eq}, depicted in Fig. 5.8. When $z < d_{eq}$, the primary concern is the rapid fluctuation of moisture. When $z > d_{eq}$, the dominant result is the gradual approach to an equilibrium value. An approximate method used for calculating this thickness relies on the assumption that only modes of spacial wavelength less than twice the value of d_{eq} participate in the fluctuations. These modes must have response times comparable to the period of the cyclic exposure. If we assume that the contribution
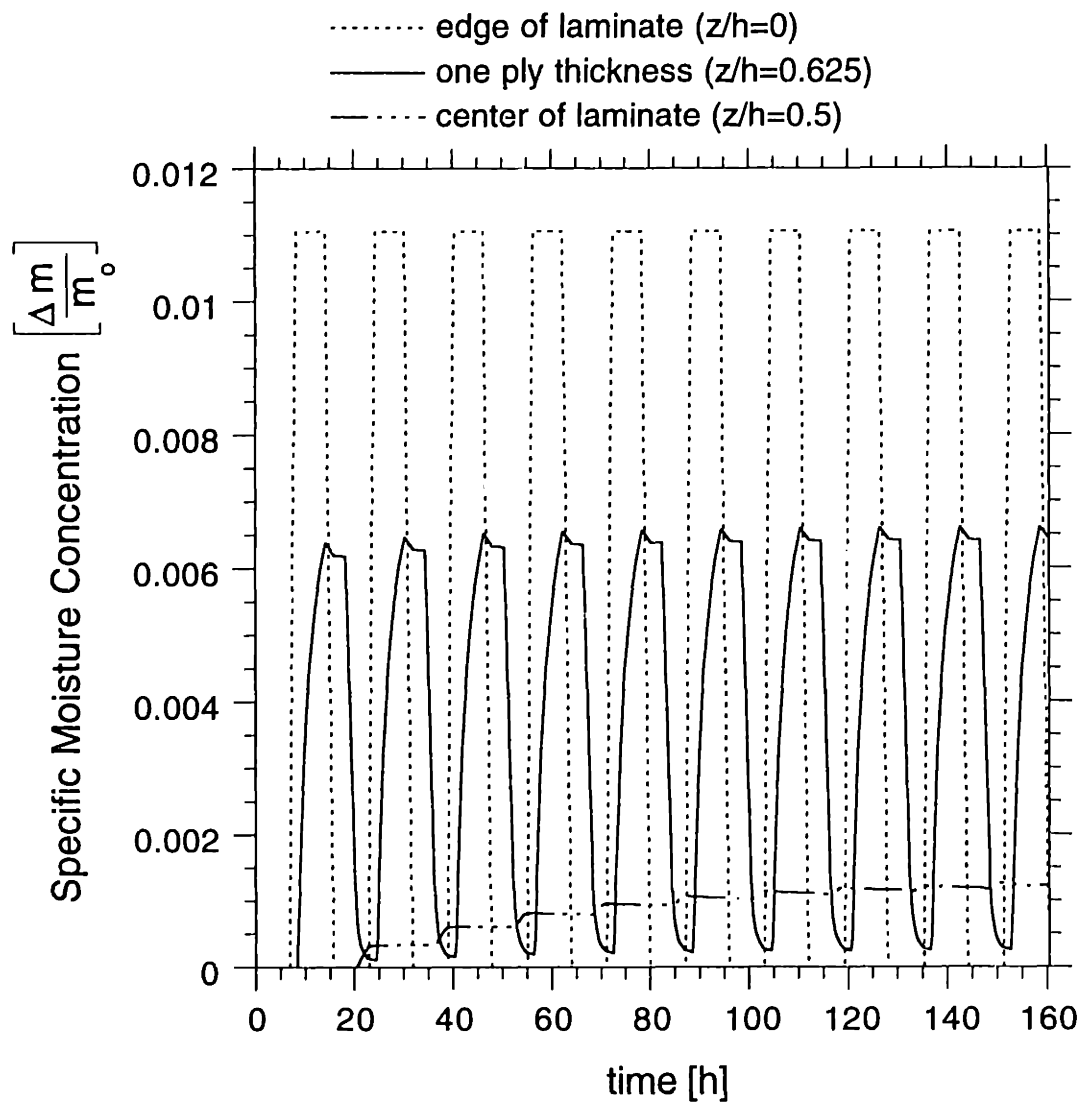
Figure 5.5: Moisture fluctuations at various points in laminate.
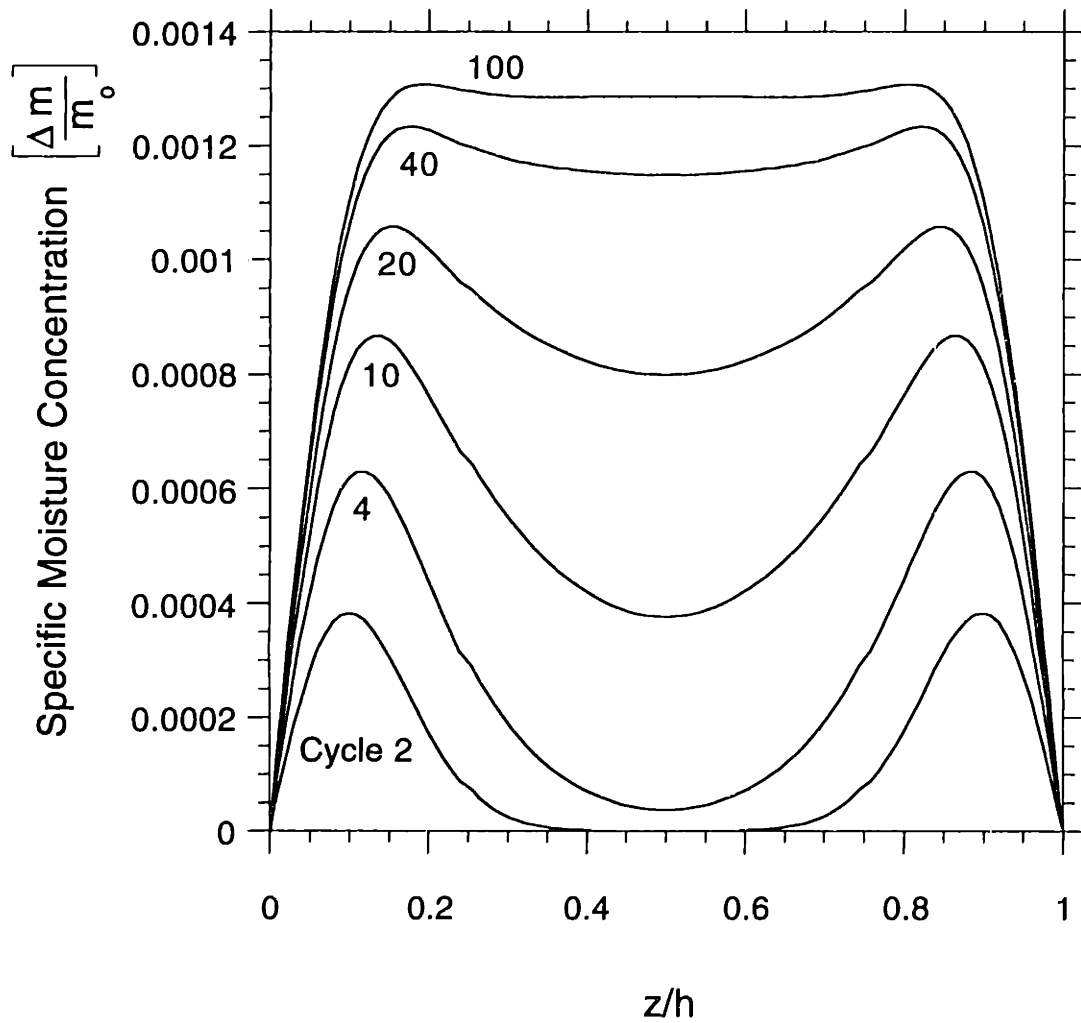
Figure 5.6: Specific moisture concentration through thickness of an initially dry 16 ply laminate at t_B in multi–cycle run.
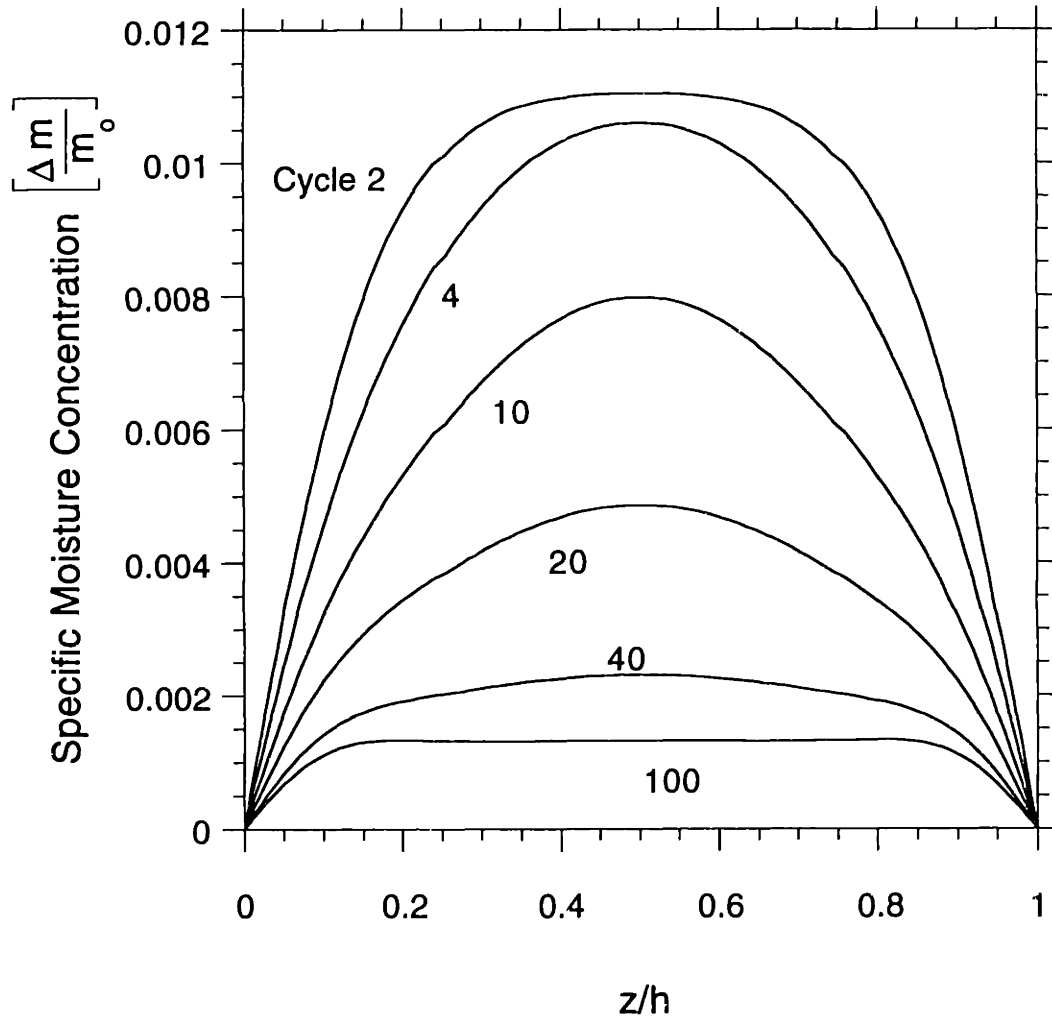
Figure 5.7: Specific moisture concentration at t_B of 16 ply laminate exposed to 85% RH for 2 weeks, then cycled.

of a mode to the cyclic response is negligible when the coefficient in Eq. 4.18 is less than $e^{-2} = 0.135$, then

$$\exp\left[\frac{-n^2\pi^2 D_o \overline{\Delta t}^*}{h^2}\right] = e^{-2} \qquad (5.2)$$

where

$$\overline{\Delta t}^* = \sum_{\text{all } i} \exp\left[\frac{E_A^m}{RT_i}\right]\Delta t_i \qquad (5.3)$$

The slowest response time, and longest spacial wavelength, mode for which this condition is met is

$$n = \frac{h}{\pi}\sqrt{\frac{2}{D_o \overline{\Delta t}^*}} \qquad (5.4)$$

If half of a spacial wavelength of this mode represents the thickness of the surface layer (suggested by the shape of the moisture concentration at t_A), the surface layer thickness can be approximated as a function only of diffusivity and adjusted time:

$$d_{eq} = \pi\sqrt{\frac{D_o \overline{\Delta t}^*}{2}} \qquad (5.5)$$

When correlated to a full analysis, this simple method tends to conservatively estimate d_{eq}. The value of the surface layer related to the cycle studied here is 0.35 mm, or 18% of the total thickness of a 16 ply laminate (see Fig. 5.8).

78

5.2.2 Total Weight Gain

During the cycle studied, there are periods of cold and dry (just before t_A), hot and dry (t_B), and hot and wet exposure (t_C). These varied conditions result in vastly different values of weight gain throughout the cycle. Figure 5.9 shows histories of the weight gain measured at t_B, at t_C, and at the end of the cycle. Even the short time allowed for the laminate to cool down after the cycle is enough to allow a large amount of moisture to diffuse out of the material. These results are significant in that they suggest that measurements of weight gain during exposure is greatly dependent on time of measurement. A specimen weighed just after the hot, wet exposure would have shown an increase in weight over fifty percent greater than a specimen weighed at the end of a cycle.

5.2.3 Parametric Studies

The plots shown in the previous section rely on several assumptions about the values of material constants and about the exposure cycle. We have used a model whose applicability is supported by both previous studies and data specific to this study. A set of parametric studies were performed in order to increase confidence in the values used and the capability of the model to predict accurate results. Two parameters were studied in detail: moisture diffusivity and temperature ramp rate.

Several other important values were not investigated. The saturation concentration is an important parameter because it scales all specific moisture concentration and weight gain predictions. A parametric study of the saturation concentration was not performed because the results would be trivial. By inspection (of Eqs. 4.19 and 4.22), a higher saturation concentration would result in more weight gain, with the same general behavior. The value used for the saturation concentration in this study was approximated from limited data.
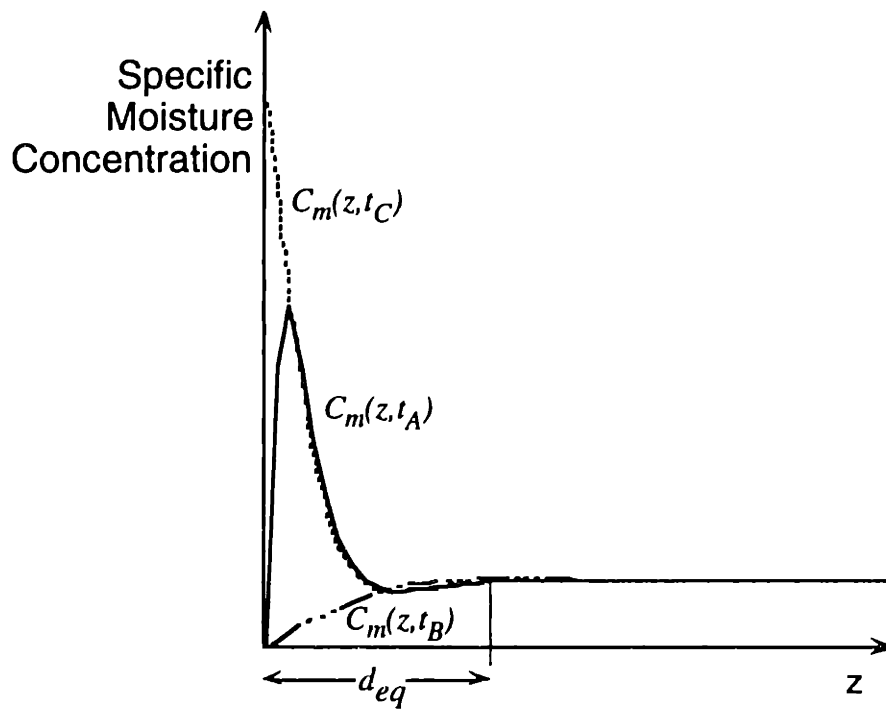
Figure 5.8 : Thickness of surface layer in which moisture fluctuations are contained.
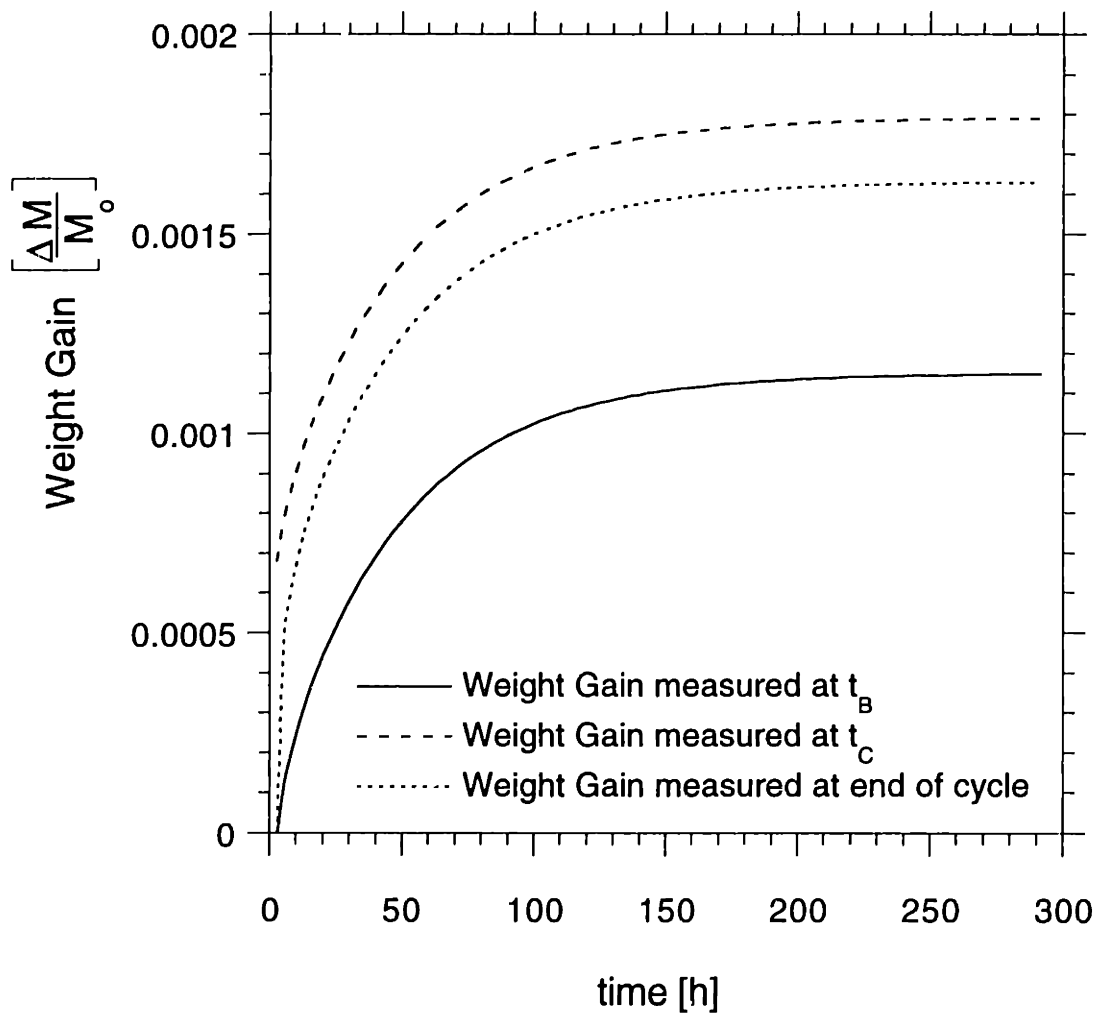
Figure 5.9: Total weight gain in laminate at t_A, t_B, and at the end of the cycle during exposure to 100 cycles.

Other parameters that were not investigated here include laminate geometry and the effect of vastly different exposure cycles. Our goal was to show that the model predicted an accurate material response for thin laminates exposed to cycles similar to the test cycle (Fig. 5.2). The current study considers this type of problem; more analysis is required for vastly different geometry and cycle specification.

A fuller set of data supports the value for diffusivity than other properties necessary for this analysis (see Fig. 5.1). To show the importance of certainty in this value, Fig. 5.10 shows the change in specific moisture concentration at the center of the laminate versus time for various values of moisture diffusivity. The material is exposed to the test cycle. It becomes clear from this plot that the diffusivity of IM7/PETI-5 lies in a critical region. A diffusivity one order of magnitude greater than the value used in the current study places the composite in a region where moisture fluctuations permeate to the center of the laminate during the test cycle. Such behavior invalidates the previous development of an equilibrium level maintained at the center of the laminate. A slower diffusivity simply requires a much longer time to reach equilibrium.

The earlier development of an expression for a surface layer in which moisture fluctuations are contained shows a dependence on the square root of the diffusion constant. For high diffusivity, this "edge zone" increases toward the center. For low diffusivities, this zone decreases and for all practical purposes ultimately disappears.

Varying the diffusivity will also effect the weight gain value; a higher diffusivity value will cause more moisture to diffuse into and out of the material during a given amount of time. Figure 5.11 shows the weight gain (measured at the end of each cycle) for a range of diffusivities.
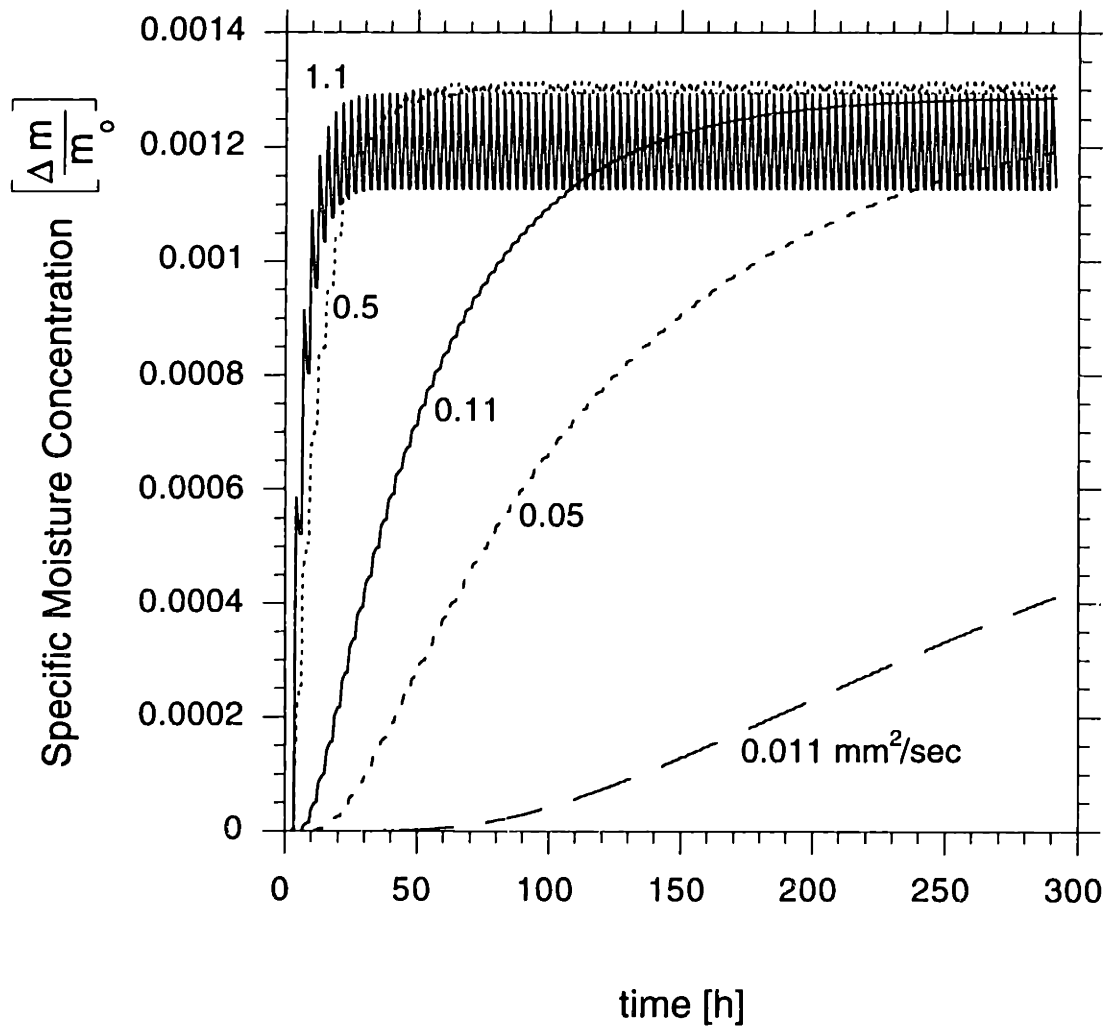
Figure 5.10: Effect of diffusivity on predicted specific moisture concentration at the center of a 16 ply laminate exposed to the test cycle.

83
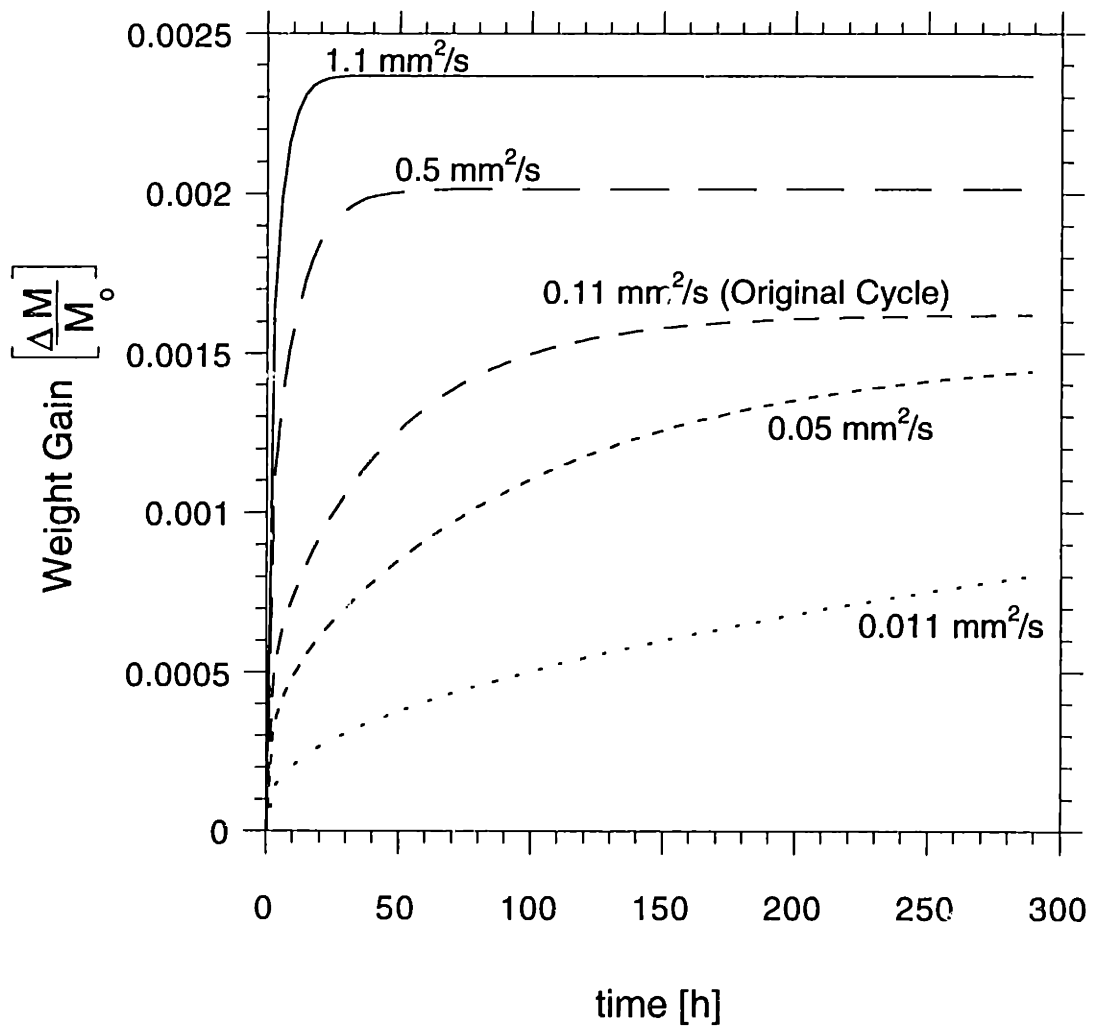
Figure 5.11: Effect of diffusivity on predicted weight gain at the end of each cycle in a 16 ply laminate exposed to the test cycle.

Another source of uncertainty lies in the rate at which temperature is ramped during the cycle. The original test cycle does not maintain a consistent ramp rate over its several temperature changes. The ramp rates in the test cycle (Fig 5.2) vary from 2°C/min to 12°C/min. Most thermocycling ovens are capable of a range of ramping rates. Figure 5.12 shows weight gain plotted against cycle number for cycles whose hold times at the constant temperatures are identical to the original test cycle, but whose temperature ramps have been varied. Each curve represents a cycle with all changes in temperature occurring at the given ramp rate. The original test cycle does not have one ramp rate, so is identified only by "Original Cycle". Altering ramp rate changes the curves slightly; the variation is due to the increase in the percentage of the total cycle time spent at the hold temperatures during each cycle as the ramp rate is increased. Varied ramp rate appears to have only a small impact on weight gain, except in the case of very slow ramp rates. A ramp rate as slow as 2°C/min effectively increases the amount of time spent at high, dry conditions so much that the equilibrium moisture concentration decreases significantly.

5.3 CHEMICAL DEGRADATION

Presented in this section are model predictions of mass loss resulting from chemical reactions in a material given the cycle shown in Fig. 5.2. Results are shown in terms of snapshots at specific times of the mass loss metric as a function of position and total mass loss during the period of exposure. Times of mass loss metric snapshots are specified by cycles elapsed. Total mass loss is given in percent change of the original mass.

85
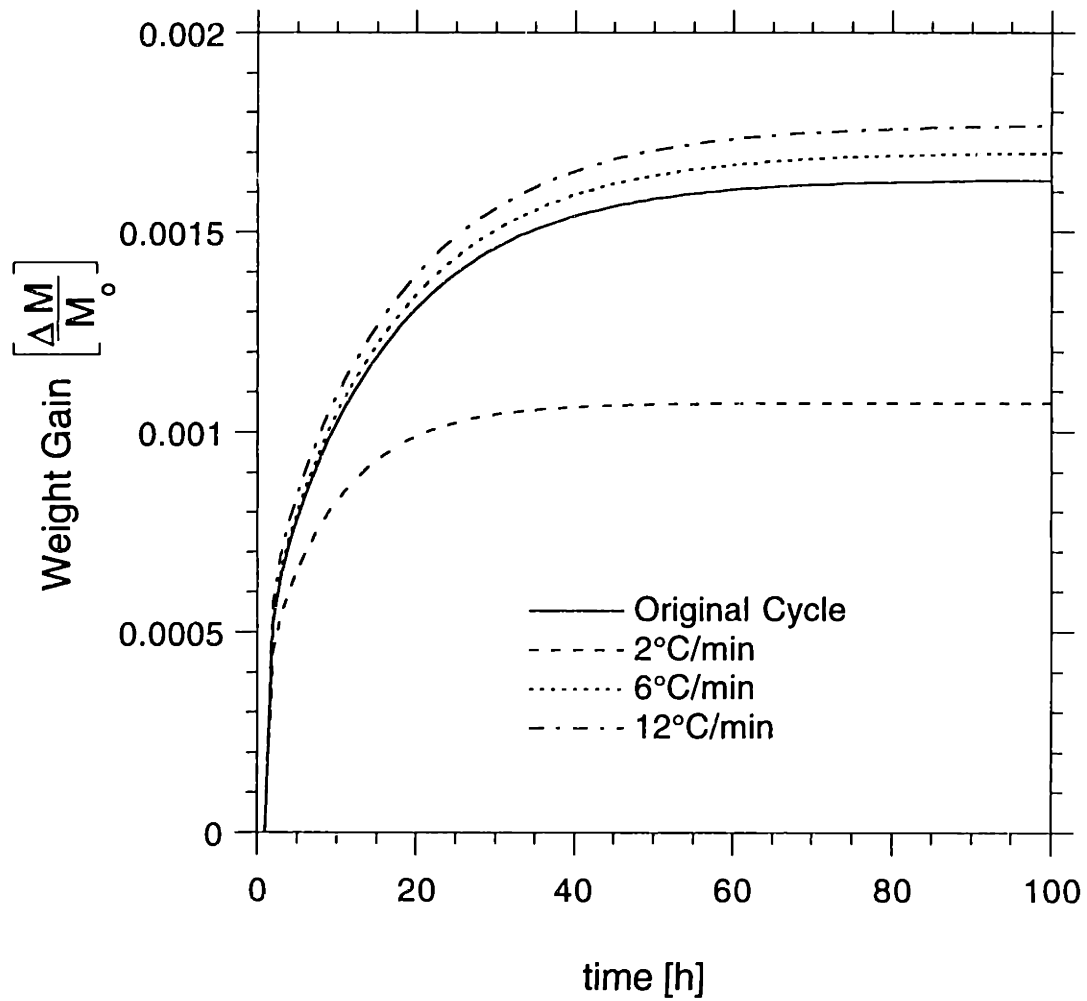
Figure 5.12: Effect of varied ramp rate on predicted weight gain at the end of each cycle in a 16 ply laminate.

5.3.1 Oxygen Diffusion and Chemical Reactions

The presence of oxygen and high temperatures in a composite activate several independent reactions in the matrix. The computer code developed for this analysis considers one oxygen dependent reaction and three thermal reactions. Experimental tests [42] which recorded the change in mass as temperature was increased showed the onset of the thermal reactions occurring at much higher temperatures than experienced in the test cycle used in the current study. For these lower temperatures, only the oxidative reaction is activated. The mass fraction available to this reaction corresponds to 16% of the material. The mass loss metric represents the progression of chemical degradation, complete when $b = 1$. Total mass loss due to chemical reactions is given as a percentage of the total original mass in order to correlate predictions with previous data.

Figure 5.13 shows a prediction of the mass loss metric through the laminate thickness after 5000 test cycles, using the material values for oxygen diffusion and reaction chemistry given in [42]. Material has degraded only a few percent at the edges, with no change in the center of the laminate. The total change in mass due to chemical reactions is shown in Fig. 5.14. The mass loss predicted by the model is small for these conditions.

5.3.2 Parametric Study

The material constants used for the analysis are for PMR-15 matrix, and may not be accurate in extrapolations to PETI-5 analysis. There are at least two ways of exploring the possibility that the PETI-5 material may be more susceptible to degradation: parametrizing the material properties or accelerating the test cycle. We have chosen not to parametrize the many diffusion and reaction constants in the absence of any data for PETI-5. By studying

Figure 5.13: Mass loss metric predicted in a 16 ply laminate exposed to 5000 test cycles.
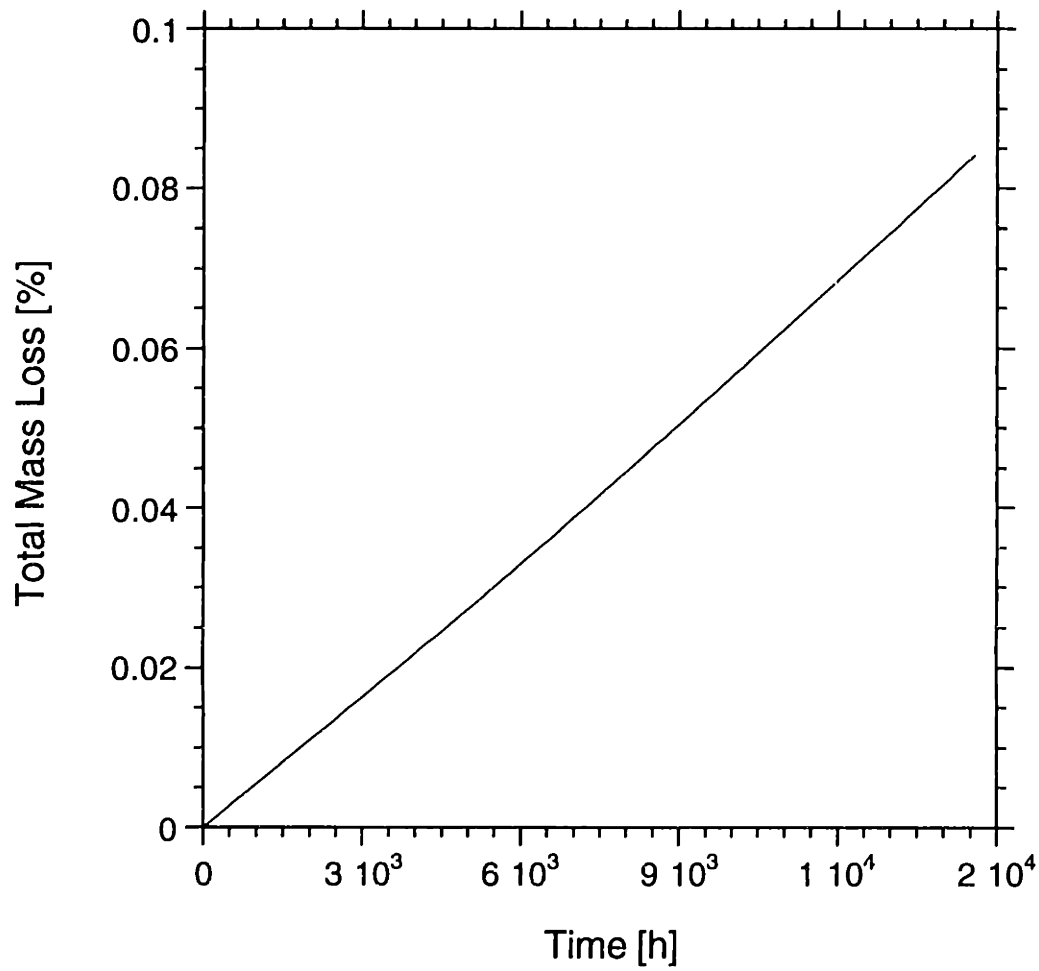
Figure 5.14: Total mass loss predicted in a 16 ply laminate over 5000 test cycles.

the effect of a temperature accelerated cycle we can investigate the results of significant material degradation. This method was chosen because temperature is a dominant factor in the chemical reactions. It also enabled us to simultaneously explore the potential of an alternate realistic exposure cycle.

Calculations were done with the same material values, but the original cycle accelerated in terms of temperature and time of exposure. The maximum temperature was 475° F (replacing the 350° F segment in the cycle in Fig. 5.2), which was held for 2.5 hours (compared with 30 minutes in the original). The cold period of exposure was omitted for this accelerated cycle because it has little impact on degradation. When the model was run simulating a 5000 cycle exposure, the mass loss shown in Figures 5.15 and 5.16 resulted. After one thousand cycles, there is significant degradation at the surface. This is in agreement with experimental observations of a visible surface layer [42]. This layer has been seen to correspond with altered material properties [38,48]. After five thousand cycles, some degradation has occurred at the center of the laminate and more mass has been lost from the material surface.

The total predicted mass loss after 5000 accelerated cycles is greater than two percent of the original material (Fig. 5.16). Continued exposure will result in additional mass loss until the mass fraction available to the active reactions is completely degraded. During the exposure period, degradation first occurs at a constant high rate. This initial period of linearly increasing mass loss can be attributed to the unlimited amount of oxygen at the surface of the material available for reactions. After the material at the surface degrades, oxygen must diffuse into the material before reactions can progress, slowing the reaction rate. After approximately 3000 hours, mass loss appears to settle down to a slower rate, controlled by diffusion.
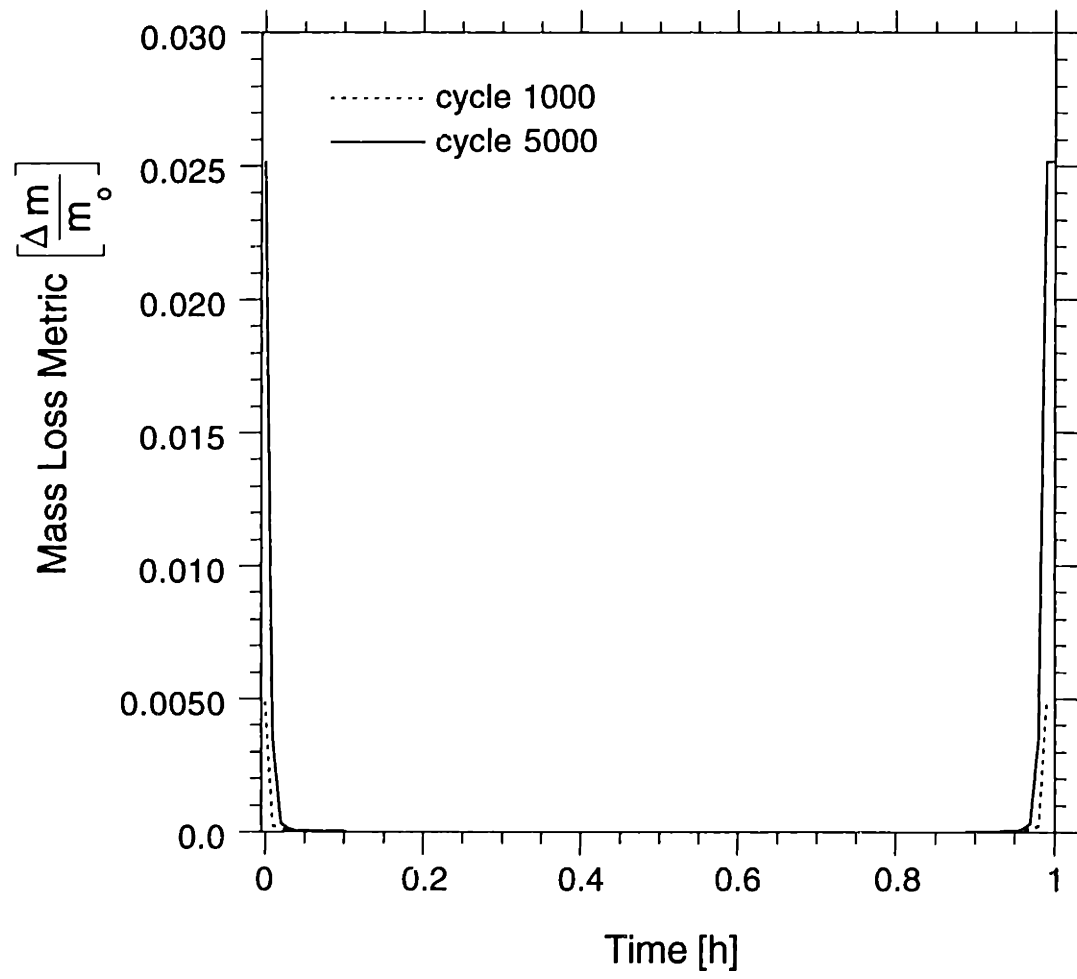
90
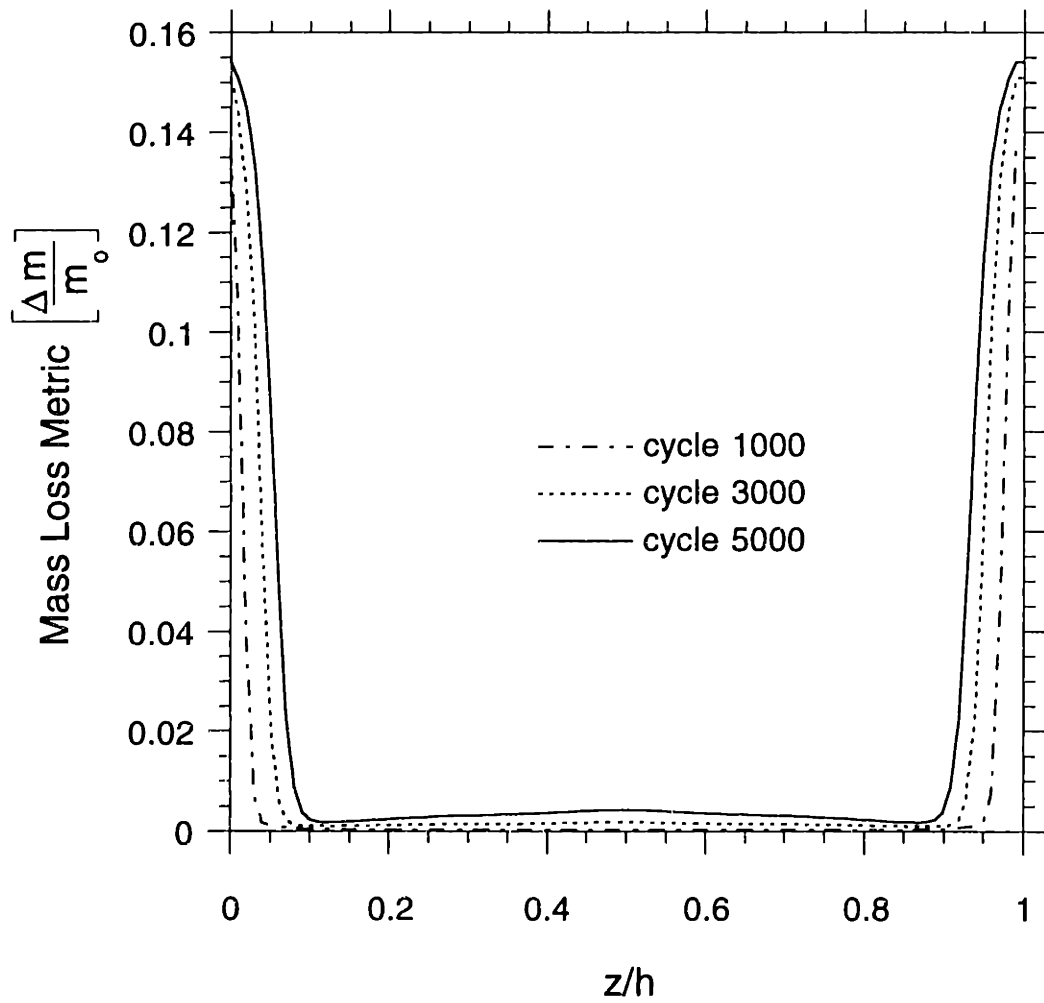
Figure 5.15: Mass loss metric in a 16 ply laminate exposed to 5000 accelerated cycles.
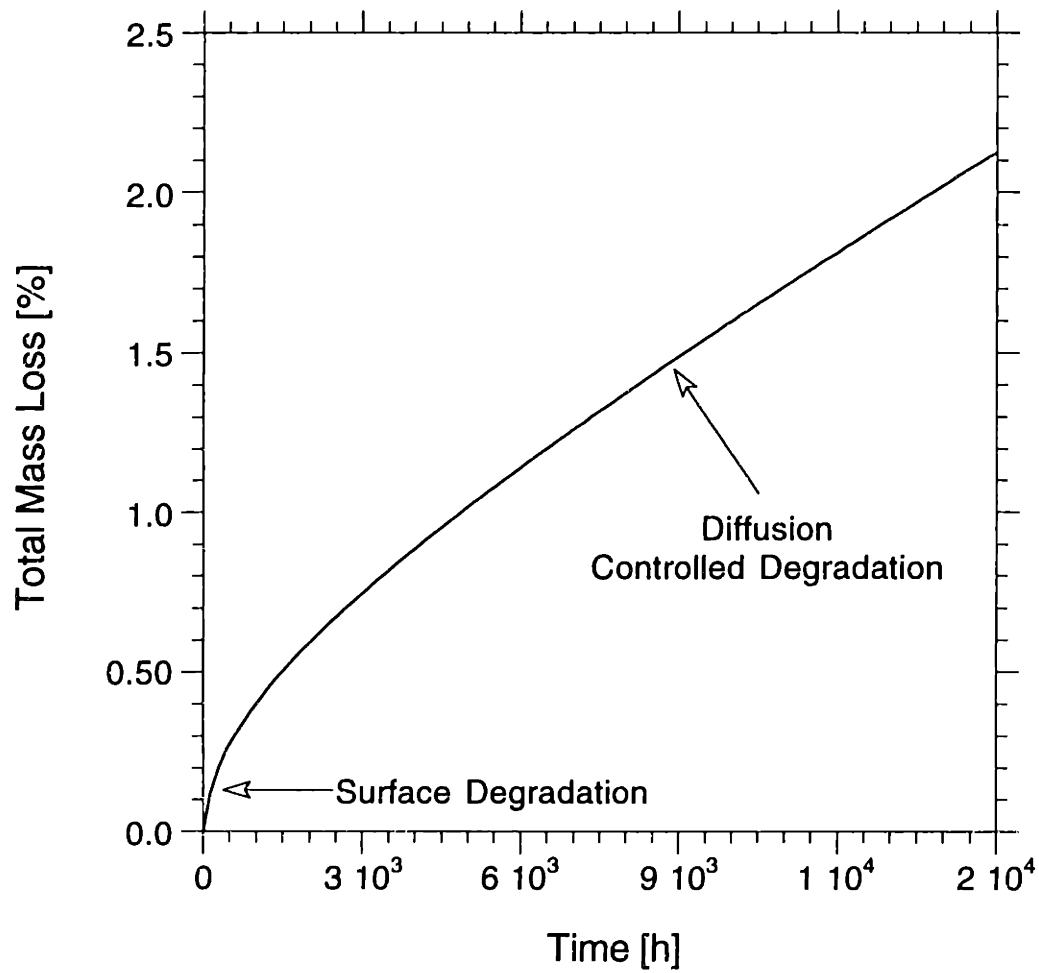
Figure 5.16: Total mass loss in a 16 ply laminate over 5000 accelerated cycles.

5.4 CORRELATION WITH DATA

Predicted weight gain and mass loss resulting from theoretical exposure to the test cycle were compared with data from tests performed at The Boeing Company [67]. Specimens were exposed to repeated cycles in a test chamber programmed to follow the test cycle given in Fig. 5.2. Figures 5.17 and 5.18 show the model prediction and measured values for the total change in mass at the end of the cycle. Each value for change in mass was calculated from the average weight of at least four coupons weighed at various times. The symbol indicates the average value, with error bars representing one standard deviation.

Mass loss caused by chemical reactions as well as weight gain due to absorbed moisture contributed to the results shown below. By subtracting the prediction of total mass loss due to degradation from the weight gained in the form of moisture, we see closer correlation between measured and predicted values after many cycles. Predicted values presented in this form also correlate with the initial experimental data points closely.

Predicted values for the total mass loss during isothermal exposure are compared with data from tests done at the Massachusetts Institute of Technology in the Technology Laboratory for Advanced Composites [42]. Results of tests performed on PMR-15 material are reported here. Neat resin specimens were exposed to constant temperature for up to 240 hours. Specimens were weighed once a day for ten days. All specimens were 3.2 mm thick. Figure 5.19 shows model prediction and data from isothermal runs at 316°C. Figure 5.20 shows runs at 343°C. Model prediction at both temperatures capture the magnitude of the total mass loss and the trends in the data.

93
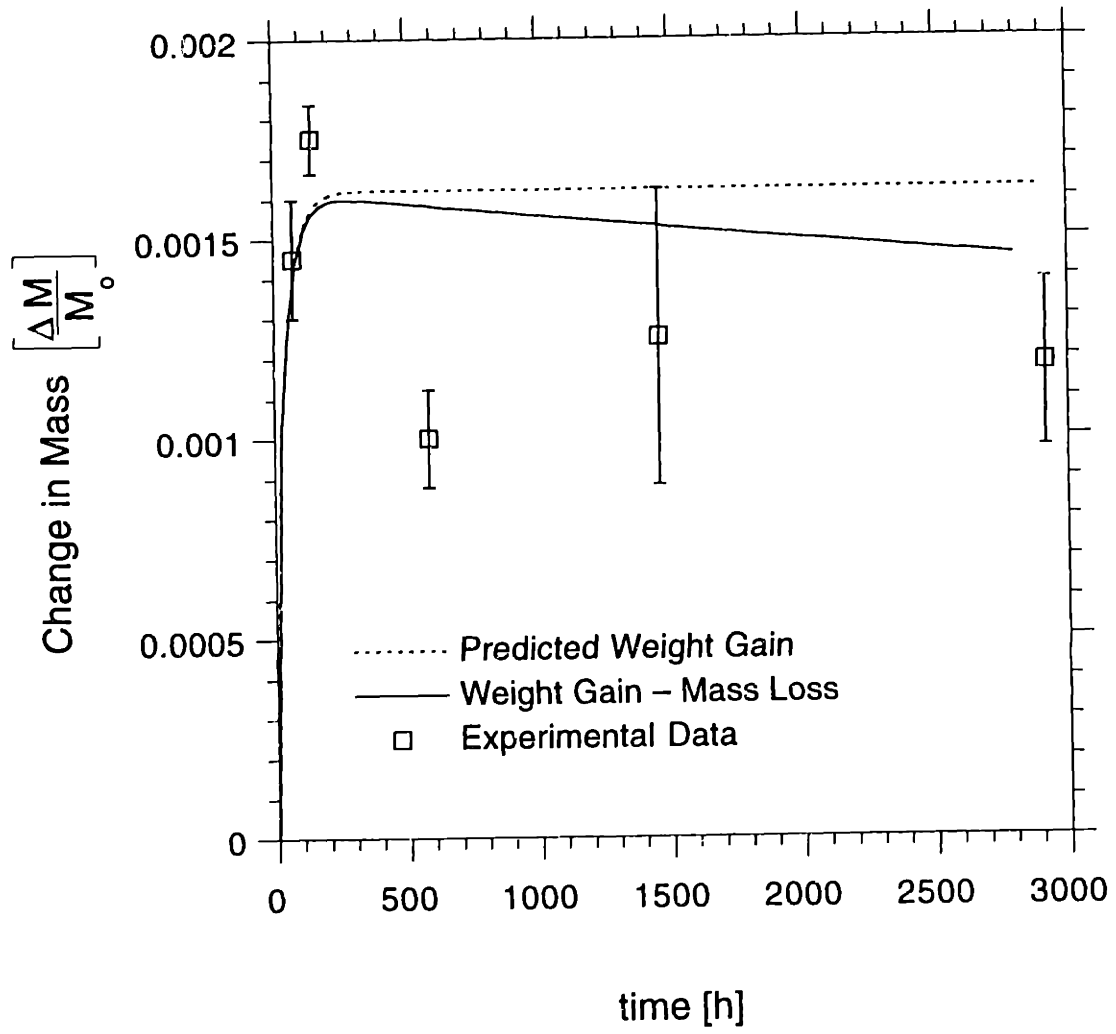
Figure 5.17: Total change in mass due to chemical reactions and moisture in an initially unexposed 16 ply laminate compared with experimental data.
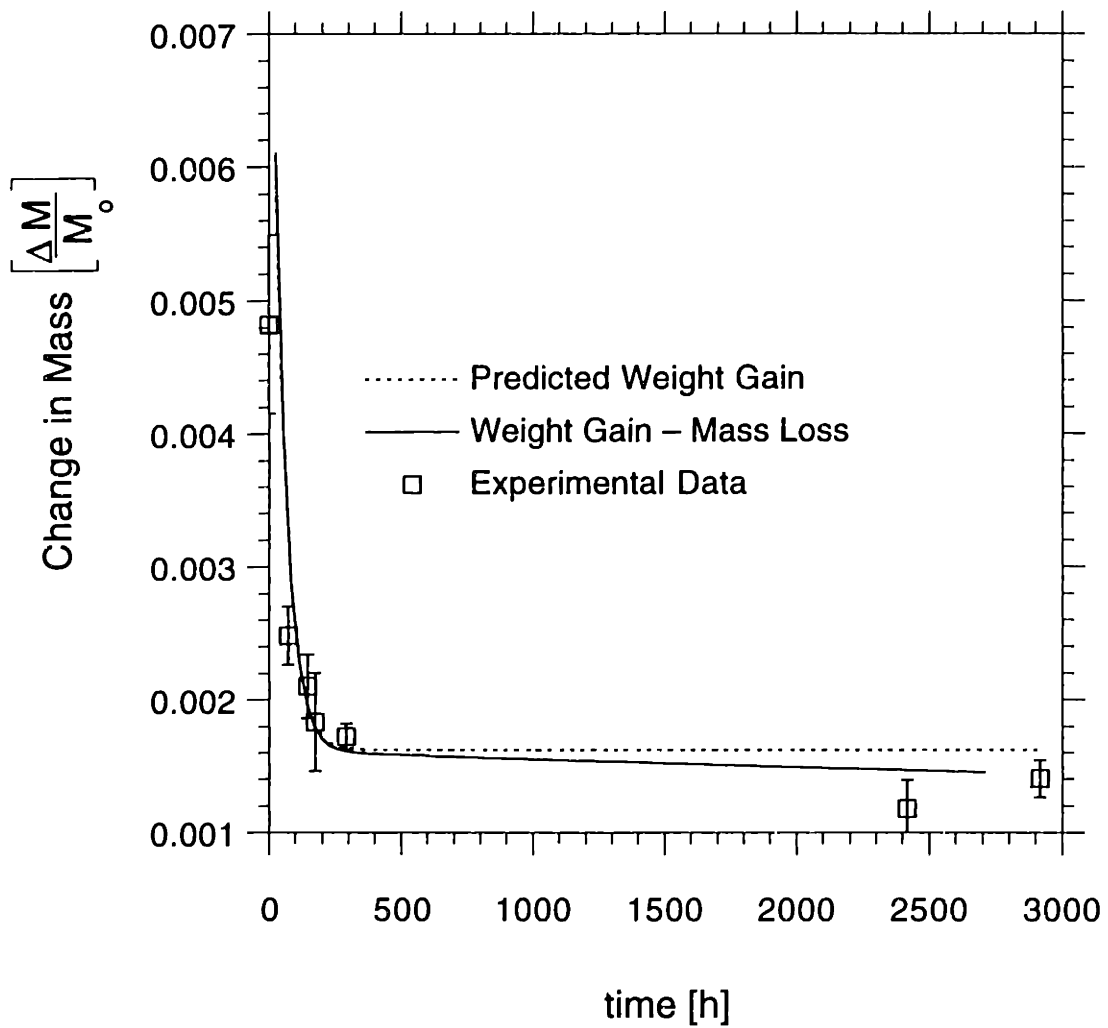
Figure 5.18: Total change in mass due to chemical reactions and moisture in a 16 ply laminate exposed to 85% RH for 2 weeks, then cycled.
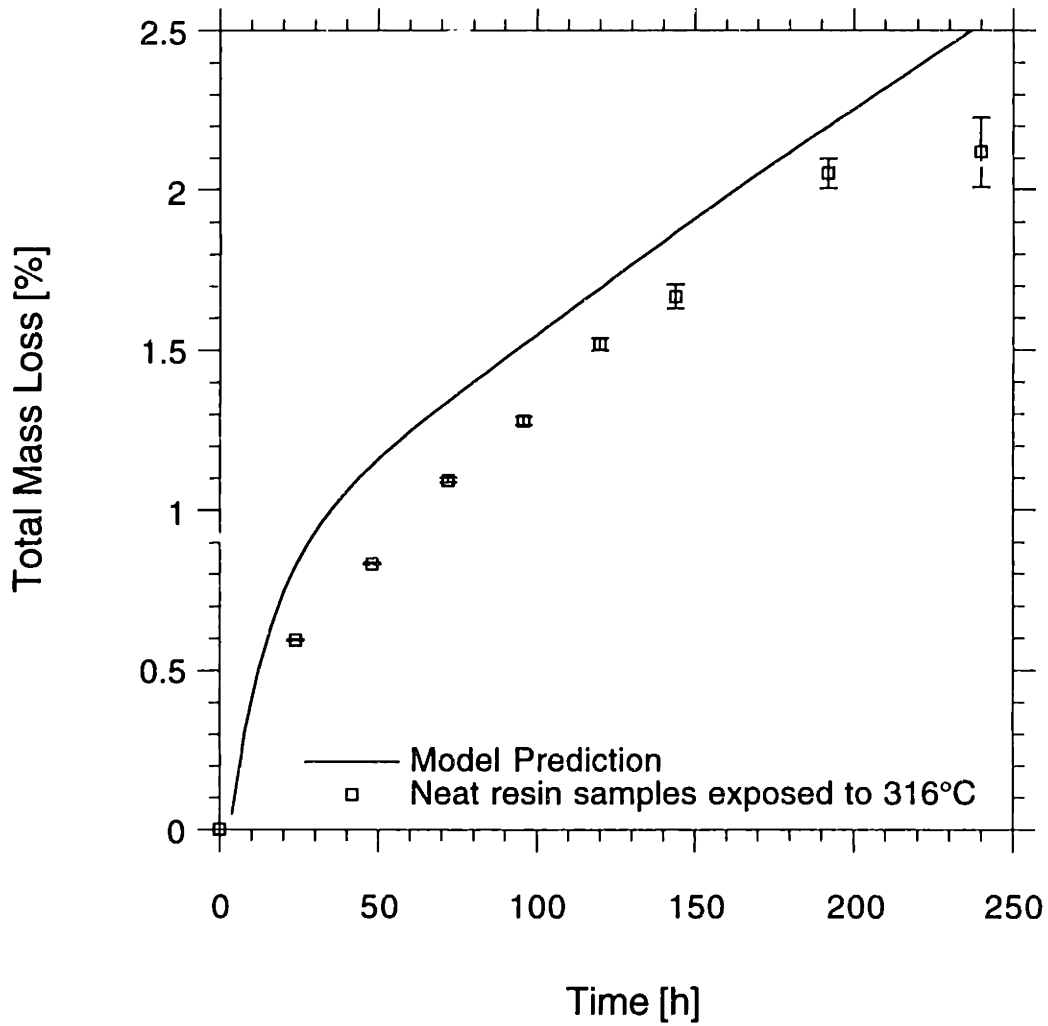
Figure 5.19: Predicted and experimental total mass loss of 3.2 mm thick PMR-15 resin samples exposed to 316°C for 10 days.
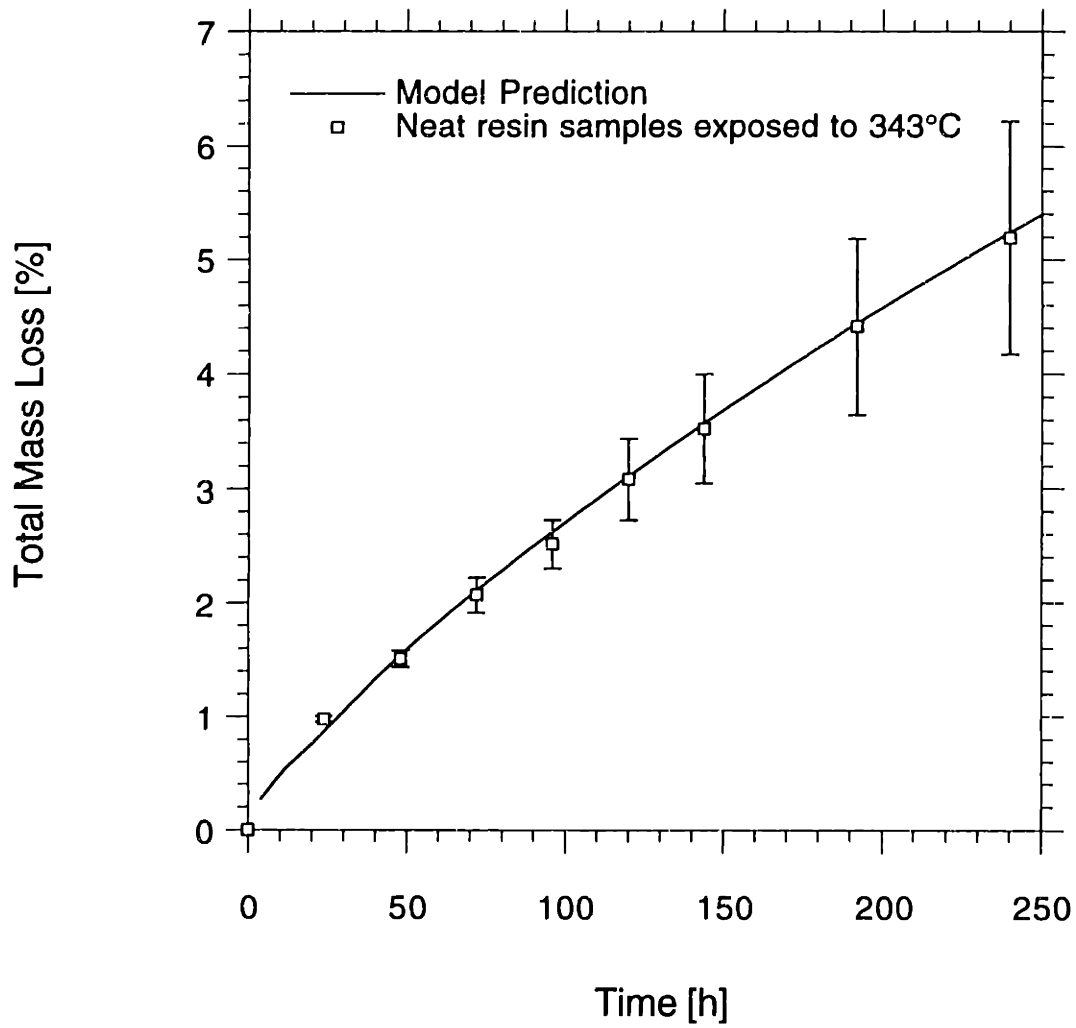
Figure 5.20: Predicted and experimental total mass loss of 3.2 mm thick PMR-15 resin samples exposed to 343°C for 10 days.

5.5 STRESS STATE

All of the effects shown above result in stresses. The presence of moisture causes swelling and softening of the matrix. Degradation of the matrix causes shrinkage and altered material properties. Changes in the ambient temperature from the stress free (cure) temperature result in expansion or shrinkage of the material. Constitutive relations which include all of these effects are used to calculate the magnitude of stresses in the matrix. Ply stresses result from swelling, shrinkage, and property changes, combined with the restraining effect of other plies. The matrix materials proposed for this project have very high cure temperatures, resulting in large thermal stresses in the quasi–isotropic (as well as others such as cross–ply) laminates at use temperatures. The gradients resulting from moisture fluctuations and degradation at the edges cause significant ply stresses. These stresses create the potential for the onset of damage in the form of surface cracking and microcracking. Calculated stresses from all of these effects are shown here as functions of position through the laminate under various conditions. Only the stresses locally transverse to the fibers are shown, as these are the stresses primarily responsible for microcracking.

5.4.1 Hygral Stresses

In Fig. 5.21, stresses in unidirectional and quasi–isotropic laminates due solely to the presence of moisture are shown. This laminate has been exposed to 85% RH for 2 weeks at 160°F prior to cycling. Symbols represent a snapshot of the model predictions of the average level of moisture in each ply. The specific moisture concentration shown represents the concentration during the first cycle, just after the hot, dry exposure (t_B). The solid line is the actual through–thickness moisture distribution, and the points represent the average value for each ply calculated using Eq. 4.43. The external ply shown has dried
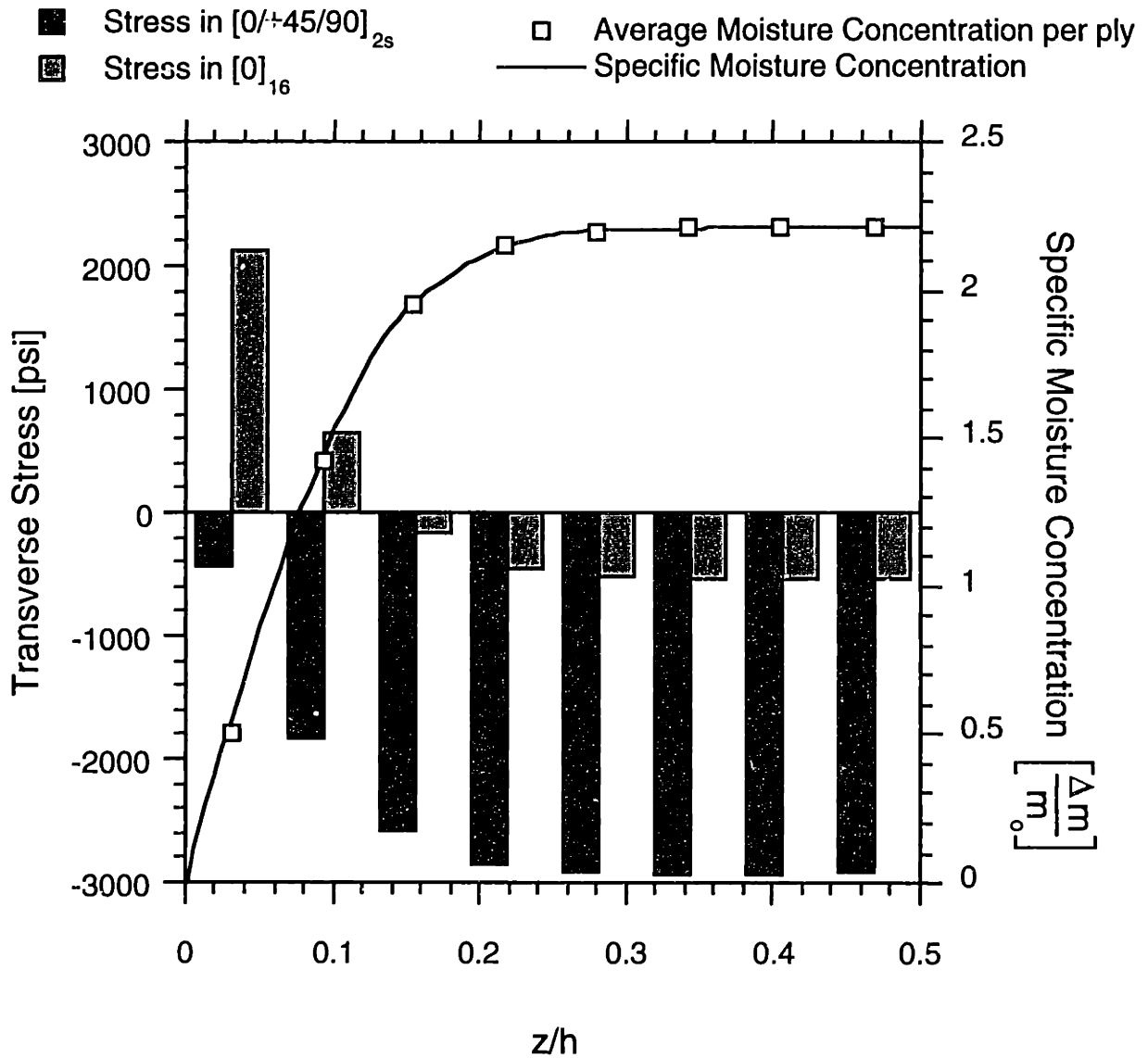
Figure 5.21: Transverse stresses due to moisture in a quasi–isotropic laminate exposed for 2 weeks at 160°F and 85% RH, then cycled.

out, leaving a high concentration of moisture in the center of the material. This situation is one of the worst cases of moisture induced stress possible during the type of exposure investigated in the current study.

Hygral stresses at the surface of the unidirectional laminate are on the same order of magnitude as the thermal stresses. The actual stress at the edges of the laminate may be greater than shown here because averaging the moisture in the first ply does not capture the actual concentration at the surface. The difference in stresses in the two laminate configurations shown is due to a restraining effect of the fibers in the quasi–isotropic lay–up. In the unidirectional laminate, the wet plies at the center expand and create a tensile stress in the outer, drier plies. As the wet plies in the center of the quasi–isotropic laminate try to expand, they are restrained by the fibers in the surrounding plies, creating a compressive stress. The tensile stresses in the outer plies of a unidirectional laminate are of the most interest, since cracking is caused by tensile stresses.

Figure 5.22 shows a snapshot of the stresses in the laminate at several times during one cycle. The specific moisture concentration correspond to the values at t_A, t_B, and t_C in cycle 2 (shown in Fig. 5.3). The laminate experiences this range of stresses during each cycle. Although the magnitude of these hygral stresses is relatively small, repeated fluctuation during exposure may result in some form of damage.

5.4.2 Stresses due to Degradation

Exposure to 5000 repeated test cycles causes only a small amount of degradation, resulting in only a small contribution to the stress state. A greater potential for damage is created by the results of the accelerated test cycle introduced in Section 5.3.2. Fig. 5.23 depicts
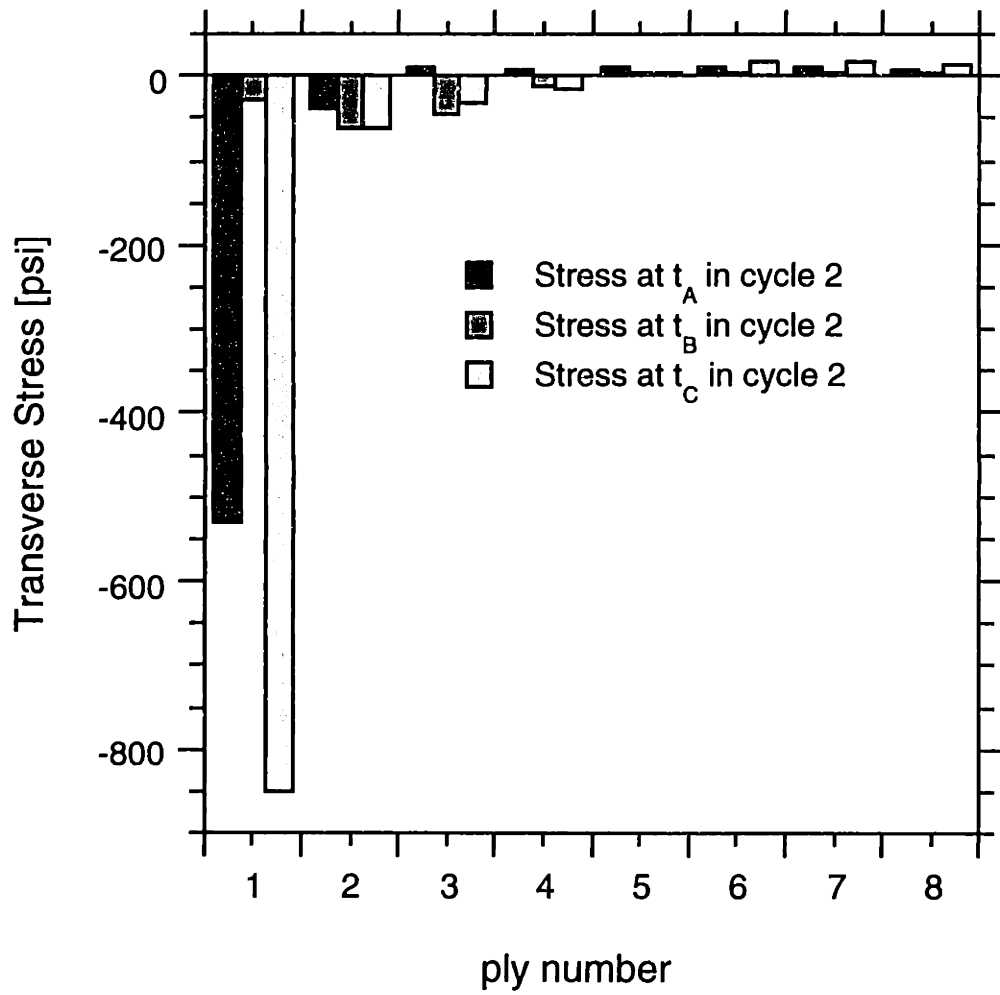
Figure 5.22: Transverse stresses due to moisture in a quasi–isotropic laminate at distinct points in 2nd cycle (corresponding to moisture concentration shown in Fig. 5.3).

stresses in unidirectional and quasi–isotropic laminates resulting from the degradation state in the laminate after 5000 of these accelerated cycles. Average mass loss per ply is represented by symbols, with the actual predicted mass loss metric shown by a solid line.

Only at the exposed surface has enough degradation occurred to affect the stresses significantly. The stresses induced by degradation and resulting shrinkage are comparable to the thermal stresses, and on the same order of magnitude as the transverse tensile strength of this composite (see Table 5.1). Stresses at the edge of the laminate reach values of 13 ksi, which exceeds the transverse tensile strength of this composite, reported as 10 ksi. The actual value for mass loss at the surface is higher than the average value in the first ply, suggesting that material right at the edges would actually experience a more severe stress than shown. These high stresses are consistent with the surface cracking observed in many studies.

5.4.3 Combined Environmental Loads

Figure 5.24 shows the stress resulting from a combination of environmental factors. This scenario represents a quasi–isotropic laminate that has been exposed to 5000 test cycles, removed from the test chamber at t_C (just after the hot, wet condition), and cooled to room temperature. Time to return to room temperature and any loss of moisture during this cool down is neglected. A uniform thermal stress exists in each ply due to the drop from cure temperature to room temperature. Matrix swelling due to moisture causes a large decrease in stress near the edges and a smaller decrease toward the center. Degradation at the edge of the laminate results in a small additional tensile stress in the surface ply. As noted above, stress would be significantly greater in material right at the surface.
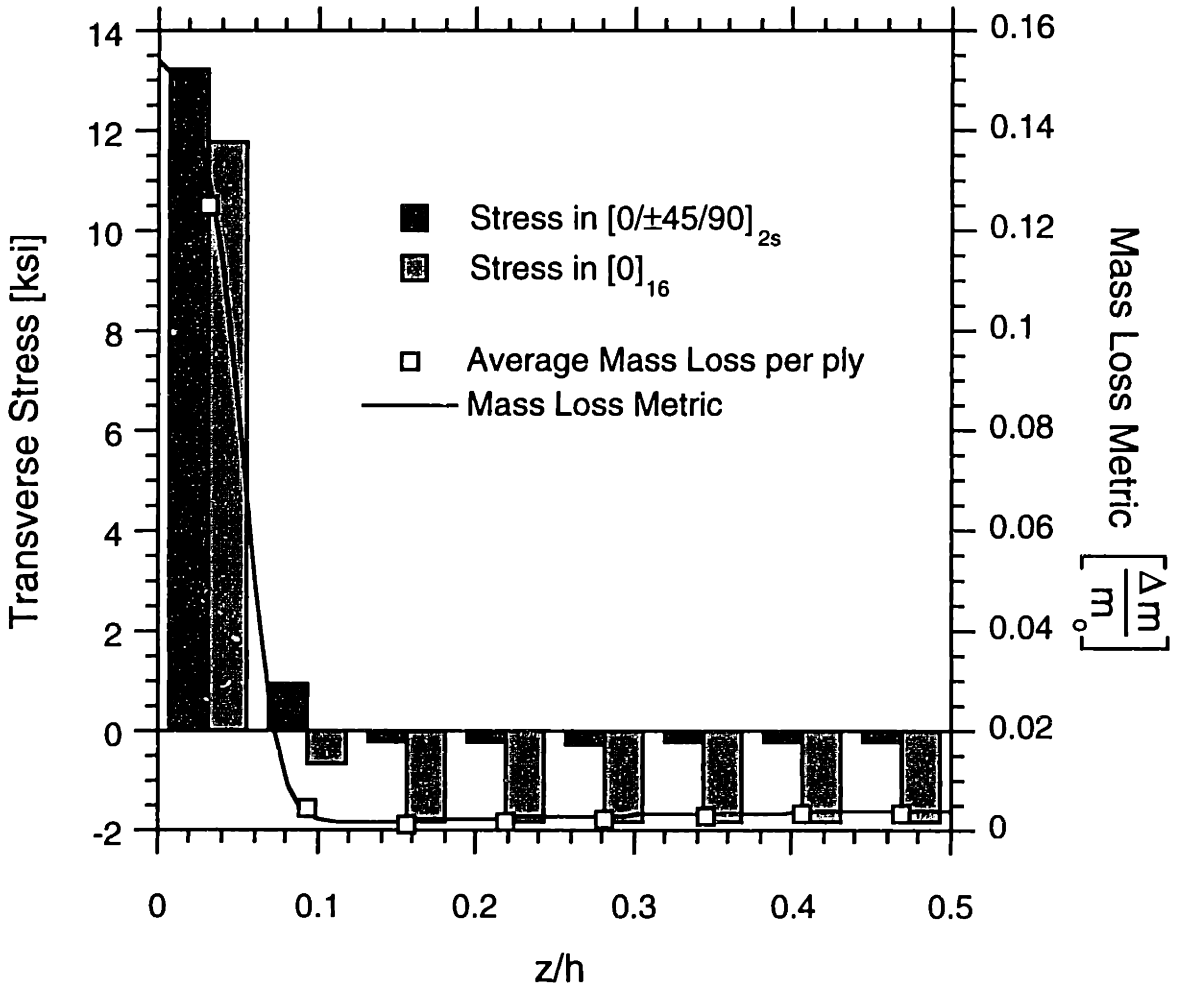
Figure 5.23: Transverse ply stresses in unidirectional and quasi–isotropic laminates exposed to 5000 repetitions of the accelerated test cycle described in Section 5.3.2.
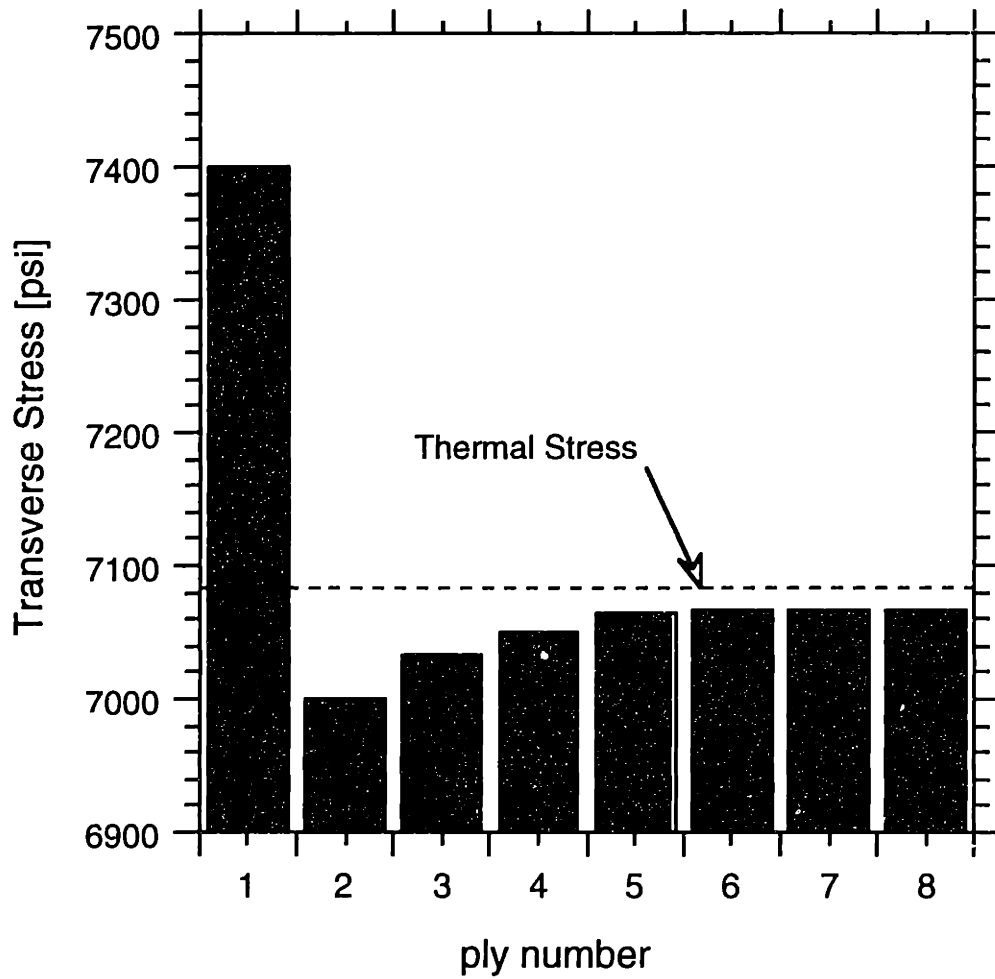
Figure 5.24: Transverse stresses in a quasi–isotropic laminate due to moisture at t_C, degradation after 5000 test cycles, and tested at room temperature.

5.4.3 Stresses Due to Isothermal Exposure

Figure 5.25 shows snapshots of the stress state resulting from 343°C isothermal exposure of a 3.2 mm thick PETI-5 neat resin specimen. Oxidative reactions have reached completion at the edges, and thermal reactions are causing mass loss to occur everywhere in the laminate. As degradation increases, both tensile stresses at the edge and compressive stresses toward the center of the laminate increase. High stresses near the surface are consistant with the surface cracking observed [42,43,47,50].

5.4.4 Microstresses

Microstresses are calculated by ICAN using a modified constitutive relation. Applied stresses cause microstresses due to local stress concentrations. Stress also arises from swelling and shrinkage in the matrix induced by moisture, degradation, and temperature, which is resisted by the more stable fibers. Stresses are calculated in two regions of the unit cell, shown in Fig. 5.26: a region of matrix only (A) and a region including fibers and matrix (B). Cracking has been observed at the fiber/matrix interface after exposure to both moisture [26,27,33] and hot, oxidative environments [39–45,47,50]. This is the region of most interest in the current study.

The microstresses in the fiber/matrix regions after exposure to 5000 accelerated test cycles are plotted in Fig. 5.27. A quasi–isotropic laminate is studied. The edge plies of the laminate have degraded approximately 12%. The shrinkage of the matrix resulting from this degradation causes a compressive stress concentration at the fiber/matrix interface. At the ply level, the undegraded plies at the center of the laminate restrain the outer degraded plies from shrinking. This causes a tensile stress in the outer plies, resulting in a tensile
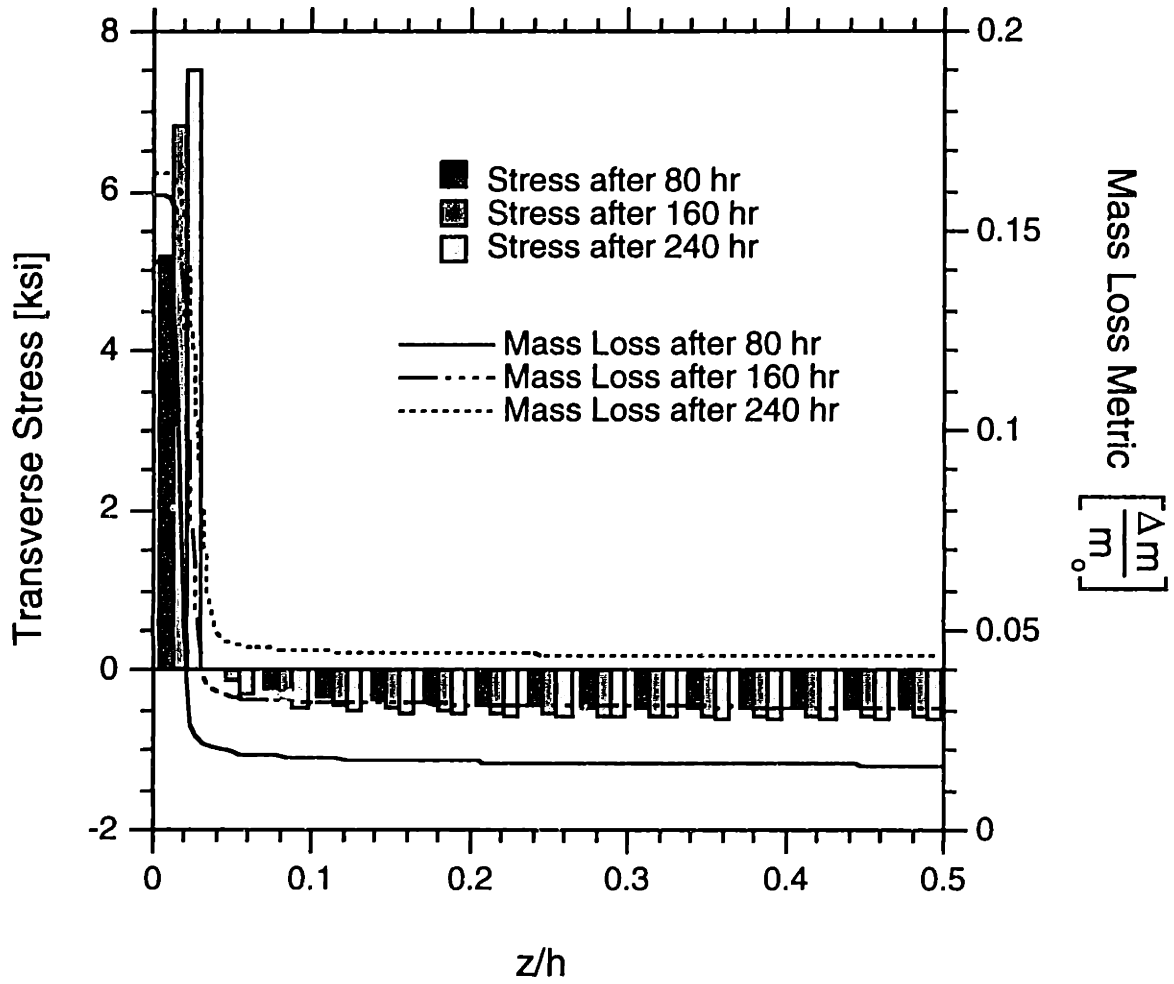
Figure 5.25: Stresses in a neat resin specimen exposed to 343°C for 240 hours.
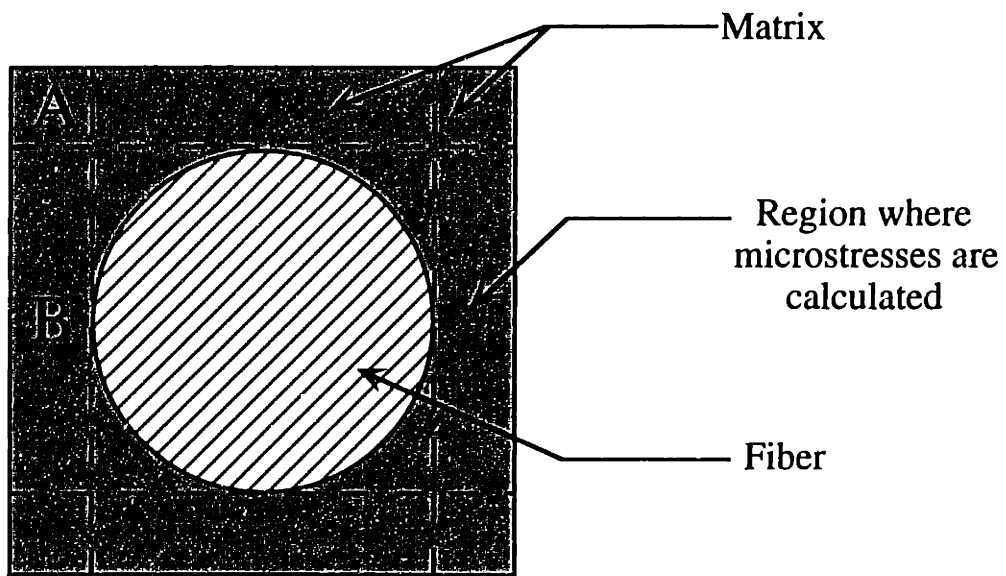
ICAN Unit Cell

Figure 5.26: Regions used in ICAN microstress calculations.
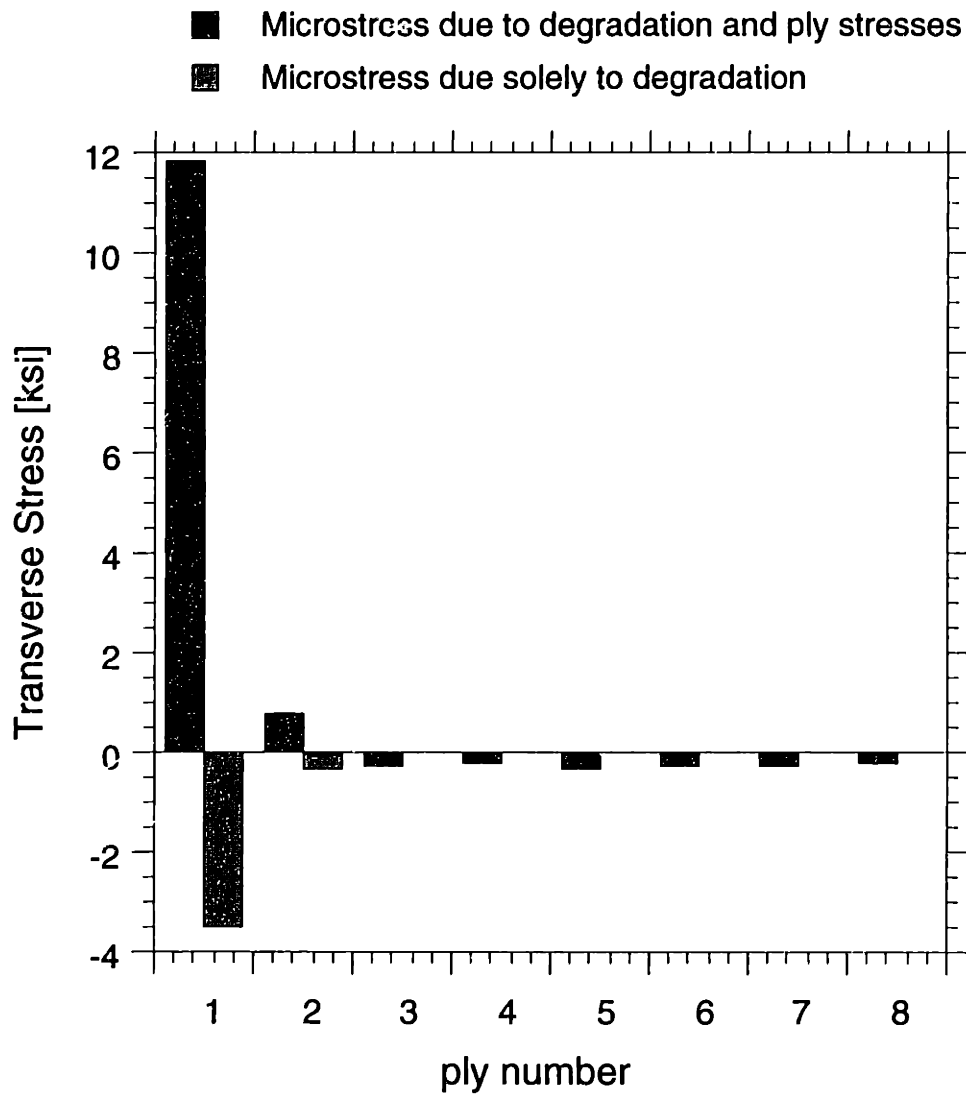
Figure 5.27: Microstresses in matrix of quasi–isotropic laminate exposed to 5000 repetitions of the accelerated test cycle described in Section 5.3.2.

microstress at the fiber/matrix interface. In Fig. 5.27, microstresses due only to local stress concentrations are plotted as well as microstresses resulting from the combination of applied stresses and ply stresses. In this particular case, microstresses are similar in magnitude to ply stresses (see Fig. 5.23). Stress concentrations near fibers are offset by compressive stress caused by shrinkage of the matrix around fibers.

5.5 SUMMARY

The computer model was used to predict the state of a material exposed to a series of test cycles. Material properties used in this analysis represent the most complete database to date for the material of interest. The sample test cycle represents the type of varied temperature and humidity exposure typical of operation.

Moisture absorbed by the laminate during multiple repetitions of this type of exposure exhibits two trends. Specific moisture concentration at the center of the laminate slowly increases towards an equilibrium value. This equilibrium value is simply a weighted average of the diffusivity conditions during the intervals of exposure. Within a region at the edge of the laminate, the moisture concentration fluctuates rapidly as the external humidity conditions change. The thickness associated with this layer is calculated by finding the mode which responds with a period approximately equal to the cycle time. The wavelength of this mode matches the thickness of the region of fluctuations.

The chemical reactions dependent on oxygen diffusing into the material and on high temperatures were predicted. Oxidative chemical reactions degrade the material starting at the edges. Total mass loss due to chemical reactions proved small for multiple runs of the test cycle studied in this investigation.

Calculated change in material weight showed reasonable agreement with experimental data. Predictions of total changes in mass due to both moisture and chemical reactions were compared with measured weight gained during 1000 test cycles. The mass lost due to reactions was small in comparison to the absorbed moisture, but significant after as many as 1000 cycles. These plots show reasonable correlation with initial values and good agreement with weight change after many cycles. Correlation with isothermal neat resin specimen data at higher temperatures gave us confidence in the correct operation of the degradation predictions. Mass loss predictions over 240 hours of isothermal testing at 316°C and 343°C agreed with the magnitude and the trends in the data.

Parametric studies of the test cycle and material properties highlighted several significant points. The diffusivity value determined experimentally for this material is critical to our assumptions about the gradual change in the center of the laminate towards an equilibrium level. A higher diffusion rate would drive fluctuations in moisture concentration even at the center of the laminate.

A test cycle with slightly higher temperatures would cause severe degradation of the material. After five thousand test cycles, predicted values suggested mass loss was occurring at the edges of the material, with material even towards the center of the laminate partially degraded. Total mass loss due to this type of exposure was significant. The rate of mass loss reached a constant after about 3000 cycles, although total mass lost continued to increase. This analysis showed a sensitivity of degradation to the exposure cycle. A similar sensitivity to the oxygen diffusion and reaction constants could also be expected.

During the exposure cycle studied, changes in the laminate take place, many of which result in an altered stress state in the laminate. Of all potential stresses, those resulting from the drop in temperature at the lowest temperature in the exposure cycle are the greatest in

magnitude. Other factors showed significant impact on the laminate, requiring attention if we are to accurately predict the potential for damage. A material that has been allowed to saturate and then begins to dry out experiences the worst hygral stresses. The degradation at the surface resulting from exposure to the test cycle causes shrinkage and altered material properties. This combination of effects causes stresses. The stresses resulting from exposure to an accelerated test cycle exceeds the transverse tensile strength of the composite.

CHAPTER 6

CONCLUSIONS AND RECCOMMENDATIONS

6.1 CONTRIBUTION AND CONCLUSIONS

This method outlined in this study provides the means for predicting the diffusion of moisture and oxygen into a material, the chemical changes that occur, and the stress field resulting from these environmental effects. This development is based on a new solution to Fick's law which allows very fast repeated calculation of the concentration of diffusing substances in laminates exposed to a changing temperature and humidity environment. A recent development predicting the progress of chemical degradation was incorporated into the present method. The result is a set of models encoded in a computer program that considers the effects of temperature, moisture and oxygen to predict the changing state of a material.

Several trends in the material behavior are better understood as a result of this analysis. The mathematical model predicts a pseudo–equilibrium moisture state, where the edges fluctuate rapidly between dry and wet, and the center sees little or no change. Diffusion of oxygen occurs much more slowly, resulting in only a small amount of material reacting with oxygen during the time periods studied.

Several new terms were introduced to describe the moisture state. The equilibrium moisture level at the center of the laminate is described by a diffusion–weighted time average of the various exposure intervals in a single cycle. The thickness of a "surface layer" is introduced in which all of the moisture fluctuations are contained.

Parametric studies provide some insight into the effects of material property values and details of the exposure cycle in the region of interest. The diffusivity value derived from experimental data lies in a critical region; a higher value would result in moisture level fluctuations even at the center of the material, while a lower one would result in a very thin region of fluctuations at the surface. Two factors prompted an investigation into the effects of slightly higher temperature exposures: the uncertainty of the equivalence between relevant properties of PMR-15 and PETI-5 and an evaluation of the relatively slow ingress of oxygen at the temperatures specific to the test cycle. A temperature–accelerated exposure cycle causes more severe oxidative degradation. Chemical effects are slow, but have the potential to cause significant mass loss and altered material properties at the surface.

The predicted levels of moisture and oxygen and the chemical degradation of the matrix create a complicated stress field. An existing code was used to calculate stresses in the laminate due to several factors: gradients in the material state across the laminate thickness and mismatch of material properties between fibers and matrix and between different plies (including elastic constants and coefficients of thermal expansion, moisture expansion, and shrinkage). For the exposure cycle studied, thermal stresses dominate. Moisture stresses, though smaller in magnitude, are non-trivial and can induce stress gradients through the thickness. The worst case hygral stresses predicted in this analysis are on the same order of magnitude as the thermal stresses. In particular, moisture stresses can be severe in unidirectional laminates undergoing dry–out from a saturated condition. If degradation takes place, it will result in significantly enhanced stresses near the surface. Transverse microstresses at the region including the fiber/matrix interface exceed the transverse strength of the composite. This could explain the surface microcracking observed in numerous studies [3,15,35,38,41,45,48].

113

6.2 RECCOMMENDATIONS FOR FUTURE WORK

The material under investigation in the current study consists of a relatively new matrix material, PETI-5. Some material properties critical for this analysis have not yet been quantified. As a more complete database of environmental properties is built for this material, reevaluation of the predicted trends is suggested.

The stress analysis included in this study is purely theoretical. Mechanical tests are necessary to verify expected behavior. Calculated stresses suggest the potential for damage. Microcracking has been observed in thermocycling tests done on the material studied here [68]. Surface cracking due to degradation has been observed in many studies [36-46]. The current code has been designed to link with an existing microcracking analysis tool, developed at M.I.T. [63]. The microcracking analysis requires information about the material toughness and its dependence on temperature and moisture level. As the understanding of the material is expanded, information about the dependence of toughness on the presence of moisture and extent of degradation would also benefit this analysis.

It was the goal of this investigation to provide a tool for predicting the changing state of a material exposed to a complex cyclic environment. The mechanisms driving changes in the material were modeled, with output consisting primarily of changes in the material mass. Using metrics of degradation, percent weight change, and empirical factors to determine changes in material properties, stresses in the laminate were predicted. From these stresses, the potential for damage was identified. The range of values predicted for the stress states suggest that this problem is worthy of additional investigation.

REFERENCES

1. Chamis, C.C., "Simplified Composite Micromechanics for Predicting Microstresses," NASA Technical Memorandum 87295, 1986.

2. Hahn, H.T. and N.J. Pagano, "Curing Stresses in Composite Laminates," *Journal of Composite Materials*, Vol. 9, No. 1, 1975, pp. 91-106.

3. Chang, W-J., T-C. Chen, and C.-I. Weng, "Transient Hygrothermal Stresses in an Infinitely Long Annular Cylinder," *Journal of Thermal Stresses*, Vol. 14, 1991, pp. 439-454.

4. Bank, L.C. and T.R. Gentry, "Accelerated Test Methods to Determine the Long-Term Behavior of FRP Composite Structures: Environmental Effects," *Journal of Reinforced Plastics and Composites*, Vol. 14, No. 6, June 1995, pp. 559-587.

5. Weitsman, Y., "Moisture in Composites: Sorption and Damage," *Fatigue of Composite Materials*, K.L. Reifsnider, Ed., Elsevier Science Publishers, New York, NY, 1991, pp. 385-430.

6. Wolff, E.G., "Moisture Effects on Polymer Matrix Composites," *SAMPE Journal*, Vol. 29, No. 3, May/June 1993, pp. 11-19.

7. Springer, G.S., "Environmental Effects," *Composites Design*, 4th Ed., S. Tsai, Ed., Think Composites, Dayton, Ohio, 1988, pp. 16-1 to 16-18.

8. Crank, J. *The Mathematics of Diffusion*, 2nd Edition, Oxford, England, Clarendon Press, 1975.

9. Shirrell, C.D. and J. Halpin, "Moisture Absorption and Desorption in Epoxy Composite Laminates," *Composite Materials: Testing and Design, ASTM STP 617*, American Society for Testing and Materials, 1977, pp. 514-528.

10. Tsai, S.W, and H.T. Hahn, *Introduction to Composite Materials*, Technomic Publishing, Lancaster PA, 1980.

11. Springer, G.S. *Environmental Effects on Composite Materials*, Technomic Publishing, Lancaster, PA, Vols. 1 and 2, 1981.

12. Jones, R.M., *Mechanics of Composite Materials*, Hemisphere Publishing Corp., New York, NY, 1975.

13. Loos, A.C. and G.S. Springer, "Moisture Absorption of Graphite-Epoxy Composites Immersed in Liquids and in Humid Air," *Journal of Composite Materials*, Vol. 13, No. 2, 1979, pp. 131-140.

14. Shen, C.H. and G.S. Springer, "Moisture Absorption and Desorption of Composite Materials," *J. Composite Materials*, Vol. 10, No. 1, 1976, pp. 2-20.

15. Ming, L, "The Environmental Effects of Carbon Fiber Reinforced Polyethersulphone Composites," *Proceedings Tenth International Conference on Composite Materials*, Whistler, B.C., Canada, August, 1995, pp. 297-303.

16. Kondo, K. and T. Taki, "Moisture Diffusivity of Unidirectional Composites," *Journal of Composite Materials*, Vol. 16, No. 1, 1982, pp. 82-93.

17. Bond, D., M. Bader, P. Smith, "Finite Element Modeling of Fibre Reinforced Composite Transverse Diffusivity," *Proceedings Tenth International Conference on Composite Materials*, Whistler, B.C., Canada, August, 1995, pp. 289-296.

18. Aditya, P.K. and P.K. Sinha, "Effects of Fiber Shapes on Moisture Diffusion Coefficients," *Journal of Reinforced Plastics and Composites*, Vol. 12, 1993, pp. 973-986.

19. Aditya, P.K. and P.K. Sinha, "Diffusion Coefficients of Polymeric Composites Subjected to Periodic Hygrothermal Exposure," *Journal of Reinforced Plastics and Composites*, Vol. 11, 1992, pp. 1035-1047.

20. Springer, G.S., "Moisture Content of Composites Under Transient Conditions," *Journal of Composite Materials*, Vol. 11, No. 1, 1977, pp. 107-122.

21. Weitsman, Y., "A Rapidly Convergent Scheme to Compute Moisture Profiles in Composite Materials under Fluctuating Ambient Conditions," *Journal of Composite Materials*, Vol. 15, No. 7, 1981, pp. 349-358.

22. Miller, R.K., "Multi-Material Model Moisture Analysis for Steady-State Boundary Conditions," *Environmental Effects on Composite Materials*, G.S. Springer, Ed., Vol. 1, Technomic Publishing, Lancaster, PA, 1981, pp. 162-169.

23. Whiteside, J.B., R.J. DeIasi, and R.L. Schulte, "Distribution of Absorbed Moisture in Graphite/Epoxy Laminates After Real-Time Environmental Cycling," *Long Term Behavior of Composites, ASTM STP 813*, T.K. O'Brien, Ed., American Society for Testing and Materials, Philadelphia, 1983, pp. 192-205.

24. Browning, C.E., G.E. Husman, and J.M. Whitney, "Moisture Effects in Epoxy Matrix Composites," *Composite Materials: Testing and Design, ASTM STP 617*, American Society for Testing and Materials, 1977, pp. 481-496.

25. Martin, W.J., "The Effect of Multiple Elevated Temperature Bonding Cycles on AS/3501-6 Mechanical Properties," *18th International SAMPE Technical Conference*, Vol. 18, Seattle, WA, October, 1986, pp. 660-669.

26. Zhou, J. and J.P. Lucas, "Effects of Water on a Graphite/Epoxy Composite," *Journal of Thermoplastic Composite Materials*, Vol. 9, October, 1996, pp. 316-328.

27. Davies, P. F. Pomies, L.A. Carlsson, "Influence of Water Absorption on Transverse Tensile Properties and Shear Fracture Toughness of Glass/Polypropylene," *Journal of Composite Materials*, Vol. 30, No. 9, 1996, pp. 1004-1019.

28. Lucas, J.P. and J. Zhou, "Moisture Interaction Characteristics and Fracture in Polymer Composites," *Proceedings Tenth International Conference on Composite Materials*, Whistler, B.C., Canada, August, 1995, pp. 247-256.

29. Upadhyay, P.C., J. Prucz, "Parametric Damage Modeling of Composites Due to Moisture Absorption" *Journal of Reinforced Plastics and Composites*, Vol. 11, 1992, pp. 198-210.

30. VanLandingham, M.R., R.F. Eduljee, and J.W. Gillespie, Jr., "Hygrothermal Effects on the Material Properties and Behavior of Thermoplastic Polyimide Composites," *Proceedings of the Tenth Technical Conference of the American Society for Composites*, Santa Monica, CA, Oct., 1995, pp. 525-535.

31. Burcham, L.J., M.R. VanLandingham, R.F. Eduljee, and J.W. Gillespie, "Moisture Effects on the Material Behavior of Graphite Polyimide Composites," *Polymer Composites*, Vol. 17, No. 5, 1996, pp. 682-690.

32. Mandell, J.F., "Origin of Moisture Effects on Crack Propagation in Composites," Dept. of Materials Science and Engineering Research Report R77-4, Massachusetts Institute of Technology, Dec. 1977.

33. Weitsman, Y., "Coupled Damage and Moisture-Transport in Fiber-Reinforced, Polymeric Composites," *International Journal of Solids and Structures*, Vol. 23, No. 7, 1987, pp. 1003-1025.

34. Cai, L.-W. and Y. Weitsman, "Non-Fickian Moisture Diffusion in Polymeric Composites," *Journal of Composite Materials*, Vol. 28, No. 2, 1994, pp. 130-154.

35. Chester, R.J. and A.A. Baker, "Environmental Durability of FA-18 Gr/Ep Composites," *Proceedings Tenth International Conference on Composite Materials*, Whistler, B.C., Canada, August, 1995, pp. 239-246.

36. Meador, M.A., P.J. Cavano, D.C. Malarik, "High Temperature Polymer Matrix Composites for Extreme Environments," *Structural Composites: Design and Processing Technologies, Proceedings of the Sixth Annual ASM/ESD Advanced Composites Conference*, Detroit, MI, October, 1990, pp. 529-539.

37. Scola, D.A, and J.H. Vontell, "High Temperature Polyimides, Chemistry and Properties," *Polymer Composites*, Vol. 9, No. 6, December 1988, pp. 443-452.

38. Roberts, G.D. and R.D. Vanucci, "Effect of Solution Concentration and Aging Conditions on PMR-15 Resin," *SAMPE Journal*, Vol. 22, 1986, pp. 24-28.

39. Bowles, K.J., D. Jayne, T.A. Leonhardt, and D. Bors, "Thermal Stability Relationships Between PMR-15 Resin and Its Composites," *Journal of Advanced Materials*, Vol. 26, No. 1, 1994, pp. 23-32.

40. Xiang, Z.D. and F.R. Jones, "Thermal Degradation of an End-Capped Bismaleimide Resin Matrix (PMR-15) Composite Reinforced with Pan-Based Carbon Fibers," *Composites Science and Technology*, Vol. 47, 1993, pp. 209-215.

41. Cunningham, R.A. and H.L. McManus, "Coupled Diffusion-Reaction Models for Predicting the Distribution of Degradation in Polymer Matrix Composites," Presented at the 1996 ASME International Mechanical Engineering Congress and Exposition, Atlanta, GA, November, 1996.

42. Cunningham, R.A., "High Temperature Degradation Mechanisms in Polymer Matrix Composites," Master of Science Thesis, Massachusetts Institute of Technology, 1996.

43. Nelson, J.B., "Thermal Aging of Graphite/Polyimide Composites," *Long-Term Behavior of Composites, ASTM STP 813*, T.K. O'Brien, Ed., American Society for Testing and Materials, Philadelphia, PA, 1983, pp. 206-221.

44. Tompkins, S.S. and S.L. Williams, "Effects of Thermal Cycling on Mechanical Properties of Graphite Polyimide," *Journal of Spacecraft*, Vol. 21, No. 3, 1984, pp. 274-280.

45. Martin, R.H., E.J. Siochi, and T.S. Gates, "Isothermal Aging of IM7/8320 and IM7/5260," *American Society for Composites 7th Technical Conference on Composite Materials*, University Park, PA, 1992, pp. 207-217.

46. Tsuji, L., Master of Science Thesis, Massachusetts Institute of Technology, expected 1998.

47. Bowles, K.J., G.D. Roberts, J.E. Kamvouris, "Long-Term Isothermal Aging Effects on Carbon Fabric-Reinforced PMR-15 Composites: Compression Strength," NASA Technical Memorandum 107129, 1996.

48. Bowles, K.J., "A Thermally Modified Polymer Matrix Composite Material with Structural Integrity to 371°C," NASA Technical Memorandum 100922, 1988.

49. Beckwith, S.W. and B.D. Wallace, "Effects of Aging and Environmental Conditions on Kevlar/Epoxy Composites," *SAMPE Quarterly*, Vol. 14, No. 4, 1983, pp. 38-45.

50. Madhukar, M.S., K.J. Bowles, D.S. Papadopolous, "Thermo-Oxidative Stability of Graphite/PMR-15 Composites: Effect of Surface Modification on Composite Shear Properties," NASA Technical Memorandum 4608, 1994.

51. Stone, M.A., J.W. Gillespie, Jr., B.F. Fink, T.A. Bogetti, "Thermo-Chemical Characterization of S2 Glass/Vinyl Ester Composites," *Advances in Polymers and Fibers*, pp. 529-538.

52. Schnabel, W., *Polymer Degradation: Principles and Practical Applications*, Macmillin Publishing Co., New York, NY, 1981.

53. Chamis, C.C., "Simplified Composite Micromechanics Equations for Hygral, Thermal and Mechanical Properties," *SAMPE Quarterly*, April, 1984, pp. 14-23.

54. McManus, H.L. and C.C. Chamis, "Stress and Damage in Polymer Matrix Composite Materials Due to Material Degradation at High Temperatures," NASA Technical Memorandum 4682, 1996.

55. Murthy, P.L.N., C.A. Ginty, J.S. Sanfeliz, "Second Generation Integrated Composite Analyzer (ICAN) Computer Code," NASA Technical Paper 3290, 1993.

56. Murthy, P.L.N. and C.C. Chamis, "Integrated Composite Analyzer (ICAN) Users and Programmers Manual," NASA Technical Paper 2515, 1986.

57. McManus, H.L., D.E. Bowles, S.S. Tompkins, "Prediction of Thermal Cycling Induced Matrix Cracking," *Journal of Reinforced Plastics and Composites*, 1995.

58. Laws, N. and G.J. Dvorak, "Progressive Transverse Cracking in Composite Laminates," *Journal of Composite Materials*, Vol. 22, No. 10, 1988, pp. 900-915.

59. Wang, A.S.D. and F.W. Crossman, "Initiation and Growth of Transverse Cracks and Edge Delamination Composite Laminates: Part 1. An Energy Method," *Journal of Composite Materials Supplement*, Vol. 14, 1980, pp. 71-87.

60. Wang, A.S.D. and F.W. Crossman, "Initiation and Growth of Transverse Cracks and Edge Delamination Composite Laminates: Part 2. Experimental Correlation," *Journal of Composite Materials Supplement*, Vol. 14, 1980, pp. 88-108.

61. Hutchinson, J.W. and Z. Suo, "Mixed Mode Cracking in Layered Materials," *Advances in Applied Mechanics*, Vol. 28, 1992, pp. 64-191.

62. Park, C.H. and H.L. McManus, "Thermally Induced Damage in Composite Space Structure: Predictive Methodology and Experimental Correlation," *Composites Science and Technology*, Vol. 56, 1996, pp. 1209-1219.

63. Maddocks, J.R., H.L. McManus, "On Microcracking in Composite Laminates Under Thermal and Mechanical Loading," *Polymers and Polymer Composites*, Vol. 4, No. 5, 1996, pp. 305-314.

64. Flaggs, D.L. and F.W. Crossman, "Analysis of the Viscoelastic Response of Composite Laminates During Hygrothermal Exposure," *Journal of Composite Materials*, Vol. 15, No. 1, 1981, pp. 21-40.

65. Harper, B.D. and Y. Weitsman, "On the Effects of Environmental Conditioning on Residual Stresses in Composite Laminates," *International Journal of Solids and Structures*, Vol. 21, No. 8, 1985, pp. 907-926.

66. Hildebrand, F.B., *Advanced Calculus for Applications*, Englewood Cliffs, N.J.: Prentice-Hall, 1976.

67. Zabora, R. Personal correspondence, July, 1996-April, 1997.

GLOSSARY

aging   term used to refer to various types of exposure (avoided here due to ambiguity)

chemical aging   additional post–manufacture cross–linking in a material at elevated temperatures; chemical degradation

chemical degradation   irreversible change in material state caused by chemical reactions

completeness of reaction   metric used to measure the progress of chemical reactions

concentration dependent reactions   reactions driven by the presence of oxygen

crazing   randomly oriented surface cracking

damage   an irreversible change in a material due to changes in its structure (e.g. cracks)

degradation   an irreversible change in a material as a continuum marked by changes in the material properties (e.g. chemical change in the matrix)

environmental effects   diffusion of, and changes in a structure due to ambient moisture, oxygen, and temperature

hygral stresses   stresses caused by swelling due to the presence of moisture in a material

mass loss   loss of material due to chemical reactions, measured in the form of change in mass from original mass

mass loss metric   local mass loss in an infinitesimal control volume

microcracks   cracks in the matrix with lengths on the scale of a fiber diameter up to the height of a ply

microstresses   stresses in regions of material on the order of a fiber diameter

moisture fluctuations   large variations in the moisture concentration at a specific location in a material over time

oxidative reaction   reactions driven by the presence of oxygen

physical aging	reversible rearrangement of molecules in matrix to a more stable state
ply cracks	cracks on the scale of a ply thickness
ply stresses	homogenized stresses in a single ply
post–curing	additional post–manufacture cross–linking
pseudo–equilibrium	relatively unchanging moisture concentration in a laminate with time
reaction rate	rate at which reactions progress
relative humidity	ambient moisture level
shrinkage	decrease in the volume of material due to degradation
snapshot	through–thickness values at a distinct time
specific moisture concentration	local moisture concentration in an infinitesimal control volume
surface cracks	cracks initiated at the surface of a laminate
surface layer	region near surface of laminate with properties or response which differ from the rest of the material
temperature ramp rate	rate at which temperature is changed from one constant interval to another in the exposure cycle
thermal reactions	reactions activated solely by elevated temperatures
weight gain	measured as a gain in mass due to moisture absorption; measured in the form of change in mass from original mass

APPENDIX A

MODCOD USERS MANUAL

The computer code described below is named MODCOD (MOisture Diffusion, Chemical reactions and Oxygen Diffusion). This code calculates weight gain due to moisture and mass loss due to degradation given material properties, material geometry, and information about the exposure profile.

A.1 INPUT FILE

MODCOD requires only a single input file. This file must be an ASCII text file and must reside in the same folder as the code. Input data includes diffusion and reaction material property values, the number of cycles run, the number of modes used for the concentration solution, the time, temperature, and humidity at distinct points in the exposure profile, and the number and thickness of plies in the laminate. A specific format is required for the data included in the input file. All values must be given in SI units, with temperature in Kelvin.

Here, a deck is shown with the required input values, followed by a variable name (which is used here for clarity; it is not required by MODCOD). All input values are FORTRAN free formatted. When more than one input is on a single line, values are separated by spaces or commas. For numbers requiring exponential notation, use E to represent base ten. Geometry of the material under investigation is given first. The first line of the input file must define the number of plies in the laminate under investigation. This must be an

integer value. The ply thickness is entered in row two (in meters).

```
16              nply
0.125e-3        tply
```

The next twelve rows are used for the material properties required in these calculations. Enter the moisture diffusion constant (D_o^m) in row three and the corresponding activation energy for moisture diffusion (E_A^m) in row four. These values must be given in m^2/sec and J/mol, respectively. Enter values describing the material saturation dependence on relative humidity in the next two rows. Enter values A and B in rows five and six, where $C_\infty = A \Phi^B$. These values are non–dimensional. Rows seven and eight are reserved for the diffusion constant and exponential constant for oxygen concentration calculations. These are in the same units as required for moisture diffusion.

The activation energy and the reaction rate for the oxygen dependent reaction are entered in rows nine and ten. These must be in J/mol and s^{-1}, respectively. The order of the oxygen dependent reaction, n_{ox} (non–dimensional), is given in row 11. The next three lines (rows 12–14) require four values each: the activation energy (J/mol), reaction rate (s^{-1}), order of reaction, and mass fraction (both non–dimensional) for each thermal reaction. Separate these values by a comma or a space. In order to turn off any reaction, enter 0.000 for the corresponding mass fraction.

```
1.108e-7                            Do
3.508e04                            Ea
0.013                               A
1.000                               B
3.36e-11                            Dox
6.611e03                            Cox
1.350e05                            Ea11
1.670e08                            k11
2.300                               n11
1.820e05,1.360e09,1.610,0.160       Ea21,k21,n21,y1
1.820e05,1.360e09,1.610,0.000       Ea12,k12,n12,y2
2.390e05,7.900e12,3.200,0.240       Ea13,k13,n13,y3
```

If an initial exposure period is desired, enter the time, temperature, and humidity of pre-exposure separated by commas in row 15. Enter time in seconds, temperature in Kelvin, and humidity as a fraction. If no previous exposure is desired, enter "0,0,0".

```
1.21e6,344,.85 initial values
```

Lines 16 and 17 are reserved for number of cycles to be run (ncycles) and the number of time steps (indices) in a cycle. The maximum number of cycles handled by the code is 5000. There can be up to 100 entries for the cycle indices.

```
100             ncycles
8               ntime nsteps in profile (nsp)
```

The final input represents the profile of the test cycle. The cycle must be identified by distinct points, each associated with a progressive time, a temperature, and a relative humidity. Up to one hundred rows may be used to describe the profile. Each index in the cycle requires a separate line of input.

```
0,255,0         t_1,T_1,Φ_1
900,219,0       t_2,T_2,Φ_2
1500,219,0      t_3,T_3,Φ_3
2700,450,0      t_4,T_4,Φ_4
4500,450,0      t_5,T_5,Φ_5
5400,355,0      t_6,T_6,Φ_6
9300,355,.85    t_7,T_7,Φ_7
10500,255,0     t_8,T_8,Φ_8
```

t_1,T_1,Φ_1
t_2,T_2,Φ_2
t_3,T_3,Φ_3
t_4,T_4,Φ_4
t_5,T_5,Φ_5
t_6,T_6,Φ_6
t_7,T_7,Φ_7
t_8,T_8,Φ_8

The number of modes used in calculation of moisture and oxygen diffusion is a user-specified value, following the cycle profile. Up to 500 modes may be included.

```
100             nmodes
```

If the user wishes to have the code alter an existing file formatted for use with the program ICAN to reflect the state of the material due to cyclic exposure, enter the name of that file in the next row. If an ICAN input file is not desired, enter the single character "N" on this line. The filename can be up to twelve characters.

```
ICAN.16.iso     ICAN input file
```

The next set of input involves the type of output the user desires. Five types of storage specifications are required. Enter either "T" for true or "F" for false to turn on or off the output of interest. The first value, smed, is true if the user wishes to record the average moisture concentration and chemical degradation in the ICAN input deck at a snapshot cycle and index during exposure. If this value is false (and an ICAN input file is given), the averages are calculated at the end of exposure. The next two values, smp and srxn, are true if the user wishes to store profiles of the moisture concentration and mass loss metric, respectively, at specific times. The total weight gain is stored if smwc is true, and the total mass loss if smlc is true.

```
T            smed    store intermediate avg profile
T            smp     store moisture profiles
T            srxn    store reaction profiles
T            smwc    store moisture dep wt change
T            smlc    store mass loss change
```

If smed is true, it is necessary to define the cycle an index at which a snapshot of moisture concentration and degradation is averaged and written to the ICAN input deck. Give the cycle number and step in cycle in the next row, separated by a space or a comma. These must be integer values. If smed is false, omit this line of input.

```
3,5                storage intermediate cycle and index
```

Moisture concentration and mass loss profiles through the thickness require a selection of the cycles at which a profile is of interest. If either smp or srxn is true, the frequency of storage is determined by the value ncsp. The code stores a profile once every ncsp cycles. The next row is reserved for the indices in the cycle at which the moisture concentration profiles should be recorded. These values should only be entered if smp is true.

```
20           n cycles stored (ncsp)
3,5,7,0,0    indices at which profiles stored
```

If you have chosen to store total moisture dependent weight change (smwc is true), the user must specify the indices in the cycle where you wish to record the weight gain. Up to three

time traces may be stored. Enter integers, separated by a comma or a space, corresponding to the index at which moisture data will be stored.

1,3,5   indices at which total moisture stored

A.2 OUTPUT

Desired output is specified in the input file. The first option (smed) gives the user the capability of calculating the average for moisture and degradation at a specific time during an exposure cycle. If this option is turned off, the average will be calculated at the end of the exposure period. The remaining options involve stored data, and are separated into moisture and oxygen effects, and into time histories and through–thickness profiles.

The value smp is a logical operator (as are all of the output options) that is true if the user wishes to store through–thickness profiles of the moisture levels in the laminate. The frequency with which the profiles are stored is determined by the value ncsp entered in line 3. If this option is turned on ("T" is entered), profiles will be stored as tab separated text in a file called "Cmprofile". The first column is the through–thickness location, and the following columns include data at each specified index in the cycles desired.

When the option smwc is true, the average weight gained by the laminate during the exposure will be stored in a tab–separated text file. There is severe fluctuations in the moisture level during any one cycle. To correctly plot the long term time histories over many cycles, weight gain at specific points in the cycle are recorded. Up to three indices may be specified. Tab–separated data will be stored in a file called "WtGain," with time (in hours) in the first column, and weight gain (in terms of fraction of dry weight) in the next three columns.

Total mass loss caused by chemical reactions are stored in a tab–separated text file called "Massloss" when smlc is true. This first column is the time in hours. The second column is the mass loss, reported as a fraction of the total original mass. The third column gives an estimation for the degraded surface layer caused by a significant degree of completion of chemical reactions at the surface. The degraded surface layer depends on an empirical estimation of the threshold value of reaction completeness. If reactions have progressed beyond this threshold value, a surface layer is visible.

Oxygen concentration and mass loss profiles through the laminate thickness are stored when srxn is true. The first column is the through–thickness location. Oxygen concentration is reported as a fraction of 1, the saturation value. The mass loss metric, b, is given as a fraction of 1, the value signifying completion. This data is stored in a tab–separated text file called "Coxprofile".

A.3 SAMPLE INPUT

A sample of the entire input file is shown below.

```
16                nply
0.125e-3          tply
1.108e-7          Di
3.508e04          E
0.013             a
1.000             b
3.36e-11          Dox
6.611e03          Cox
1.350e05          Eox
1.670e08          kox
2.300             nox
1.820e05,1.360e09,1.610,0.160
1.820e05,1.360e09,1.610,0.000
2.390e05,7.900e12,3.200,0.240
1.21e6,344,.85 initial values
100               ncycles
8                 ntime indices in cycle
0,255,0
900,219,0
1500,219,0
```

```
2700,450,0
4500,450,0
5400,355,0
9300,355,.85
10500,255,0
100             nmodes
ICAN.16.iso     ICAN input file
T               smed      store intermediate avg profile
T               smp       store moisture profiles
T               srxn        store reaction profiles
T               smwc      store total moisture dep wt change
T               smlc      store mass loss change
3,5             storage intermediate cycle and index
20              n cycles stored
3,5,7,0,0       indices at which profiles stored
1,5,7           total m storage
```

A.4 SOURCE CODE

The source code for MODCOD is given below.

```
C********************************************************************
C                           M O D C O D
C
C                      CODE FOR THE PREDICTION OF
C        MOISTURE AND OXYGEN DIFFUSION AND RESULTING CHEMICAL REACTIONS
C
C              © 1997 Bethany J. Foch and Hugh L. McManus
C                   Massachusetts Institute of Technology
C                      Rm 33-311, 77 Massachusetts Ave.
C                   Cambridge MA 02139   (617) 253-0672
C
C********************************************************************
C
C  Version 1.0  5/97
C
C  Written in MPW FORTRAN
C  © 1988-1995 Fortner Research
C
C********************************************************************
C Permission to use, copy, and modify this software and its documentation
C for internal purposes only without fee is hereby granted provided that
C the above copyright notice and this permission appear on all copies of
C the code and supporting documentation. For any use of this software, in
C original or modified form, including but not limited to, adaptation as
C the basis of a commercial software or hardware product, or distribution
C in whole or part, specific prior permission and/or the appropriate
C license must be obtained from MIT. This software is provided "as is"
C without any warranties whatsoever, either expressed or implied,
C including but not limited to the implied warranties of merchantibility
C and fitness for a particular purpose. This software is a research program
C and MIT does not represent that it is free of error or bugs or suitable
C for any particular task.
C********************************************************************
C
C
C MOISTURE/OXYGEN DIFFUSION AND CHEMICAL REACTION PREDICTION CODE
C    all values in SI units
      PROGRAM MODCOD
      PARAMETER (maxn=5000)
      PARAMETER (Nsp=10)
      PARAMETER (maxmodes=500)
      PARAMETER (maxdt=100)
      CHARACTER*12 matfile,ICANin
      CHARACTER*20 ps
      CHARACTER*80 Aline,ican1,ican2
      CHARACTER*8 Mpct,Dpct
      CHARACTER*1 TAB
      REAL Ant(maxmodes),Hmt,Hit,Dit,tt,zt
      REAL th,h,dz,dx,z,ht
      REAL a,b,Di,Temp,E,rgc,Diff,maxt,D,t
      REAL Hinf1,Hinit,Hinf2,Gtot,Gstart,Gend,Hsat
```

```fortran
      REAL timetemp,dTdt,smdt,dt,thick,Stot(3),Dtot(3),dttot(3)
      REAL Ceq1,Ceq2,Ceq,Tmax,Aold(maxmodes)
      REAL Astore1(maxmodes),Astore2(maxmodes),Astore3(maxmodes)
      DIMENSION zloc(maxn),dTemp(maxdt),timetot(1000),Hsv(maxn,1000)
      DIMENSION Temp(maxdt),Ho(maxdt),time(maxdt),cyc(maxdt)
      DIMENSION ttot(maxdt),dtstar(maxdt,6),Htot(3,maxn),Cm(maxn)
      DIMENSION Hm(maxn),An(maxmodes),Bn(maxmodes),Am(maxmodes)
      DIMENSION G(maxn),Gavg(maxn),x(maxn),u(maxn),Havg(maxn),Davg(maxn)
      DATA rgc,pi/8.314,3.14159265359/
      DATA Hm/maxn*0./,An/maxmodes*0./,dtstar/600*0./,Bn/maxmodes*0./
      DATA Htot/15000*0./
      INTEGER filein,nply,ntime,nsmp,ncsp,ntot,nm,S,nx,nmt,nmodes
      INTEGER sic,ssic,Np,Nz,nsm,in,out,kstep,i1,i2,i3
      INTEGER ic1,ic2,ic3,ic4,ic5,ns
C  Reaction code variables
      CHARACTER*1 title(2),switch
      CHARACTER*2 title2(3)
      LOGICAL W,smed,smp,smwc,smlc,srxn
      PARAMETER (nplts=10)
      PARAMETER (splts=20)
      DIMENSION save(splts,maxn),tp(nplts),aprof(splts,maxn)
      DIMENSION r(3),rdt(3),atot(maxn),prfct(nplts)
      DIMENSION Ea(3),rk(3),y(3),Oi(3),alphaoxy(maxn)
      REAL Dox,Doxy,box,dlt,rml,rmli,rml1,rmlnstep
      REAL Cox,Eox,rkx,Ox,Bn2,roxy,roxydt,rthermdt,cavg
      COMMON/stuff/ c(maxn), alpha(3,maxn)
      DATA c/maxn*0./,alpha/15000*0./,atot/maxn*0./,alphaoxy/maxn*0./
      DATA title/'C','A'/
      DATA thold/0.02/
      DATA ic1/0./,ic2/0./,ic3/0./,ic4/0./,ic5/0./
      WRITE(*,*) 'Please input file name'
      READ(*,*) matfile
C  Read in material property values
      filein=2
      TAB=CHAR(9)
      OPEN(filein,FILE=matfile,STATUS='old')
      REWIND(filein)
      READ(2,*) nply
      READ(2,*) th
      READ(2,*) Di
      READ(2,*) E
      READ(2,*) a
      READ(2,*) b
      READ(2,*) Dox
      READ(2,*) Cox
      READ(2,*) Eox
      READ(2,*) rkx
      READ(2,*) Ox
      DO 10 i=1,3
        READ(2,*) Ea(i),rk(i),Oi(i),y(i)
10    CONTINUE
      READ(2,*) tinit,tempinit,Hinit
      READ(2,*) ncycles
      READ(2,*) ntime
CC  READ IN EXPOSURE PROFILE, CALC DTSTAR
      Tmax=1
      ns=0
      Ceq1=0
```

```fortran
      Ceq2=0
      DO 150 j=1,ntime
90        READ(2,*) ttot(j),Temp(j),Ho(j)
        IF (Temp(j).GT.Tmax) Tmax=Temp(j)
          IF (j.GT.1) THEN
            time(j)=ttot(j)-ttot(j-1)
            dTemp(j)=Temp(j)-Temp(j-1)
            IF (dTemp(j).NE.0) THEN
              dt=0
              smdt=time(j)/20
              dTdt=dTemp(j)/time(j)
              DO 100 nn=1,20
              dt=dt+smdt
+             dtstar(j,1)=dtstar(j,1)+smdt*
               exp(-E/(rgc*(dTdt*dt+Temp(j-1))))
              dtstar(j,2)=dtstar(j,2)+smdt*
+              exp(-Ea(1)/(rgc*(dTdt*dt+Temp(j-1))))
              dtstar(j,3)=dtstar(j,3)+smdt*
+              exp(-Ea(2)/(rgc*(dTdt*dt+Temp(j-1))))
              dtstar(j,4)=dtstar(j,4)+smdt*
+              exp(-Ea(3)/(rgc*(dTdt*dt+Temp(j-1))))
              dtstar(j,5)=dtstar(j,5)+smdt*
+              exp(-Eox/(rgc*(dTdt*dt+Temp(j-1))))
              dtstar(j,6)=dtstar(j,6)+smdt*
+              exp(-Cox/(dTdt*dt+Temp(j-1)))
100           CONTINUE
              Ceq1=Ceq1+a*Ho(j)*dtstar(j,1)
              Ceq2=Ceq2+dtstar(j,1)
            ELSE
              dtstar(j,1)=time(j)*exp(-E/(rgc*Temp(j-1)))
              dtstar(j,2)=time(j)*exp(-Ea(1)/(rgc*Temp(j-1)))
              dtstar(j,3)=time(j)*exp(-Ea(2)/(rgc*Temp(j-1)))
              dtstar(j,4)=time(j)*exp(-Ea(3)/(rgc*Temp(j-1)))
              dtstar(j,5)=time(j)*exp(-Eox/(rgc*Temp(j-1)))
              dtstar(j,6)=time(j)*exp(-Cox/Temp(j-1))
              Ceq1=Ceq1+a*Ho(j)*exp(-E/(rgc*Temp(j)))*time(j)
              Ceq2=Ceq2+exp(-E/(rgc*Temp(j)))*time(j)
            ENDIF
          ELSE
            time(j)=ttot(j)
            dTemp(j)=0
            dtstar(j,1)=time(j)*exp(-E/(rgc*Temp(j-1)))
            dtstar(j,2)=time(j)*exp(-Ea(1)/(rgc*Temp(j-1)))
            dtstar(j,3)=time(j)*exp(-Ea(2)/(rgc*Temp(j-1)))
            dtstar(j,4)=time(j)*exp(-Ea(3)/(rgc*Temp(j-1)))
            dtstar(j,5)=time(j)*exp(-Eox/(rgc*Temp(j-1)))
            dtstar(j,6)=time(j)*exp(-Cox/Temp(j-1))
            Ceq1=Ceq1+a*Ho(j)*exp(-E/(rgc*Temp(j)))*time(j)
            Ceq2=Ceq2+exp(-E/(rgc*Temp(j)))*time(j)
          ENDIF
150   CONTINUE
      READ(2,*) nmodes
      READ(2,*) ICANin
      CALL STORAGE(smed,filein)
      CALL STORAGE(smp,filein)
      CALL STORAGE(srxn,filein)
      CALL STORAGE(smwc,filein)
      CALL STORAGE(smlc,filein)
```

```fortran
        IF (smed) READ(2,*) sic,ssic
        IF (smp.OR.smwc) READ(2,*) ncsp
        IF (smp) READ(2,*) ic1,ic2,ic3,ic4,ic5
        IF (smwc) READ(2,*) i1,i2,i3
        h = th*nply
        nstep=nply*Nsp
        Ceq=Ceq1/Ceq2
        WRITE(*,180) 'Ceq = ',Ceq
180     FORMAT(A7,1pe9.3)
        npp=ncycles/ncsp
        IF (ncycles.GT.100) THEN
          nsm=int(ncycles/100)
        ELSE
          nsm=1
        ENDIF
200     CLOSE(2)
        IF (smlc) THEN
          OPEN (23,file='Massloss',status='new')
          WRITE(23,210) 'Time [h]',TAB,'Mass %',TAB,'Deg layer'
        ENDIF
210     FORMAT(2(a11,a1),a11)


C
C  INITIAL EXPOSURE
        rmli=0
        box=.01
        Bn2=0
        c(1)=1
        dz=h/(nstep-1)
        z=0
        Hinf1=a*Hinit**b
        Hinf2=a*Ho(1)**b
        IF (tinit.NE.0) THEN
         DO 250 n=1,nmodes,2
          An(n)=-Hinf1*4/(pi*float(n))
          Bn(n)=4/(pi*float(n))
250       CONTINUE
        Diff=Di*exp(-E/(rgc*tempinit))
        Doxy=Dox*exp(-Cox/tempinit)
        DO 350 k=1,nstep
          DO 300  n=1,nmodes,2
           Hm(k)=Hm(k)+An(n)*SIN(n*pi*z/h)*
     +     EXP(-(n**2*pi**2*Diff*tinit)/h**2)
           c(k)=c(k)+Bn(n)*SIN(n*pi*z/h)*
     +     EXP(-(n**2*pi**2*Doxy*tinit)/h**2)
300       CONTINUE
          Hm(k)=Hinf1-Hm(k)
          c(k)=1-c(k)
          zloc(k)=z
          z=z+dz
          DO 310 i=1,3
          IF (i.LE.1) THEN
           roxy=ABS(c(k))*(1.0-alpha(i,k))**Ox*rkx*
     +       exp(-Eox/(rgc*tempinit))
           roxydt= min(roxy*tinit,1.0-alpha(i,k),ABS(c(k)/box))
           alphaoxy(k)=alphaoxy(k)+roxydt
           r(i)=(1.0-alpha(i,k)-roxydt)**Oi(i)*rk(i)*
     +       exp(-Ea(i)/(rgc*tempinit))
```

```fortran
                rthermdt= min(r(i)*tinit,1.0-alpha(i,k)-roxydt)
                rdt(i)=roxydt+rthermdt
              ELSE
                r(i)=(1.0-alpha(i,k))**Oi(i)*rk(i)*
     +            exp(-Ea(i)/(rgc*tempinit))
                rdt(i)= min(r(i)*tinit,1.0-alpha(i,k))
              ENDIF
              alpha(i,k)=alpha(i,k)+rdt(i)
              atot(k)=atot(k)+(y(i)*rdt(i))
310         CONTINUE
            rmli=rmli+atot(k)/nstep
            Bn2=Bn2+dz*2/h*roxydt*box*sin(n*pi*zloc(k)/h)
350       CONTINUE
          Diff=Di*exp(-E/(rgc*Temp(1)))
          Doxy=Dox*exp(-Cox/Temp(1))
          DO 400 n=1,nmodes,2
            An(n)=4/(float(n)*pi)*(Hinf2-Hinf1)
     +        +An(n)*EXP(-(n**2*pi**2*Diff*time(1))/h**2)
            Bn(n)=Bn(n)*EXP(-(n**2*pi**2*Doxy*time(1))/h**2)+Bn2
400       CONTINUE
        ELSE
          DO 600 k=1,nstep
            zloc(k)=z
            z=z+dz
600       CONTINUE
          DO 700 n=1,nmodes,2
            An(n)=4*(Hinf2-Hinf1)/(pi*float(n))
            Bn(n)=4/(pi*float(n))
700       CONTINUE
          rmli=0
        ENDIF
C
CC    BODY OF PROGRAM
C
        nn=0
        ntot=0
        timetemp=0
        nsmp=0
        dlt=0
        DO 4400 m=1,ncycles
         DO 4000 j=1,ntime
           timetemp=timetemp+time(j)
           rml=rmli
           dlt=0.0
           Hinf1=a*Ho(j)**b
           Hinf2=a*Ho(j+1)**b
           Bn2=0
C Oxygen/thermal reactions
           IF (smp.AND.(mod(m,ncsp).EQ.0).AND.(j.EQ.ic1)) THEN
             nsmp=nsmp+1
             cyc(nsmp)=m
           ENDIF
           DO 2500 k=1,nstep
            IF ((k.GT.3).AND.(k.LT.nstep-2)) THEN
             cavg=(c(k-1)+c(k)+c(k+1))/3
            ELSE cavg=c(k)
            ENDIF
             DO 2050 i=1,3
```

135

```
            IF (i.LE.1) THEN
              roxydt=ABS(c(k))*(1.0-alpha(i,k))**Ox*rkx*dtstar(j,5)
              roxydt= min(roxydt,1.0-alpha(i,k),ABS(c(k)/box))
              alphaoxy(k)=alphaoxy(k)+roxydt
              rthermdt=(1.0-alpha(i,k)-roxydt)**Oi(i)*rk(i)*dtstar(j,2)
              rthermdt= min(rthermdt,1.0-alpha(i,k)-roxydt)
              rdt(i)=roxydt+rthermdt
            ELSE
              rdt(i)=(1.0-alpha(i,k))**Oi(i)*rk(i)*dtstar(j,i+1)
              rdt(i)= min(rdt(i),1.0-alpha(i,k))
            ENDIF
            alpha(i,k)=alpha(i,k)+rdt(i)
            atot(k)=atot(k)+(y(i)*rdt(i))
2050        CONTINUE
            rml=rml+atot(k)/(nstep-1)
C
C     CALCULATE NEW OXYGEN/MOISTURE CONCENTRATION
C
            c(k)=0
            IF (smp.AND.(mod(m,ncsp).EQ.0).AND.
     +      (j.EQ.ic1.OR.j.EQ.ic2.OR.j.EQ.ic3.OR.j.EQ.ic4.OR.j.EQ.ic5)) THEN
              Hm(k)=0
              DO 2200  n=1,nmodes,2
                Hm(k)=Hm(k)+An(n)*SIN(n*pi*zloc(k)/h)*
     +          EXP(-(n**2*pi**2*Di*dtstar(j,1))/h**2)
                c(k)=c(k)+Bn(n)*SIN(n*pi*zloc(k)/h)*
     +          EXP(-(n**2*pi**2*dtstar(j,6)*Dox)/h**2)
2200          CONTINUE
              Hm(k)=Hinf1-Hm(k)
              Hsv(k,nsmp)=Hm(k)
            ELSE
              DO 2300 n=1,nmodes,2
                c(k)=c(k)+Bn(n)*SIN(n*pi*zloc(k)/h)*
     +          EXP(-(n**2*pi**2*dtstar(j,6)*Dox)/h**2)
2300          CONTINUE
            ENDIF
            c(k)=1-c(k)
            IF (c(k).GT.box*roxydt) c(k)=c(k)-box*roxydt
            Bn2=Bn2+dz*2/h*roxydt*box*sin(n*pi*zloc(k)/h)
2500        CONTINUE
            rml1=0.5*atot(1)/(nstep-1)
            rmlnstep=0.5*atot(nstep)/(nstep-1)
            rml=rml-(rml1+rmlnstep)
            DO 2600 n=1,nmodes,2
              IF (smwc) THEN
                IF (j.EQ.i1) Astore1(n)=An(n)
                IF (j.EQ.i2) Astore2(n)=An(n)
                IF (j.EQ.i3) Astore3(n)=An(n)
              ENDIF
              Aold(n)=An(n)
              An(n)=4/(float(n)*pi)*(Hinf2-Hinf1)
     +          +An(n)*EXP(-(n**2*pi**2*Di*dtstar(j,1))/h**2)
              Bn(n)=Bn(n)*EXP(-(n**2*pi**2*Dox*dtstar(j,6))/h**2)+Bn2
2600        CONTINUE
            IF (smwc.AND.j.EQ.i1) THEN
              dttot(1)=dtstar(j,1)
              Stot(1)=Hinf1
            ELSEIF (smwc.AND.j.EQ.i2) THEN
```

```
                    dttot(2)=dtstar(j,1)
                    Stot(2)=Hinf1
                  ELSEIF (smwc.AND.j.EQ.i3) THEN
                    dttot(3)=dtstar(j,1)
                    Stot(3)=Hinf1
                  ENDIF
C    Degraded layer thickness (visible if alpha>threshold)
            DO 3900 k=1,nstep
               IF (alphaoxy(k).GT.thold.AND.k.LE.50) THEN
                IF (alphaoxy(k+1).NE.1) THEN
                  dadz=(alphaoxy(k+1)-alphaoxy(k))/dz
                  dlt=(k-1)*dz-(alphaoxy(k)-thold)/dadz
                ELSE
                  dlt=k*dz
                ENDIF
               ENDIF
 3900       CONTINUE
            IF (smed.AND.(m.EQ.sic).AND.(ssic.EQ.j)) THEN
              CALL MOISTURE(nmodes,nstep,Aold,Hm,Hinf1,h,Di,dtstar(j,1),zloc)
              CALL AVG(nply,nstep,Nsp,Hm,Havg)
              CALL AVG(nply,nstep,Nsp,atot,Davg)
            ENDIF
 4000       CONTINUE
            IF (mod(m,ncsp).EQ.0) WRITE(*,*)'Cycle',m,' complete.'
            IF ((smlc).AND.(mod(m,nsm).EQ.0.OR.m.EQ.1)) THEN
              WRITE(23,4110) timetemp/3600,TAB,rml*100,TAB,dlt
 4110         FORMAT(F9.2,a1,2(1pE11.3,a1))
            ENDIF
            IF (srxn.AND.mod(m,ncsp).EQ.0) THEN
              ns=ns+1
              tp(ns)=timetemp
              prfct(ns)=m
              DO 4220 k=1,nstep
                save(ns,k)=c(k)
 4220           save(ns+npp,k)=atot(k)
            ENDIF
C
C    STORE CENTER AND TOTAL MOISTURE
C
            IF (smwc.AND.((mod(m,nsm).EQ.0).OR.(m.EQ.1))) THEN
              ntot=ntot+1
              CALL TOTALM(nmodes,Astore1,Htot(1,ntot),Stot(1),Di,dttot(1),h)
              CALL TOTALM(nmodes,Astore2,Htot(2,ntot),Stot(2),Di,dttot(2),h)
              CALL TOTALM(nmodes,Astore3,Htot(3,ntot),Stot(3),Di,dttot(3),h)
              timetot(ntot)=timetemp
            ENDIF
 4400   CONTINUE
        OPEN(50,FILE='dump',STATUS='new')
        IF (smed) GOTO 4444
        CALL MOISTURE(nmodes,nstep,Aold,Hm,Hinf1,h,Di,dtstar(j,1),zloc)
        CALL AVG(nply,nstep,Nsp,Hm,Havg)
        CALL AVG(nply,nstep,Nsp,atot,Davg)
 4444   WRITE(50,4500) (i,TAB,100*Havg(i),TAB,Davg(i),i=1,nply)
 4500   FORMAT(I9,A1,F8.4,A1,F8.6)
 4550   FORMAT(I9,',',1PE8.2)
        REWIND(50)
C
C    ICAN input file adjustments
```

```
C
      in=3
      out=4
      IF (ICANin.NE."N") THEN
        OPEN(in,FILE=ICANin,STATUS='old')
        OPEN(out,FILE='ICANin',STATUS='new')
        DO 4700 i=1,200
         READ(in,4800,END=4775) Aline
         IF (Aline(1:8).EQ.'       PLY') THEN
          READ(50,4750) i,Mpct,Dpct
          Aline(41:48)=Mpct(2:9)
          Aline(73:80)=Dpct(1:8)
         ENDIF
         WRITE(out,4850) Aline
4700    CONTINUE
4775    CLOSE(in)
        CLOSE(out)
      ENDIF
4750  FORMAT(I9,A9,A9)
4800  FORMAT(A80)
4850  FORMAT(A80)
      CLOSE(50)
C
C  Data storage
C
      IF (smp) THEN
       OPEN(10,FILE='Cmprofile',STATUS='new')
       WRITE(10,9040) (TAB,cyc(j),j=1,nsmp)
       DO 5000 k=1,nstep
        WRITE (10,9050) zloc(k),(TAB,Hsv(k,j),j=1,nsmp)
5000    CONTINUE
      ENDIF
      IF (smwc) THEN
       OPEN(24,FILE='WtGain',STATUS='new')
       WRITE(24,9020) TAB,i1,TAB,i2,TAB,i3
       WRITE(24,9030) (timetot(m)/3600,TAB,Htot(1,m),
     + TAB,Htot(2,m),TAB,Htot(3,m),m=1,ntot)
      ENDIF
1010  FORMAT(50(e11.2))
C  Reaction Profile storage
      IF (npp.NE.0.AND.srxn) THEN
       OPEN(22,FILE='Coxprofile',STATUS='new')
       WRITE(22,9080)TAB,((title(k),prfct(i),TAB,i=1,npp),k=1,2)
       ncols=2*npp
       DO 6300 k=1,nstep
6300    WRITE(22,1090) zloc(k),TAB,(save(j,k),TAB,j=1,ncols)
      ENDIF
1090  FORMAT (2000(1pe11.4,A1))
9020  FORMAT ('time [h]',A1,'Wtgain',I2,A1,'Wtgain',I2,A1,'Wtgain',I2)
9030  FORMAT (1PE9.3,A1,1pe11.3,A1,1pe11.3,A1,1pe11.3)
9040  FORMAT (2x,'z',500(A1,'Cyc',F5.0))
9050  FORMAT (f7.5,500(A1,1pe11.3))
9080  FORMAT('Z',a1,10(a,F5.0,a1))
      IF (smlc) CLOSE(23,STATUS='keep')
      IF (smp) CLOSE(10,STATUS='keep')
      IF (smwc) CLOSE(24,STATUS='keep')
      IF (srxn) CLOSE(22,STATUS='keep')
      IF (smp)WRITE(*,*)'Moisture profiles stored in file ''Cmprofile'''
```

```fortran
      IF (smwc)WRITE(*,*)'Moisture dep wt change stored in ''WtGain'''
      IF (smlc)WRITE(*,*)'Mass loss stored in file ''Massloss'''
      IF (srxn)WRITE(*,*)'Ox conc. and mass loss stored ''Coxprofile'''
      IF (ICANin.NE."N")WRITE(*,*) 'ICAN input written to ''ICANin'''
      STOP
      END

      SUBROUTINE MOISTURE(nm,kstep,Am,Cm,Hsat,ht,D,t,u)
      INTEGER nm,kstep
      REAL Hsat,ht,D,t
      REAL Am(nm),Cm(kstep),u(kstep)
      DO 44 k=1,kstep
       Cm(k)=0
       DO 32  n=1,nm,2
        Cm(k)=Cm(k)+Am(n)*SIN(n*pi*u(k)/ht)*
     +  EXP(-(n**2*pi**2*D*t)/ht**2)
32     CONTINUE
       Cm(k)=Hsat-Cm(k)
44    CONTINUE
      RETURN
      END

      SUBROUTINE TOTALM(nmt,Ant,Hmt,Hit,Dit,tt,zt)
      INTEGER nmt
      REAL Ant(nmt),Hmt,Hit,Dit,tt,zt
      Hmt=0
      DO 50 n=1,nmt,2
       Hmt=Hmt+Ant(n)*2/(n*pi)*EXP(-(n**2*pi**2*Dit*tt)/zt**2)
50     CONTINUE
      Hmt=Hit-Hmt
      RETURN
      END

      SUBROUTINE STORAGE(W,FILE)
      LOGICAL W
      INTEGER FILE
      CHARACTER*1 switch
    1 READ(FILE,3,END=4) switch
      IF (switch.EQ.'$') GOTO 1
      IF (switch.EQ.'T') THEN
       W=.TRUE.
      ELSEIF (switch.EQ.'F') THEN
       W=.FALSE.
      ELSE
       TYPE*, 'Storage commands incorrectly formatted'
      ENDIF
    3 FORMAT(A1)
    4 RETURN
      END

      SUBROUTINE AVG(Np,Nz,S,G,Gavg)
      INTEGER Np,Nz,S,j
      REAL Gtot,Gstart,Gend
      REAL G(Nz),Gavg(Np)
      j=0
      Gtot=0
      Gstart=G(1)/2
      DO 10 i=1,Nz
```

```
        Gtot=Gtot+G(i)
        IF (mod(i,S).EQ.0) THEN
         j=j+1
         IF (j.GT.Np) GOTO 11
         Gend=G(i)/2
         Gavg(j)=(Gtot-(Gstart+Gend))/(S-1)
         Gstart=Gend
         Gtot=0
        ENDIF
10      CONTINUE
11      RETURN
        END
```